EFFECTS OF PHYSICAL STIMULI ON EXTRACELLULAR MATRIX ASSEMBLY BY CHONDROCYTES AND MESENCHYMAL STEM CELLS: EXPERIMENTAL AND FINITE ELEMENT ANALYSES

A Dissertation

Presented to the Faculty of the Graduate School

of Cornell University

In Partial Fulfillment of the Requirements for the Degree of

Doctor of Philosophy

by

Omotunde Mobolaji Babalola

May 2010

EFFECTS OF PHYSICAL STIMULI ON EXTRACELLULAR MATRIX ASSEMBLY BY CHONDROCYTES AND MESENCHYMAL STEM CELLS: EXPERIMENTAL AND FINITE ELEMENT ANALYSES

Omotunde Mobolaji Babalola, Ph. D.

Cornell University 2010

Using cells, materials, physical and/or chemical factors, tissue engineering (TE) is being researched extensively for the repair or regeneration of tissues and organs after damage/disease. With arthritis being the leading cause of disability in the United States, cartilage TE and associated techniques are actively being researched as potential solutions to halting the progression of the disease.

This thesis investigated how physical stimuli used in cartilage TE affect the formation of functional TE cartilage. The lack of sufficient metrics available in the field for defining cell response is highlighted, which has hindered faster advancement of the field. The overall hypothesis of this work was that different levels of physical stimuli regulate the functionality of TE constructs and these levels differentially affect mesenchymal stem cells (MSCs). The first aim addressing this hypothesis established a baseline on the effects of cell density, type and species on engineered constructs. The second aim developed finite element (FE) models of scaffolds commonly used in cartilage TE undergoing dynamic compression, to quantify the physical stimuli present within them. Finally, the third and fourth aims investigated the effects of scaffold composition and physical stimuli on matrix metabolism by chondrocytes and differentiated MSCs, respectively.

Chondrocytes and MSCs differed in their ability to metabolize matrix proteins. This difference was dependent on cell density, cell species and scaffold composition.

For example, MSCs lacked the ability to retain and aggregate produced proteoglycan, and the absence of link protein may play a role. FE models showed that scaffolds generally used for cartilage TE yielded gradients of physical stimuli spanning orders of magnitude, for similar loading conditions. The consequence of such variations in physical stimuli was evident in cells seeded in lower weight percent scaffolds (i.e. less complaint and more permeable) producing more matrix proteins, but retaining the least amounts compared to higher weight percent constructs.

These results highlight a limitation in the use of MSCs for cartilage TE; although MSCs are capable of matching the amounts of matrix produced by chondrocytes, they lack retention capabilities. The results also makes evident, the difficulty in comparing studies on the use of dynamic compression for the enhancement of cartilage TE constructs.

BIOGRAPHICAL SKETCH

Tunde was born in Buffalo, NY and raised in Lagos, Nigeria by a physician and economist/entrepreneur. She grew up as the second of four children. Though she started high school in Nigeria, she finished in Brooklyn, NY; a move which proved to be a huge culture shock for her. She received her B.S. degree in Biomedical Engineering with a minor in Mechanical Engineering from the University of Rochester, in Rochester, NY. Prior to starting graduate school, Tunde worked as a research engineer at the Hospital for Special Surgery, in Manhattan, NY. It was during her two year tenure there that she fostered a fascination with the musculoskeletal system and advancements being made in orthopaedic research and medicine.

In 2004, Tunde returned to school to embark on a graduate career in Biomedical Engineering at Cornell University in Ithaca, NY. Working under the advisement of Larry Bonassar, Ph.D. and with help from Marjolein van der Meulen, she worked on her dissertation research, continuing with her fascination with orthopaedics. In addition to her dissertation research, she has participated in numerous outreach activities which have ranged from educating the community about science and engineering through fairs to hosting demo sessions about the endless possibilities provided by tissue engineering techniques.

For my family; immediate, extended and adopted.

ACKNOWLEDGMENTS

I would first like to extend sincere thanks to my special committee, Prof. Larry Bonassar, Prof. Marjolein van der Meulen and Dr. Alan Nixon, for their constant encouragements, guidance, technical advice and support. Tissue engineering and mechanobiology was a research area I had only read in articles and textbooks, and never would I have thought that I would be completing a dissertation on these two very topics, especially under the guidance of world renowned researchers. I am truly grateful and honored to have had them on my committee and have them as mentors.

I must thank Judy Thoroughman and Belinda Floyd for their constant support, assistance and availability, both of whom have been instrumental in making sure I could actually run experiments smoothly. Thanks also go out to past and present members of the Bonassar lab, most of who have helped shape me to be a better researcher, teacher, communicator, mentor and friend. I thank past and present members of the Biomechanics group, Nixon lab, Diversity programs in engineering office and Hospital for Special Surgery friends all of whom have been a constant encouraging and supportive presence in my tenure as a doctoral candidate. Many thanks to the Biomedical Engineering and Mechanical Engineering department members (faculty, students and staff) for their mentorship and friendship, and for giving me countless opportunities to be a respected member of such great departments. I also thank members of the histology and necropsy facilities for their patience and help in acquiring samples and getting samples processed.

Most importantly, I thank my parents and siblings for their unwavering love and support and my extended family and friends for providing much needed balance in my life. I am truly indebted to you all.

Funding for this dissertation was primarily provided by the Alfred P. Sloan Foundation, Graduate Assistance in Areas of National Need fellowship, Cornell Nanobiotechnology Center and the Office of the Provost at Cornell University.

TABLE OF CONTENTS

LIST OF FIGURES

CHAPTER 1

CHAPTER 2

CHAPTER 3

CHAPTER 4

CHAPTER 5

LIST OF ABBREVIATIONS

ANOVA	Analysis of Variance
BMP	Bone morphogenetic protein
CO_2	Carbon dioxide
DMAB	Dimeththylaminoborane
DMEM	Dulbecco's Modified Eagle Medium
DMMB	1, 9 Diethylmethylene blue
DNA	Deoxyribonucleic acid
dw	Dry weight
EDTA	Ethylenediaminetetraacetic acid
FBS	Fetal bovine serum
FGF	Fibroblast growth factor
g	Grams
GAG	Glycosaminoglycan
GF	Growth factor
HA	Hyaluronan
IHC	Immunohistochemistry
IGF	Insulin-like growth factor
Kg	Kilogram
kPa	Kilopascal
mm	Millimeters
mm/s	Millimeters per second
mg/ml	Milligrams per milliliter
mM	Millimolar
μm	Microns

Microns per second	μm/s
Megapascal	MPa
Mesenchymal stem cell	MSC
Microgram per milliliter	μg/ml
Osteoarthritis	OA
Pascals	Pa
Phosphate buffered saline	PBS
Polyethylene glycol	PEG
Poly glycolic acid	PGA
Polylactic acid	PLA
Poly-l-lactic acid	PLLA
Standard deviation	SD
Tissue engineering	TE
Transforming growth factor beta	TGF-b
Wet weight	ww

LIST OF SYMBOLS

Symbol	Variable or Parameter	Dimensions
ρ_f	fluid density	kg m^{-3}
θ_s	solid fraction	---
ν	fluid velocity	μ/s
η	viscosity	Pa.s
∇p	pressure gradient	---
$\frac{\partial}{\partial t}$	partial derivative	---
σ	normal stress	N/m^2
T	shear stress	N/m^2
K	permeability	$m^4/N.s$

CHAPTER 1

Introduction

This dissertation focuses on the ability of the terminally differentiated cell of cartilage tissue (chondrocytes) and its progenitor cell (mesenchymal stem cells) to produce and retain glycosaminoglycan, a key component of cartilage tissue that plays a major role in its ability to function normally. The properties, development and pathology of cartilage tissues are first introduced to give a background and preface to the work presented here. The use of cartilage tissue engineering techniques for therapeutic interventions is then detailed. The first aim established a baseline for the behavior of mesenchymal stem cells and chondrocytes in alginate scaffolds as a function of standard conditions (cell density, type and species) perturbed in cartilage engineering research. The aim also highlighted caveats for the use of mesenchymal stem cells for cartilage tissue engineering with current techniques and scaffolds. The second aim develops a finite element model for the analysis of dynamic loading on cartilage tissue engineered constructs. The studies of this aim also included the parametric analysis of physical stimuli generated within various scaffolds used in the field. The third aim related extracellular matrix assembly by chondrocytes to the ranges in physical stimuli present in engineered constructs due to dynamic loading. And finally, the last aim details the differential behavior of mesenchymal stem cells when subjected to the same ranges in physical stimuli during dynamic loading of engineering constructs.

Cartilage

Characteristics

Cartilage, an avascular, aneural and alymphatic tissue, is present in several forms within the human body. This tissue is a dense fibrous connective tissue that depends highly on diffusion and convection for nutrient transport and waste removal. Cartilage plays a crucial role in the growth and development of vertebrate organisms by forming a majority of the temporary skeletal system of an embryo (1). This temporary template is then used as the pattern for the development of the adult skeleton. The development of this tissue involves series of highly choreographed temporally and spatially varying factors including chemical, physical and mechanical cues, that culminate in the development of a functional skeletal system.

A thin layer of hyaline cartilage lining the ends of long bones, articular cartilage is a specialized type of cartilage with low frictional properties (1, 2). This tissue aids in the distribution of loads efficiently within diarthrodial joints and also functions as a shock absorber during high impact loading. The unique zonal extracellular matrix (ECM) architecture of cartilage is responsible for its ability to resist compressive, tensile and shear forces upon loading. This architecture is produced by the small population of chondrocytes (10% of the tissue volume), cells intrinsic to cartilage tissue. These cells are responsible for laying the predominantly rich network of type II collagen (50-75% of its dry weight) interwoven with proteoglycans (15-40% of dry weight) (1, 2) that make up the major matrix constituents of the tissue. Water is its most abundant component at approximately 70% of its wet weight.

Proteoglycans are macromolecules made up of one or more glycosaminoglycans (GAG) chains covalently bound to a protein core (3, 4).

Aggrecan, the major proteoglycan of articular cartilage, is formed by numerous proteoglycan monomers bound by non-covalent bonds via link protein molecules to long hyaluronic acid (HA) chains to form aggregates. These aggregates, hydrated due to their high fixed negative charge, are responsible for the high water content (5) and subsequently, the compressive resilience of the tissue during joint loading. The inhomogeneous and zonal distribution of type II collagen fibers within this tissue forms networks that inhibit the full hydration of glycosaminoglycans by acting as a restraint. This thereby restricts proteoglycan swelling, giving the tissue its ability to withstand compressive, shear and tensile forces.

Damage, Disease and Current Therapies

As a result of the characteristic low cellularity and avascular nature of cartilage, age, damage and/or disease can result in irreversible loss of function of cartilage tissue *in vivo*. These factors can result in changes in the composition of its ECM that lead to changes in mechanical properties and functionality. Compositional changes include increased cell proliferation and cell death, increased matrix production and enzymatic activity, and the formation of osteophytes, all leading to proteoglycan degradation and collagen fibrillation (6-10). These changes result in the loss of functional capabilities of the tissue that predispose cartilage to arthritis. Significant changes in structural, matrix components and mechanical properties of articular cartilage are also associated with ageing (7-9, 11-13). These changes include increased surface fibrillation, loss of glycosaminoglycans and decrease in cell function that can ultimately lead to the onset of osteoarthritis.

Osteoarthritis is a complex disease that affects the whole joint and occurs as a result of an imbalance between catabolic and anabolic pathways. This disease usually

occurs due to aging, genetics, or environmental factors, or a combination of these factors (14, 15). Being the most common form of arthritis, osteoarthritis is the leading cause of disability in the United States. According to the Centers for Disease Control and Prevention and related sources, 46 million adults (22%) reported physician-diagnosed arthritis, bases on data from a 2003-2005 national health interview survey (16-18). The pathophysiology of this disease is characterized by the breakdown of cartilage that leads to the development of fibrillation and fissures, and the disappearance of the full thickness surface of the joint. This results in bone remodeling, overgrowth and cartilage degradation, and decrease in joint space (19).

Mechanical forces play an important role in the initiation or progression of damage and disease to cartilage. Joint immobilization via casts inhibits the long-term healing response of cartilage (20), and controlled experimental studies have studied the evolution of osteoarthritis after initiation by impact loading (21-23). As a result of cartilage's limited ability for self repair, several types of interventions and replacement therapies have been explored. The current state of the art for the repair or replacement of this tissue involves the use of metal- or plastic- based implants for joint replacement. Unfortunately, as a result of their relatively short longevity *in vivo* (compared to the increasingly young age of patients), more biologically based therapeutic interventions are being researched. One such potential therapeutic intervention involves the use of tissue engineering techniques.

Biological interventions in the form of cell solutions for cartilage tissue repair, especially for defect repair, has been extensively studied and used clinically. When applied clinically, this method has widely been used in the form of autologous chondrocyte transplantation or implantation (ACT/ACI). ACT relies on implanted cells, harvested from the non-weight bearing region of a joint, to produce and replace damaged tissue (24-26). This procedure has been used with or without growth factors,

with the cells secured (in place) by a periosteal flap sutured over the defect. Since its evolution, this procedure has included the use of biomaterials as carriers and restraints of the implanted cells. The incorporation of biomaterials in this technique has only strengthened the capacity of research involved in tissue engineering for cartilage repair due to favorable outcomes observed clinically (27-29).

Tissue engineering, a field that combines the use of cells and biomaterials, and the application of suitable environmental factors (Fig. 1.1) (30), can provide a basis for the systematic control of in vitro studies on tissue growth and function. Most importantly, tissue engineering can serve as model for engineering replacement tissue. Although progress has been made in defining the relevant parameters of tissue engineering, much still needs to be explored about how variations in the aforementioned factors and their combination, affect the formation and maintenance of functional tissues and structures.

Cartilage Tissue Engineering

Engineering cartilaginous tissue involves the use of cells (either chondrocytes or progenitor cells), natural or synthetic scaffolds (e.g. alginate, agarose and poly ethylene glycol) and environmental factors (ranging from the use of cytokines and growth factors to mechanical stimulation). Numerous studies have highlighted the success of combinations of these factors for the generation of cartilaginous tissues (31-45). Using techniques related to tissue engineering, neocartilage, articular and fibrous cartilage-like tissues have been successfully engineered both *in vitro* and *in vivo*. Although these engineered tissues contain most of the components characteristic of native cartilaginous tissues, they occur in different quantities/concentrations with little to no architectural arrangement, which is key for the functionality of this tissue. The

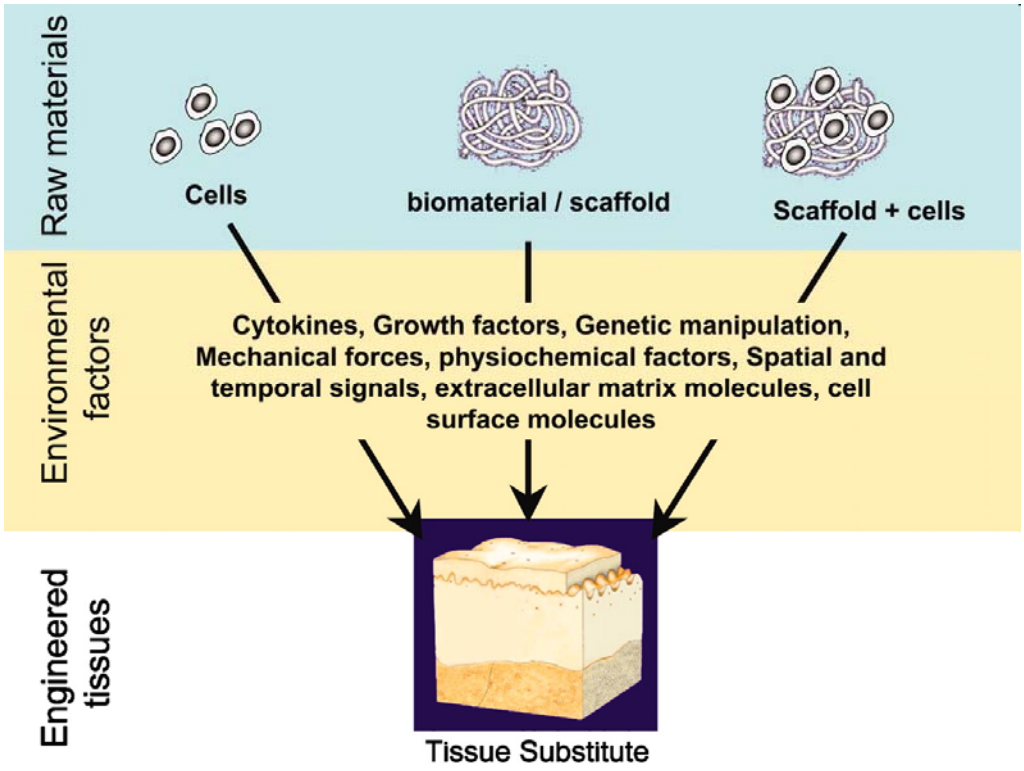

Figure 1.1: Factors used independently or in combination for tissue engineering applications. Figure reprinted from "Khademhosseini et. al. Microscale technologies for tissue engineering and biology. *PNAS*, 2006" and with permission from the National Academy of Sciences, USA.

resultant engineered tissues are normally of homogeneous cartilage-like tissues that lack the functional architecture indicative of articular cartilage. In an effort to increase the concentration of and/or improve the functionality of ECM molecules within engineered cartilage constructs, recent studies have focused on the use of mechanical stimulation devices/bioreactors. These devices have been used to replicate in vivo mechanical forces present during cartilage development and tissue maintenance, and have ranged from either custom designed or commercially available bioreactors (33, 34, 37, 43, 45-50).

Role of Mechanical Forces In vivo

The development of articular cartilage tissue is highly dependent on the sequence of events that occur prior to, during and after joint cavitation. Muscle contractions, which begin *in ovo/in utero* in the late embryonic stages, have been hypothesized to generate forces that impose a time-dependent, distributed pattern of stresses and strains throughout nearly all of the musculoskeletal tissues (51-57). These physical cues have been thought to guide the growth and differentiation of progenitor cells and their importance has been elucidated using *in vitro* cultures of cartilage rudiments (55) and in embryos immobilized using neuromuscular blocking agents (58, 59). The use of neuromuscular blocking agents or the prevention of static or dynamic loading results in either partial or absent joint cavitation in growing embryos. Shear stresses and hydrostatic (dilatational) pressures are the types of physical stimuli that have been postulated to be responsible for the cavitation process and subsequently, joint development (60-63).

Mechanical loading also plays a major role in the maintenance of cartilage tissue (21, 61, 64-66). In a study by Vanwanseele et. al., mean articular cartilage

thickness was found to be significantly less in the patella and medial tibia of spinal-cord injured patients six months post-injury, when compared to healthy volunteers (67). Defined by cells' ability to translate mechanical signals to biochemical ones(68-70), mechanotransduction occurs via cell surface receptors (integrins) binding to ligands (6-10, 71-73). Ligands are regions present on extracellular matrix proteins to which cells can bind. Cell binding to ligands allows cells respond to mechanical loads imposed on their surrounding extracellular matrix (ECM).

Use of Mechanical Loading Devices In vitro

With compression, shear, and hydrostatic forces all present in the native loading environment, the mechanical loading devices (mentioned above) have been designed to recapitulate these forces individually or in combination, and to enhance mass transfer within engineered constructs. Although bioreactors applying all these mechanical forces are being studied, the use of direct scaffold compression bioreactors is the most prevalent. Perfusion (74), hydrostatic (47, 75) and rotating wall bioreactors (76) have been used to a lesser extent, and have been generally beneficial as evident by increased extracellular matrix production. The benefits of loading bioreactors have also been highly variable both among studies using similar systems and across systems. The variations in response found in studies utilizing mechanical loading bioreactors stems from differences in the loading parameters, scaffolds and cells used.

The paradigm followed by a majority of the studies on mechanical stimulation of chondrocytes to date simply seek to relate mechanical environments (i.e. applied strains, frequencies and duty cycles) to cell activity and tissue development (Fig. 1.2). Although these studies have attempted to determine the loading conditions that are most advantageous for cartilage tissue growth, less is known about the physical stimuli the cells experience as a result of a particular loading protocol imposed on scaffolds

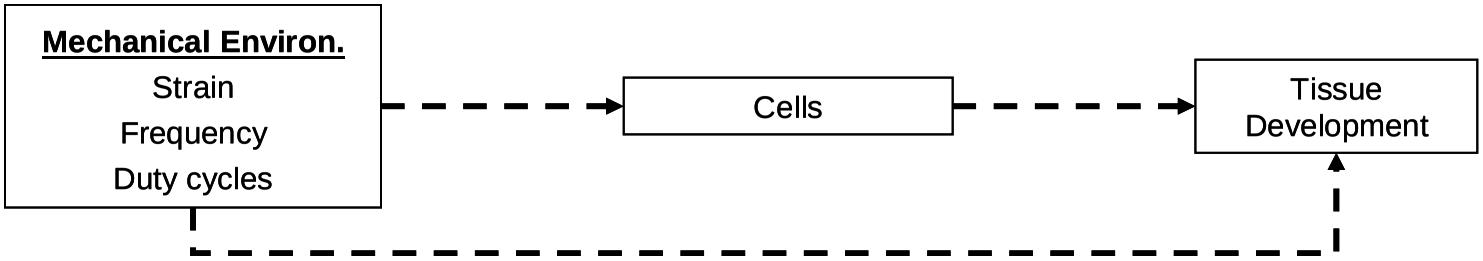

Figure 1.2: Top: Schematic of paradigm followed (dotted lines) by most studies on mechanical stimulation of chondrocytes. Bottom: Proposed change in paradigm (solid

that may be correlated to cell anabolic or catabolic activities. Unfortunately, the efficacy of bioreactors cannot be assessed solely based on the type of stimuli they provide due to numerous differences in all these study parameters. And in actuality, the physical stimuli sensed by cells will not only depend on the mechanical loading conditions and parameters, but also on the material properties of the scaffolds and resultant stresses, strains and fluid velocity profiles they generate upon loading.

Other Components for Engineering Cartilage Tissue

Cells

Although the efficacy of acellular constructs has been examined for cartilage tissue regeneration (77, 78) their use in studies has generally been to served as controls in experiments using cells. Their success post-implantation for cartilage replacement is unfortunately limited due to poor ability of acellular constructs to integrate and adhere with surrounding tissues. Due to this limitation, most studies utilize cells in the generation of replacement tissues with the idea that the encapsulated cells will synthesize and remodel the surrounding matrix to enhance integration. To this end, chondrocytes are the most widely used cell type, with the use of progenitor cells, particularly mesenchymal stem cells, becoming more prevalent in the past couple of years. Chondrocytes are cells derived from the mesenchymal lineage; therefore, the use of mesenchymal stem cells for cartilage tissue engineering purposes is not surprising.

As previously mentioned, cartilage has low cellularity, therefore acquiring a functional volume of cells to make a construct can be challenging. To circumvent this limitation, different approaches have been taken to increase cell numbers. One approach involves the use of cells harvested from neonatal/young tissues that are still

highly cellular and thicker than adult tissues (46, 47, 79, 80). Cells of this tissue age are the most commonly used in cartilage tissue engineering studies. Another approach relies on passaging of chondrocytes to achieve functional numbers for the construction of engineered constructs (80-82). Although both approaches have the benefit of providing large numbers of cells, they also come with associated disadvantages. As previously mentioned, one of the consequences of ageing cartilage is a reduction in cell function and ability to function normally. Unfortunately, cells from older tissue are more readily available than neonatal/younger cells. Hence the translation of tissue engineered constructs for clinical use will require more studies and analysis on the use of aged tissues/cells and not their younger counterparts. The disadvantage of using passaged chondrocytes to acquire functional volumes of chondrocytes has been elucidated (80) and includes to their loss in phenotype due to de-differentiation when cultured in monolayer for passaging. These de-differentiated cells are more fibroblastic in nature and as a result produce high amounts of type I collagen that is only present in healthy articular cartilage at extremely low concentrations (80, 82).

The limitations in the availability of chondrocytes make the use of mesenchymal stem cells very attractive, and indeed this idea has generated a great deal of excitement and promise. Stem cells are defined as undifferentiated cells capable of self renewal, with the ability to be differentiated into more than one specialized cell type (83). Specifically, mesenchymal stem cells are pluripotent cells that have the capacity to differentiate into chondrocytes, osteocytes or myoblasts, depending on the culture conditions and growth factors used (84-88). They are usually isolated from bone marrow, but can also be obtained from periosteum (89), muscle (90), adipose tissues (91), and synovial fluid (92), amongst other tissues. Their added attractiveness stems from their ability to be amplified via passaging, without loss in phenotype or

multipotentiality (86, 93). Unfortunately, they constitute only 0.001-0.01% of the total population of nucleated cells in the marrow (86).

To date, mesenchymal stem cell isolation has depended on either their phenotypic expression or lack of expression of cell surface markers (e.g. CD45, CD71, CD90 and CD102). Stem cell isolation via adherence to tissue culture plastic was one of the first methods of isolation discovered when the presence of fibroblastic colony forming cells was observed in *in vitro* cultures (94). This process has become the standard method for the isolation of mesenchymal stem cells from bone marrow tissue volumes. Unfortunately, this technique produces a heterogeneous population of cells that are thought to consist mainly of progenitor cells in different stages of differentiation, but fortunately, no terminally differentiated cells. The use of the adherent cell populations of bone marrow for cartilage tissue engineering has been sufficient in producing cartilage-like constructs (95), although no study on the ability of the different progenitor populations to form cartilage tissue has been done.

A more robust method of acquiring more homogeneous populations of stem cells is selection via the presence or absence of cell surface makers. These markers include SH2, SH3, CD14, CD29, CD34, CD44, CD45, CD71, CD90, CD106 and many more (83, 86). To date, no cell surface marker has been found to be solely indicative of a bone marrow derived mesenchymal stem cell; therefore studies have depended on (the absence or presence) of particular markers to determine cell stemness using flow cytometry.

Scaffolds

Biomaterials used for cartilage tissue engineering provides the three dimensional support necessary for seeded cells to maintain their differentiated function, proliferate and/or produce matrix proteins. The numerous scaffold types that

are being used have consisted of either natural, synthetic or hybrid materials, fabricated using a wide range of processes. Natural materials that have been used include agarose (33, 43, 46), alginate (47, 79, 96), hyaluronic acid (97, 98), gelatin (31, 99), fibrin glue (99, 100) and collagen derivatives (100, 101). Synthetic varieties include polyhydroxyacid based scaffold such as poly(l-lactic acid), poly(glycolic acid), poly(lactide-ε-caprolactone) and poly(ethylene glycol) based scaffolds (36, 37, 49, 102-105). Several varieties of hybrid biomaterials using both natural and synthetic polymers have also been successfully used as cartilage tissue engineering scaffolds (103, 106).

Several characteristics determine the success of a biomaterial as a scaffold, especially for the replacement of a weight bearing tissue like cartilage. These features include scaffold biocompatibility, mechanical properties, porosity, ease of fabrication, and degradation properties and by products. For the successful production of functional constructs, scaffold chemistry, which can differ from scaffold to scaffold, is also of concern (107). The fabrication of these materials includes techniques like hydrogel formation (33, 79, 108, 109), solvent casting/salt leaching (110), electrospinning (102, 111), non woven meshes (97), 3D fiber deposition (112) and gas foaming (113). The resulting scaffolds acquire different forms and architecture such as hydrogels, sponges and fiber meshes.

Other Factors

Lastly, combined with the use of cells and/or scaffolds, other environmental factors can enhance the formation of engineered cartilage. These factors fall under one of three categories, namely biochemical, architectural, and mechanical/physical factors, the last of which has been discussed above. Biochemical factors are generally in the form of growth factors or cytokines, and have included the sole or combined use

of the transforming growth factor beta superfamily, insulin-like growth factor, basic fibroblast growth factor, and bone morphogenic proteins (114-117). Their use has been in an effort to mimic the biochemical environments present during either the development or repair of cartilage, with the hopes of increasing cell proliferation and up-regulating matrix production. In a review by Darling and Athanasiou (35), the use of transforming growth factor superfamily was reported to range from no effect on cell activity to a 250% increase in either glycosaminoglycan production or ^{35}S-sulfate incorporation by chondrocytes encapsulated either within a scaffold or in cartilage explants. This variation was also found for collagen production, although the range was narrower and on average yielded a 50% increase in production.

Assessing the Efficacy of Cartilage Tissue Engineering Parameters

To assess matrix production, the most widely used assessment tools are biochemical assays of DNA, glycosaminoglycan and collagen (37, 43, 96). Gene expression analysis of matrix component levels and radioactive isotope incorporation by cells (e.g. [^{35}S]sulfate, [^{3}H]leucine and [^{3}H]proline) to assess rate of matrix biosynthesis are both also widely used (47, 95, 106, 118, 119). Although gene expression analysis does not give insight into the functionality of the constructs produced, the method serves as an excellent first order determinant of cell activity. Matrix localization within the constructs is also routinely analyzed via histological and immunohistochemical techniques. Although the collective use of these techniques has shown that cells seeded within a scaffold are capable of making matrix components found in native tissues, analysis of retention or architecture of the matrix synthesized is still uncommon. For a tissue such as cartilage, where structure-function relationships are very important, few studies include the assessment of the ability of

cells within the scaffold to not only retain the matrix molecules being made, but also to form a structural ECM that would result in a functional tissue. These assessments can be done with all the current techniques mentioned above.

Research Objectives

In light of the limitations discussed above and to elucidate the effects the discussed variations in cell type, scaffold properties and mechanical factors have on engineering functional cartilage, this dissertation sought to explore variations in cell, scaffold and environmental factors affect *in vitro* cartilage formation. The work presented in this dissertation also highlights the lack of standards in the field that may have hindered faster advancement in knowledge of the roles these conditions/parameters play in the generation of functional tissue. The hypothesis of this dissertation is that mechanical stimulation differentially regulates glycosaminoglycan production and assembly by chondrocytes when compared specifically to mesenchymal stem cells. We also hypothesize that this difference is modulated by scaffold composition. To address these hypotheses, the first aim focused on establishing the baseline effects of cell type, density, and species on engineered constructs. The second aim developed finite element (FE) models of scaffolds subjected to dynamic compression to quantify the physical stimuli present within scaffolds commonly used in cartilage tissue engineering. To study the response of cells to particular levels of physical stimuli, the third aim investigated the effects of scaffold composition on glycosaminoglycan production and assembly by chondrocytes when dynamically stimulated. Lastly, the fourth aim assessed the differential response of mesenchymal stem cells to scaffold composition and mechanical loading.

Specific Aims

Specific Aim I (Chapter 2):

This aim established baseline effects of cell species, type and density on engineered cartilage constructs. Glycosaminoglycan production and assembly, and construct mechanical properties were used as a metric to quantify the differential response to the aforementioned factors.

Motivation

Additional limitations, beyond those already highlighted, exist that hinder the advancement of cartilage tissue engineering as a viable clinical option. One such added complexity is the characteristics of cells used in the field. For example, assessing benefits of certain conditions between different studies has been difficult due to the use of different cell species. Variations in cell species affect the functionality of engineered tissue and as such create difficulties when trying to determine the efficacy of cells, scaffolds or environmental factors in such constructs. Another level of difficulty arises with the use of different cells densities when engineering cartilage tissues. Using cell densities similar to native tissue is unrealistic due to the low cellularity of the tissue and the need to generate large volumes of matrix proteins. Therefore, various densities of cells have been used in studies for cartilage tissue engineering and have ranged from 0.5 to 60 million cells per milliliter. This range in cell densities used has added another level of complexity when trying to compare outcomes between studies.

Furthermore, once again due to the low cellularity of the native tissue, chondrocytes have limited cell-cell interaction due to their sparse population within such a dense tissue. When seeded in scaffold constructs at high densities, cell-cell interaction occurs which provides added stimuli to the cell that are not present their in

native environment. This increased level of cell-cell interaction has been shown to be beneficial for the formation of cartilage-like tissues, although substantial increase in the functionality (modulus) of the tissue is not seen (42, 101, 116, 120). This finding suggests that the density of cells needed to create a functional construct has a limit. Unfortunately, the ideal initial seeding density, the cell species most applicable to study human cartilage engineering or the ability of MSCs to overcome the limitations in the use of chondrocytes all still remain elusive.

Approach

Using bovine and equine chondrocytes and equine mesenchymal stem cells, cartilage tissue engineering constructs were made by encapsulating cells within alginate hydrogel scaffolds using standard techniques. The bovine and equine chondrocyte laden constructs were seeded at densities of 1-, 10-, 25 and 50 million cells per ml. Due to the limited number of mesenchymal stem cells available in bone marrow tissue, first passage MSCs were encapsulated at a density of 25 million cells per ml, and second passage at densities of 1-, 10 and 25 million cells per ml. The resulting constructs were then cultured for up to 6 weeks, with culture medium being changed and harvested every 3 days and gels harvested every 2 weeks. Biochemical analysis of glycosaminoglycan and mechanical analysis of aggregate modulus and permeability was used to assess progression of tissue formation.

This aim sought to highlight the role initial seeding density played in the formation of a functional matrix. It also sought to highlight differences in metabolic capacities of chondrocytes from two different species, as well as differences between mesenchymal stem cells and the terminally differentiation chondrocytes. Glycosaminoglycan was used as a metric of functionality, and aggregate moduli and permeability as metrics for construct integrity and functionality. Construct and media

GAG content were analyzed to attain total amounts made, amounts loss to the surrounding medium and amount retained within the constructs that may have contributed to construct integrity and functionality. Link protein localization within the constructs was assessed to elucidate mechanism of loss of proteoglycan for all the groups studied.

Specific Aim II (Chapter 3):

To develop a finite element model of dynamically loading scaffold for the parametric analysis and quantification of physical stimuli being imposed on cells seeded within them.

Motivation

The successful creation of engineered cartilage is determined by a set of techniques that assess matrix production and construct functionality, which as would be expected, are determined by the cells, scaffolds and environmental factors used. Scaffold stiffness and permeability are the properties generally reported when assessing scaffold efficacy. And indeed, cells have been shown to respond to both these properties (103, 112), which are generally good indicators of a success. Unfortunately, with the recent increase in the use of mechanical loading devices, these properties play a more significant role in cell behavior. To begin to elucidate the effect of scaffold properties during the application of mechanical factors, finite element models are valuable to assess the physical environments created within the scaffolds during loading (121-123). These studies are looking to quantify specific levels of stimuli that are responsible for specific cell response. The studies have shown the presence of a gradient of stimuli within a scaffold, e.g. gradients of stimuli in the

radial direction when scaffolds are dynamically compressed. This results in gradients of matrix deposition by cells within the scaffold.

Approach

To quantify the physical stimuli present within dynamically compressing cell seeded scaffolds, a finite element model was developed in COMSOL multiphysics. Using principles from solid mechanics and flow through porous media, the model quantifies gradients of pressure, velocity, stresses and strains within cyclically straining scaffolds. These gradients can then be correlated to the behavior of cells within such scaffolds. Correlating specific physical stimuli to cell behavior gives a better understanding of the effects of particular stimuli on functional tissue production and metabolism, rather than scaffold mechanical properties, levels of strain, duty cycle or one of the other numerous factors that are currently used to define cell response.

Parametric analyses of 360 different combinations of scaffold modulus and permeability were examined to represent over 16 different scaffold material types. The analysis sought to quantify the physical stimuli present within the scaffolds when subjected to dynamic compression, and subsequently, sought to explain the variations in results reported in the literature for reportedly similar conditions.

Specific Aim III (Chapter 4):

To relate proteoglycan assembly by chondrocytes to ranges in physical stimuli present within engineered constructs due to dynamic loading.

To begin mapping the physical stimuli responsible for specific cell response to scaffold loading, this aim focused on quantifying the metabolic activity of chondrocytes encapsulated within varying scaffold compositions when subjected

different loading conditions and models. Using alginate as a model scaffold, bovine chondrocytes were encapsulated at a density of 25 million cells per ml and cultured for up to 2 weeks. The constructs were cultured under free swell, static or dynamic loading. As with the first aim, the metric for cell metabolism was the production, retention within the constructs and release to the surrounding medium, of glycosaminoglycans. Histological and immunohistochemical analysis were used to assess GAG and collagen and link protein localization, respectively.

To assess the physical stimuli present within the scaffolds being loaded, finite element analyses using the model developed in aim 2 were performed on tissue engineered cartilage. The stimulatory and inhibitory effects of the applied static and dynamic loading was assessed by normalizing the matrix content and aggregate modulus of constructs cultured under these conditions, to those cultured under free swell. Matrix production was correlated to mechanical integrity (i.e. GAG to aggregate modulus) and the amount of GAG within the constructs was compared to the levels of physical stimuli present within them during loading.

Specific Aim IV (Chapter 5):

Quantifies the differential behavior of mesenchymal stem cells when subjected to the same ranges in physical stimuli present during dynamic loading of engineered constructs.

To assess the differential response of MSCs to scaffold composition and dynamic loading, the studies carried out in this aim quantified MSC response to loading and hence, physical stimuli. The MSC seeded constructs were subjected to the same loading regimen imposed on the chondrocytes seeded constructs detailed above. The metric for cell metabolism was, once again, the production and retention of

glycosaminoglycans within the constructs and release to the surrounding medium. Histological and immunohistochemical analysis were used for GAG and collagen and link protein localization, respectively.

The physical stimuli present within the scaffolds, as assessed by finite element analyses, were then correlated to glycosaminoglycan assembly. The stimulatory and inhibitory effects of the applied static and dynamic loading was also assessed by normalizing the matrix content and aggregate modulus of constructs cultured under these conditions, to those cultured under free swell. Glycosaminoglycan production was correlated to aggregate modulus and the amounts of GAG retained within the gels were compared to the levels of physical stimuli present during loading.

CHAPTER 2

Effects of Seeding Density on Proteoglycan Assembly of Passaged Mesenchymal Stem Cells*

Abstract

Cartilage repair strategies have utilized a wide range of cell types at a similarly wide range of seeding densities, both of which may affect ECM assembly. In this study, we investigated the effects of cell type and seeding density on proteoglycan assembly and the associated mechanical properties of tissue engineered constructs. Bovine and equine articular chondrocytes (AC) and first (P1) and second passage (P2) equine mesenchymal stem cells (MSCs) were encapsulated into alginate disk gels at densities of 1-, 10-, 25-, & 50x10^6cells/ml for chondrocytes, and 25 x10^6cells/ml for P1-MSCs and 1-, 10-, & 25 x10^6cells/ml for P2-MSCs. Glycosaminoglycan content of the gels and surrounding media, as well as the resulting aggregate modulus of the disks was quantified at times up to 6 weeks. GAG accumulation was found to depend on cell type and density, and was observed to change with time. P1-MSCs produced the most total GAG (gel + media). Retention of GAG in gels was highest for bovine AC gels (which were used as a gold standard comparison), with equine MSCs retaining the least GAG. Although P1-MSCs were able to produce the largest amount of GAG, their ability to retain the produced GAG was very limited. This deficiency in retention by MSCs may be related to the lack of accumulation of link protein in MSC seeded gels. This is consistent with the lower amounts of GAG found in stem cell seeded gels by several studies, but also begins to elucidate metabolic patterns of MSCs. Future

* Babalola, O.M. and Bonassar, L.J. "Effects of Seeding Density on proteoglycan Assembly by Passaged Mesenchymal Stem Cells," Accepted for publication in February , 2010 in Cellular and Molecular Bioengineering.

studies in cartilage engineering utilizing MSCs should explore ways of enhancing GAG retention.

Introduction

Tissue engineering approaches have been investigated extensively as treatments for articular cartilage and osteochondral tissue injuries including chondral defects, avascular necrosis, and trauma related injuries (33, 124-126). Chondrocytes, the cells intrinsic to cartilage, have been the most common source used in cartilage tissue engineering to date, with bovine chondrocytes being the most studied species. Other species that have been studied include porcine (127), equine (109), ovine (128), canine and human (81). This variety of species has made direct comparisons difficult when trying to assess functional tissue regeneration in different animal models.

Due to the low density of these cells in cartilage tissue and the characteristic de-differentiation when expanded in monolayer (129-131), cells types other than primary chondrocytes have been investigated as a source for cartilage repair. Mesenchymal stem cells (MSCs), which have been shown to differentiate into cells of several lineages including chondrocytes, osteoblast and adipocytes (84, 86), show great promise as a potential cell type for the regeneration of articular cartilage tissue (84, 86, 132-134). Previous studies have shown a link between cell species (81), cell passage (80, 82) and seeding density (42) on chondrogenesis by chondrocytes. Unfortunately, less is known about the effects of these parameters on chondrogenically differentiated MSCs. Phenotypic similarities between chondrogenically differentiated MSCs and chondrocytes have not been fully characterized, especially with regards to extracellular matrix production and assembly.

Based on these observations, we developed the following hypotheses: 1) glycosaminoglycan (GAG) assembly differs between chondrogenically differentiated MSCs and chondrocytes; 2) that the difference in GAG assembly is a function of passage number and cell density; 3) these differences in ECM assembly will regulate the material properties (i.e. aggregate modulus) of cell laden constructs. To test these hypotheses, the objectives of this study were to quantify GAG production and retention by equine articular chondrocytes and chondrogenically differentiated MSCs and the resultant construct material properties. To put this study in the perspective of the gold standard of cells used by the field, a study on GAG assembly by bovine articular chondrocytes was conducted in parallel to these experiments.

Materials and methods (Fig. 2.1)

All materials were purchased from MediaTech Inc. unless otherwise noted.

Experimental Setup

Chondrocyte harvest and isolation

Equine and bovine articular chondrocytes (AC) were harvested using previously described protocols (96, 135). Briefly, articular cartilage tissue was harvested from the patellofemoral, scapulohumeral, and fetlock joints of an 11 month and 2 and a half year old horse within one hour of euthanasia. The harvested tissues were chopped into smaller pieces and digested overnight at 37°C and 5% CO_2 in Dulbecco's modified Eagle medium (DMEM) containing 0.3% collagenase (Worthington Biochemicals, Lakewood, NJ) and 100 U/mL penicillin G sodium, 100 μg/mL streptomycin sulfate, 25 μg/mL amphoterocin B. The digest solution was filtered with a 100 μm cell strainer and articular chondrocytes were isolated from the strained digest solution by centrifugation at 338 x g for 7 min. Cells were washed twice with Dulbecco's

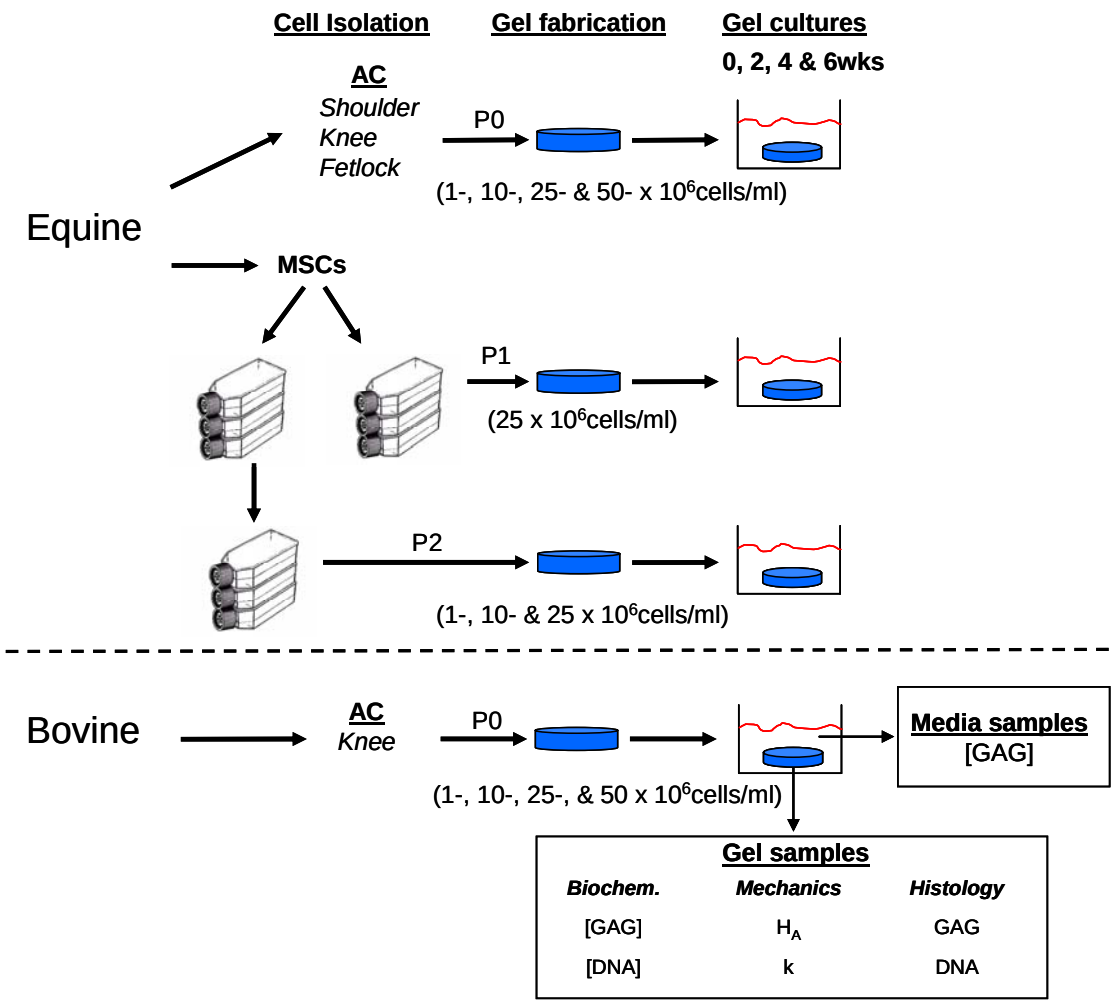

Figure 2.1: Schematic of experimental groups studied (AC = articular chondrocytes, P0 = primary articular chondrocytes, P1 = first passage MSCs and P2 = second passage MSCs). The studies were compared to a study on bovine ACs, the gold standard of cells used in cartilage tissue engineering.

phosphate-buffered saline (PBS) and viability was determined using trypan blue. Only cell solutions with viabilities of 85% or higher were used for these studies. Primary chondrocytes were seeded at densities of 1-, 10-, 25-, and 50 x 10^6 cells/ml in 6mm alginate disks as described below.

To establish a frame of reference for the many studies on cartilage tissue engineering that use bovine articular chondrocytes (33, 48, 125, 136), parallel cultures were performed using cells obtained from the patellofemoral grooves and femoral condyles of two joints from 1-3 day-old calves using the same techniques described above.

MSC harvest and isolation

Equine sternal MSCs were harvested and passaged using established protocols (79, 88). Bone marrow aspirates were obtained aseptically from the sternum of 11 month old to 2 year old horses within two hours of euthanasia. Aspirates were collected in 60 cc syringes containing 8 ml of 10,000 USP units of chilled heparin sodium solution (Baxter Healthcare corp., Deerfield, IL). Four to six 60cc syringes were obtained per animal. Under sterile conditions, 30 ml of aspirate was resuspended in 15 mls of PBS and centrifuged at 338 x g for 10 min to remove red blood cells. The cell pellet was resuspended in 30 ml of DMEM containing 4.5 g/L sodium pyruvate supplemented with 10% Fetalplex (Gemini Bioproducts, West Sacramento, CA), 100 μg/ml penicillin G sodium, 100 U/ml streptomycin sulfate, 25 μg/mL amphoterocin B, 4.5 g/L L-glutamine, 25 mM HEPES buffer (Sigma Aldrich, St. Louis, MO.) and 1 ng/ml basic fibroblast growth factor (PeproTech, Rocky Hill, NJ),) and plated in 175 cm^2 flasks at 5% CO_2, 95% humidity, and 37°C. Twenty-four hours after incubation, half the volume in each flask was transferred to a new flask and the media level was supplemented up to 30 ml/flask. The medium was changed twice a week until 80%

confluency was achieved to attain first passage cells (P1). Second passage cells (P2) were obtained by trypsinizing flasks containing 80% confluent P1 cells, replating the cells at a concentration of 10,000 cells/cm^2 in T-175cm^2 flasks and treated as above until they formed 80% confluent monolayer. Each flask yielded 6-8 million cells and the resulting monolayer cultures appeared homogeneous and morphologically resembled cells commonly described as MSCs (86). Some cell heterogeneity may have persisted, despite phenotypic similarities. Trypsinized cells (P1 and P2) were encapsulated in 6 mm alginate gel disks by injection molding as described below.

Gel formation

Two percent by weight (i.e. 20 mg/ml), steri-filtered, Pronova™ UPLVG (ultrapure, low viscosity, 67% guluronic acid, MW 160 kDa) alginate (FMC Biopolymers, Drammen, Norway) was crosslinked with sterilized 2 wt % calcium sulfate (Sigma Aldrich, St. Louis, MO.) using established injection molding techniques (79). Briefly, cell pellets were resuspended in sterile 20 mg/ml alginate in PBS and crosslinked with 2 mg/ml $CaSO_4$ in PBS at a 2:1 ratio. The crosslinked solution was molded into a 1 mm thick sheet, from which 6 mm diameter disks were acquired using a dermal biopsy punch. Isolated primary equine and bovine chondrocytes were seeded at densities of 1-, 10-, 25-, and 50 x 10^6 cells/ml in the alginate disks. P1-MSCs were seeded at a density of 25x10^6 cells/ml and P2-MSCs at densities of 1-, 10-, and 25 x 10^6 cells/ml.

Gel disk culture

Chondrocyte and MSC cells encapsulated in alginate gels disks were cultured in an incubator for 0, 2, 4, or 6 weeks at 5% CO_2, 95% humidity, and 37°C. Chondrocyte laden disks were cultured in DMEM containing 10% fetal bovine serum, 100 μg/ml penicillin, 100 U/ml streptomycin, and 50 μg/ml ascorbic acid. MSC seeded disks

were cultured in DMEM containing 4.5 g/L sodium pyruvate, 10% fetalplex, 100 μg/ml penicillin G sodium, 100 U/ml streptomycin sulfate, 25 μg/mL amphoterocin B, 4.5 g/L L-glutamine and 25 mM HEPES buffer and supplemented with 5 ng/ml transforming growth factor-beta (TGF-β1 – PeproTech, Rocky Hill, NJ). This media has been previously shown to be chondrogenic for equine MSCs as indicated by type II collagen and aggrecan expression (88) as well as significant matrix assembly in 3D culture (96). Disks harvested at the 0, 2, 4 and 6 week time points and used media samples (from media changes every three days) were stored at -80°C for further analysis.

Chondrogenesis analysis

Biochemical Analysis

A 1, 9-dimethylmethylene blue dye (Sigma) based assay (137) was used to quantify sulfated GAG content on papain digested disks and collected media samples. Gel samples were weighed upon removal from culture, lyophilized, and weighed again, before digestion in 1 ml of 0.125 mg/ml papain in phosphate buffer with EDTA at 60°C for 18hrs. Papain digests and frozen media samples were treated with 1 μl of a 10 unit alginate lyase (Sigma Aldrich, St. Louis, MO) solution in PBS, to further reduce the effect of cross reaction of DMB with macromolecular alginate. Both the collected media and disks were assayed for GAG content with serial dilutions of chondroitin-6-sulfate (Sigma) from shark cartilage in papain digest buffer (for gel samples) or medium (for collected media samples) used as standards, with DMB-GAG binding observed at 525 nm. DNA was quantified using a Hoechst 33258 dye based assay following standard protocol (138). Briefly, papain digested samples were reacted with Hoechst 33258 dye excited, at 358 nm and emission observed at 458 nm. Calf thymus DNA at serial dilutions were used as standards.

Mechanical Analysis

Confined compression tests were used to assess the mechanical integrity of the gels at the different time points according to established protocols (79, 96) (n=5-10 samples per condition). A uniaxial testing system (EnduraTec, Bose, IN) was used to determine the aggregate modulus. Harvested and frozen samples were thawed in 0.5 ml of an EDTA-free protease inhibitor cocktail (Sigma Aldrich, St. Louis, MO) in PBS solution in a 37°C water bath. Thawed samples were then placed in a confined compression chamber and loaded with a porous platen to 40% strain in sequential 50 μm increments, with relaxation loads recorded with each strain step. Constructs were allowed to relax to equilibrium (approx. 7mins) before the next strain step was imposed. The stress relaxation data was fit to a poroelastic model of material behavior that yielded the aggregate modulus (H_A) of the constructs (139, 140).

Histological Analysis

Samples reserved for histology (n = 5-6 samples per group) were fixed in 10% formalin supplemented with 1% calcium sulfate to help maintain gel integrity. Samples were then dehydrated in increasing concentrations of ethanol to 100% ethanol and cleared in 3 changes of Xylene, before being embedded in paraffin, sectioned (5μm thick slices), and mounted onto slides. Sections were stained with Safranin O (0.1% in DI water) for glycosaminoglycan deposition and localization, and Hematoxylin and eosin (H&E) for nuclei and general matrix distribution. Samples with the highest GAG retention from each group, as indicated by biochemical analysis, were immunohistochemically analyzed for link protein. Briefly, rehydrated sections were predigested with a 300U/ml hyaluronidase solution (Sigma Aldrich, St. Louis, MO) for 30mins at 37°C for epitope recovery. Sections were then rinsed in three changes of phosphate buffered solution at room temperature for 5mins each and

analysis of link protein was performed using a Diaminobenzidine histochemistry kit with streptavidin-horseradish peroxidase (Invitrogen Corp., Carlsbad, CA), in accordance with the manufacturer's protocol. Mouse monoclonal antibodies to link protein (Hybridoma Bank, University of Iowa, Iowa City, IA) were used. Sections samples of bovine articular cartilage tissue were treated as above and used as positive controls. Slides were imaged using a Spot Jr Digital camera attached to an inverted Nikon TS 200 microscope (MicroVideo Instruments, Avon, MA), and photomicrographs were obtained of stained regions. Some H&E stained slides were also used to assess cell density. To do this, sample micrographs of five areas per slide were taken and assessed for cell density per area. Image J (NIH Bethesda, MD) was used to analyze the total number of cells per image after threshold and size exclusion analysis. Similarly, the number of cells with pericellular staining for link protein was analyzed with this process.

Statistical analysis

Data in all graphs were recorded as means +/- standard deviation of 5 to 10 samples/group. Statistical comparisons of μg GAG/mg ww, H_A and cell density between all groups were performed on the data from all groups using two way analysis of variance (ANOVA) with mixed procedure analysis ($p<0.001$) in SAS 9.1 (Cary, NC). The mixed procedure analysis uses standard linear models that allow for both fixed and random effects. This approach was utilized due to the non-normal and unbalanced nature of our data set. Tukey's HSD post hoc test was used for all pairwise comparisons ($p<0.05$).

Results

Glycosaminoglycan assembly

To calculate the average total GAG produced (media + gel) per disk, the average GAG content within disks at each time point was summed with the average cumulative GAG released to the surrounding medium by the disks by that time point. Total GAG production was found to vary with cell type, density and culture time (Fig. 2.2), with all groups showing increase in production with time. At lower cell densities (1- & 10 x 10^6 cells/ml), equine AC seeded disks produced more GAG than either bovine ACs or MSCs. Disks seeded with P2 MSCs at the lower densities had similar average amounts of total GAG. In gels seeded at 25 x 10^6 cells/ml GAG production by MSCs depended on MSC passage number, with the highest production seen in P1-MSCs gels at 6 weeks (~125 μg) and equine and bovine ACs having similar values of GAG by day 42. Bovine AC at 50 x 10^6 cells/ml showed the highest GAG production (~172 μg) and no difference was observed in P2 MSCs with increasing cell density. The GAG content in the gels varied with cell species, type, and density ($p<0.05$, mixed mode ANOVA, Fig. 2.3). Gels seeded with ACs had higher GAG content than those seeded with MSCs. Gels seeded with bovine ACs had higher GAG content than those seeded with equine ACs, particularly at higher seeding densities and longer culture times. Both bovine and equine ACs seeded gels at 10 x 10^6 cells/ml showed a significant increase in GAG content after 2 weeks ($p <0.05$). In contrast to chondrocyte seeded gels, only equine P2-MSCs seeded gels at 1 x 10^6 cells/ml gels showed a significant increase in GAG content ($p<0.05$) by the 6 week time points when compared to their 0 week value, with all other densities and P1-MSCs showing no significant increase in gel GAG content.

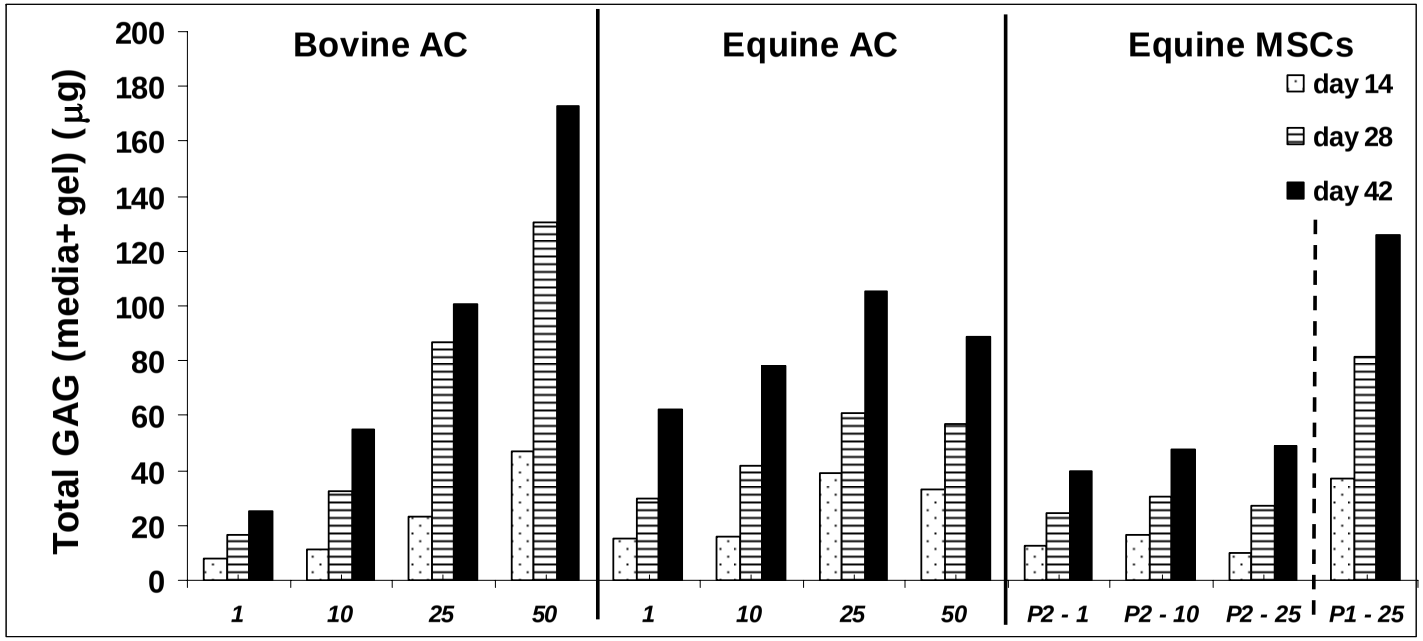

Figure 2.2: Average total GAG produced as a function of species, density and passage (n = 6–9). Samples seeded with bovine articular chondrocytes are represented as "Bovine AC", equine articular chondrocytes as "Equine AC", equine passage 1 MSC as "P1" and equine passage 2 MSC as "P2".

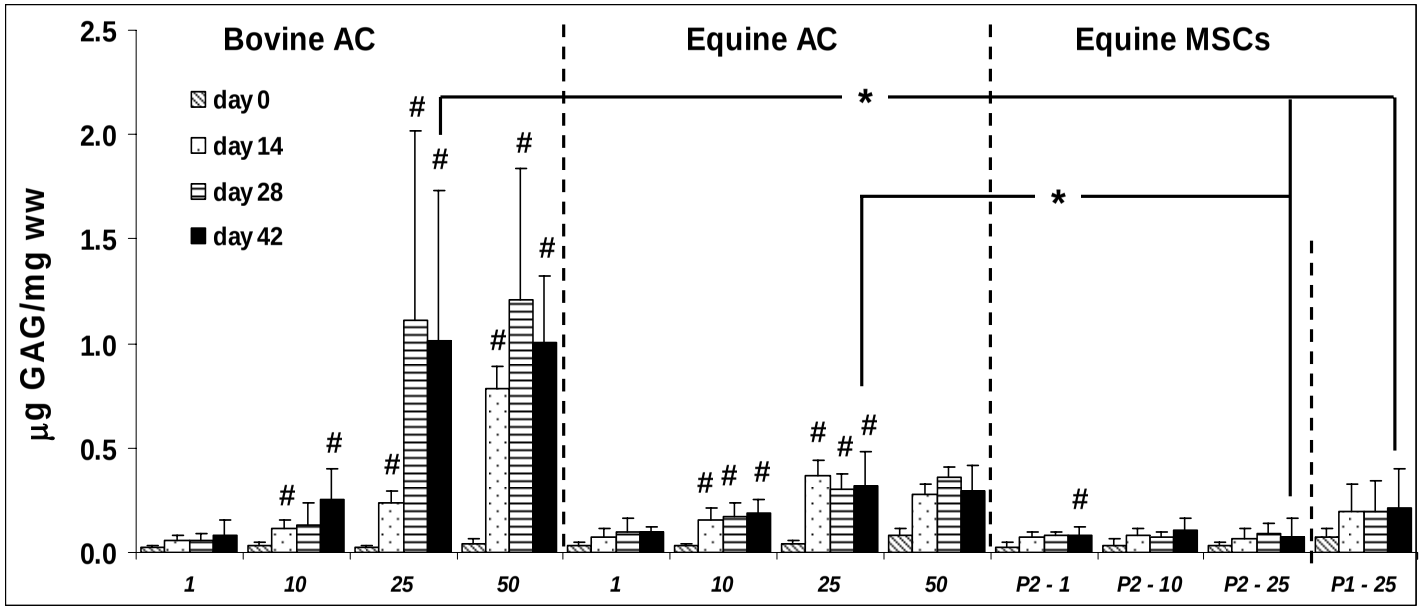

Figure 2.3: Average concentration of GAG in gels normalized to wet weight for bovine and equine AC and equine MSCs (n = 7–9 ± st. dev.). # indicates significant difference from 0 week values of P2-MSCs at 1 x 10^6 cells/ml, equine and bovine AC both at 10-, 25- and 50 x 10^6 cells/ml. * indicates significant differences between bovine AC and both P1 and P2-MSCs, and equine AC and P2-MSCs all at 25 x 10^6 cells/ml at 6 weeks (all $p < 0.05$). † indicates significant difference between equine and bovine AC at 50 x 10^6 cells/ml at 6 weeks ($p < 0.05$).

Comparison of GAG content in gels across cell types and species showed no difference amongst all groups at 6 weeks for the gels seeded at 1- or 10 x 10^6 cells/ml ($p>0.32$). Within the group of gels seeded at 25 x 10^6 cells/ml, bovine ACs were found to be significantly higher than both P1- and P2 MSC seeded gels ($p = 0.018$ and $p < 0.0001$, respectively) and equine ACs, significantly higher than only P2-MSCs ($p = 0.0002$) by 6 weeks. No difference was found either between P1- and P2-MSCs seeded gels ($p = 0.12$) or bovine and equine ACs seeded gels ($p = 0.64$) at 25 x 10^6 cells/ml at 6 weeks. Bovine and equine AC seeded at 50 x 10^6 cells/ml both showed a significant increase in GAG content by 6 weeks when compared to 0 week, and were also significantly different from each other at throughout the culture period (all $p < 0.05$).

Analysis of GAG loss to the surrounding medium showed bovine ACs at 50 x 10^6 cells/ml released the largest amounts (140 μg) by day 42 (data not shown). For cells seeded at 1-, 10-, and 25 x 10^6 cells/ml, equine cells (ACs and MSCs) released more GAG to their surrounding medium than bovine cells, with the equine ACs releasing the most at lower densities and P1-25 MSCs releasing the most amongst all gels seeded at 25 x 10^6 cells/ml. Cumulative loss to media increased with time, with bovine ACs at 50 x 10^6 cells/ml displaying the highest rate of release, at 3.0 μg GAG/day, followed by P1-MSCs at 25 x 10^6 cells/ml releasing at a rate of 2.6 μg GAG/day.

GAG retention (percent GAG in disk / total GAG) depended on both species and cell density, with equine MSCs (P1 and P2) retaining the least amount at lower cell densities (Fig. 2.4). In all groups studied, with the exception of bovine ACs seeded gels at 25 x 10^6 cells/ml, GAG retention either stayed the same (Bovine ACs at 1- and 10 x 10^6 cells/ml) or decreased with time (all other groups). Retention ranged from as little as 4% in 1 x 10^6 cells/ml equine AC and P2-25 equine MSCs gels at 6

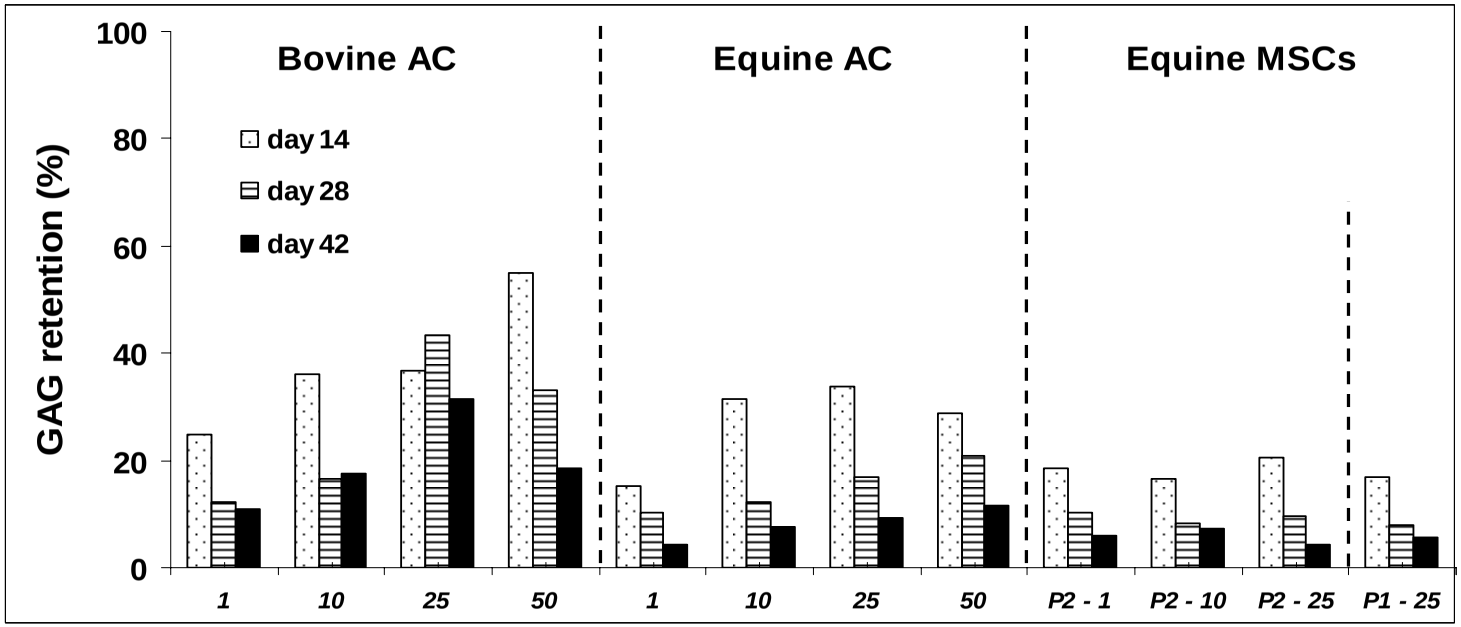

Figure 2.4: Percentage of GAG retained (GAG in disks/total GAG) for bovine AC, equine AC and equine MSCs. GAG in disks was summed for n = 7–9 samples and compared to GAG lost from disks in pooled media.

weeks, to as high as 55% in 25 x 10^6 cells/ml bovine chondrocyte gels at 2 weeks. No difference was found between equine ACs and passaged MSCs.

Mechanical analysis

Confined compression analysis of samples harvested at 0, 2, 4, and 6 weeks showed large variations in aggregate modulus over time, especially with bovine chondrocyte seeded gels (Fig. 2.5). Although increasing trends in aggregate modulus with time in culture were seen for certain groups (e.g. bovine ACs at 25 x 10^6 cells/ml and P2-MSCs at 1- and 10 x 10^6 cells/ml) there was no significant difference in aggregate modulus with time for all cell species, type, passage and density studied. Comparisons of all groups at the 6 week time point showed a significant difference between bovine and equine AC gels seeded at 10 x 10^6 cells/ml ($p = 0.011$) and 25 x 10^6 cells/ml ($p = 0.013$), and between equine AC and P1-MSCs ($p = 0.03$) and P2-MSC ($p = 0.024$) gels seeded at 25 x 10^6 cells/ml.

Histological analysis

Hematoxylin and eosin stains of the gels showed evenly seeded gels at 0wks for all groups studied, but a decrease in cellularity by 6 weeks (Fig. 2.6). Quantification of cell density revealed a significant decrease from 0 to 4 weeks for P2-MSCs seeded at 10 x 10^6 cells/ml ($p = 0.004$), decrease between 0 and 2, 4 and 6 weeks for P1-MSCs seeded at 25 x 10^6 cells/ml ($p < 0.04$) and a decrease between 0 week and 2 and 4 weeks, as well as between 2 and 4 week samples for P2-MSCs seeded at 25 x 10^6 cells/ml ($p < 0.05$) (Fig. 2.7).

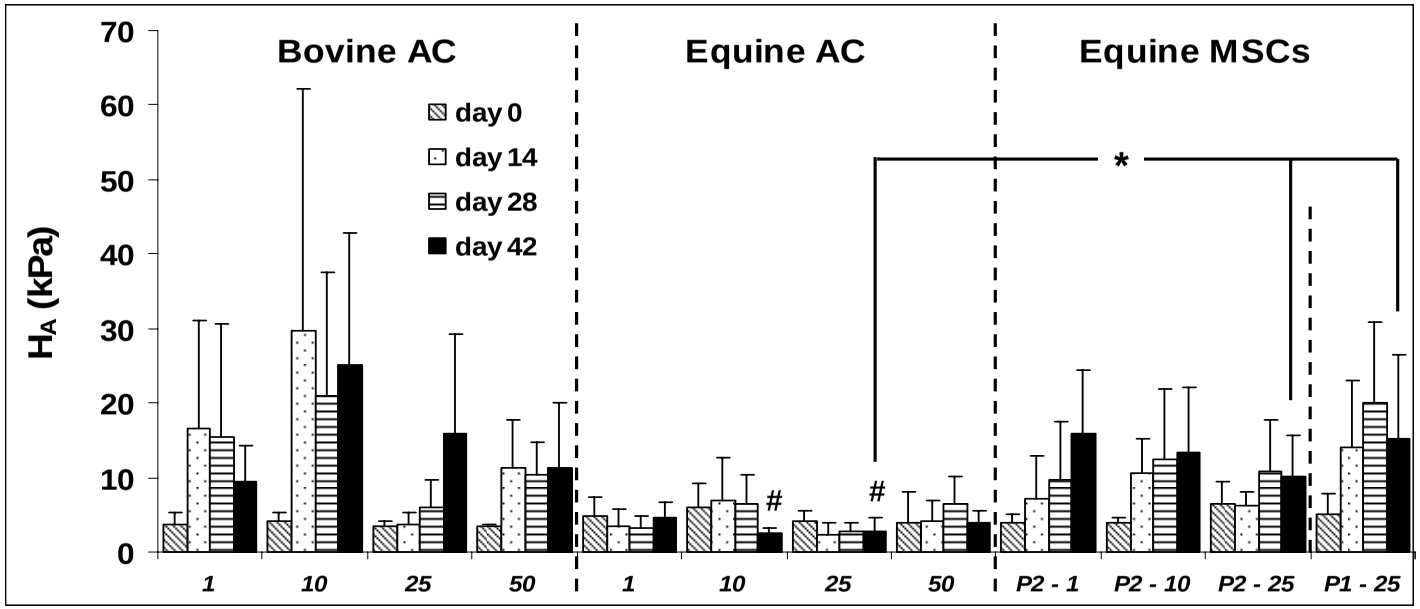

Figure 2.5: Aggregate moduli (kPa ± st. dev.) of gels per time point (n = 5–10). * indicates significant difference between 6wk bovine AC and equine AC gels at 25 x 10^6 cells/ml and between equine AC and both P1 and P2 MSCs seeded gels at 25 x 10^6 cells/ml, also at 6wks.

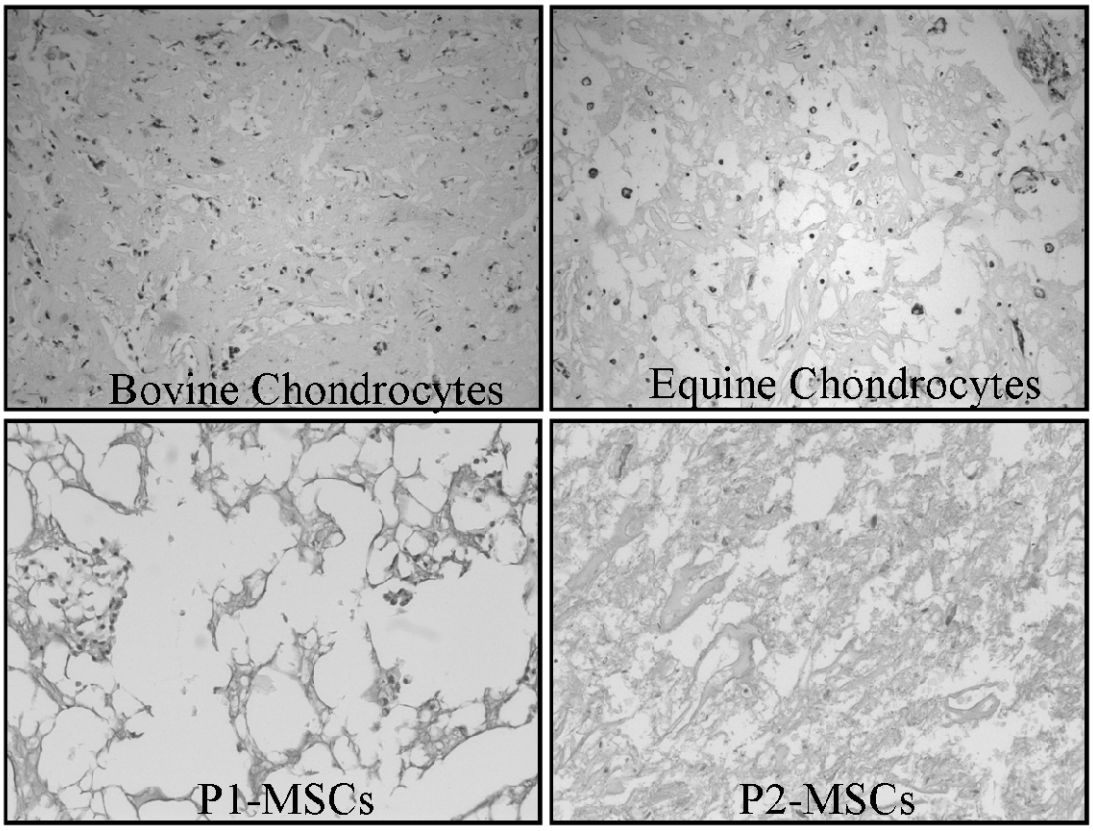

Figure 2.6: Grayscale sample images of histological samples stained with Hematoxylin and eosin at 6 weeks (images at 100x magnification).

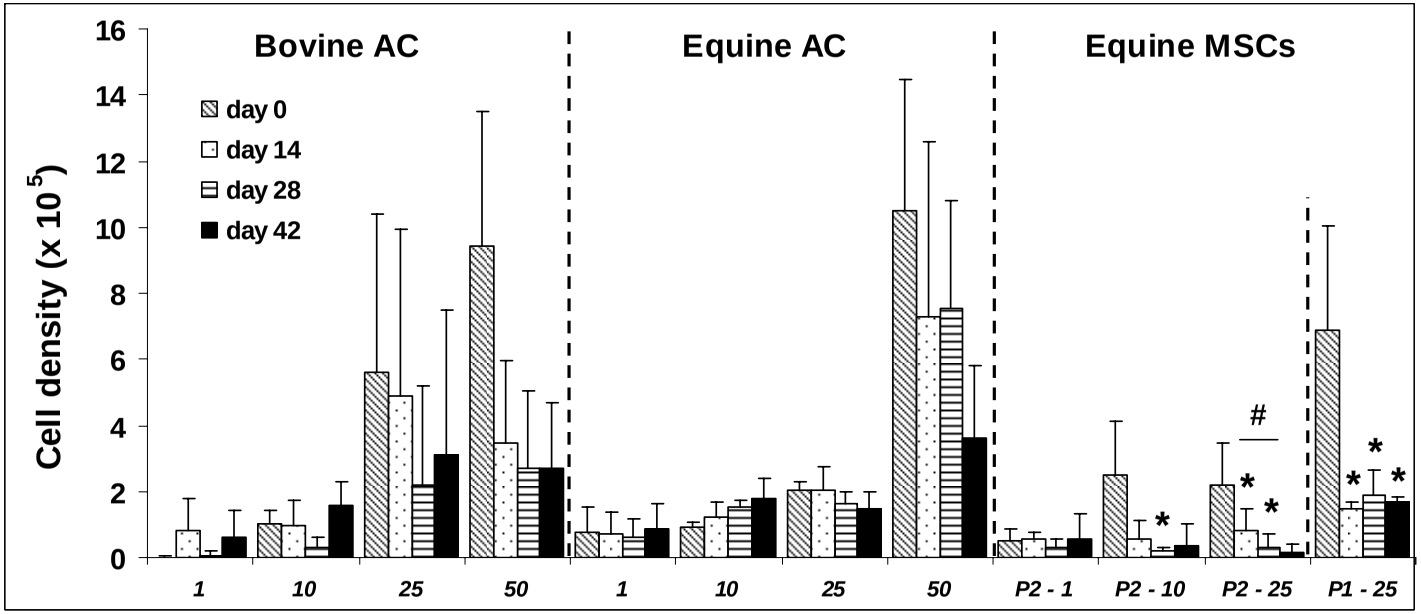

Figure 2.7: Average number of cells/disk per time point (± st. dev.) # indicates significant differences between 0 and 6wk values for P1- and P2-MSC samples at 25 x 10^6 cells/ml ($p = 0.03$ and $p = 0.022$, respectively).

Immunohistochemical analysis demonstrated the presence of link protein in both equine and bovine chondrocyte seeded gels, but not MSC seeded gels (Fig. 2.8, micrographs). Link protein was localized to regions surrounding cells or clusters of cells, with immunostaining being intense in these areas. Quantitative analysis showed bovine and equine chondrocytes having significantly higher fraction of cells stained for link protein when compared to either P1 or P2-MSCs ($p<0.05$) (Fig. 2.8, plot). There was no difference in percent of cells stained between bovine and equine chondrocyte or between P1 and P2-MSC seeded gels ($p>0.05$).

Discussion

This study demonstrated that GAG assembly by chondrocytes depends on cell density and is different between chondrocytes and chondrogenically differentiated MSCs. GAG retention increased with seeding density and was higher in chondrocytes than chondrogenically stimulated MSCs. In contrast, chondrogenically differentiated first passage MSCs produced the largest amount that was mostly lost to the surrounding culture medium. GAG production and retention by equine chondrocytes and MSCs were lower than that of the bovine chondrocytes, the cell type most commonly used to study cartilage matrix assembly.

Passage two MSCs gels seeded at $1x10^6$/ml were the only group to show significant increase in GAG content, which may be a statistical aberration. The GAG content of these gels at 0wk was smaller than that of MSC samples seeded at either 10 or $25x10^6$/ml, although not statistically different ($p=0.3733$ and $p=0.9568$, respectively). This smaller amount in the $1x10^6$/ml seeded gels at 0wk, when compared to the 6wk samples resulted in the significant difference in GAG content.

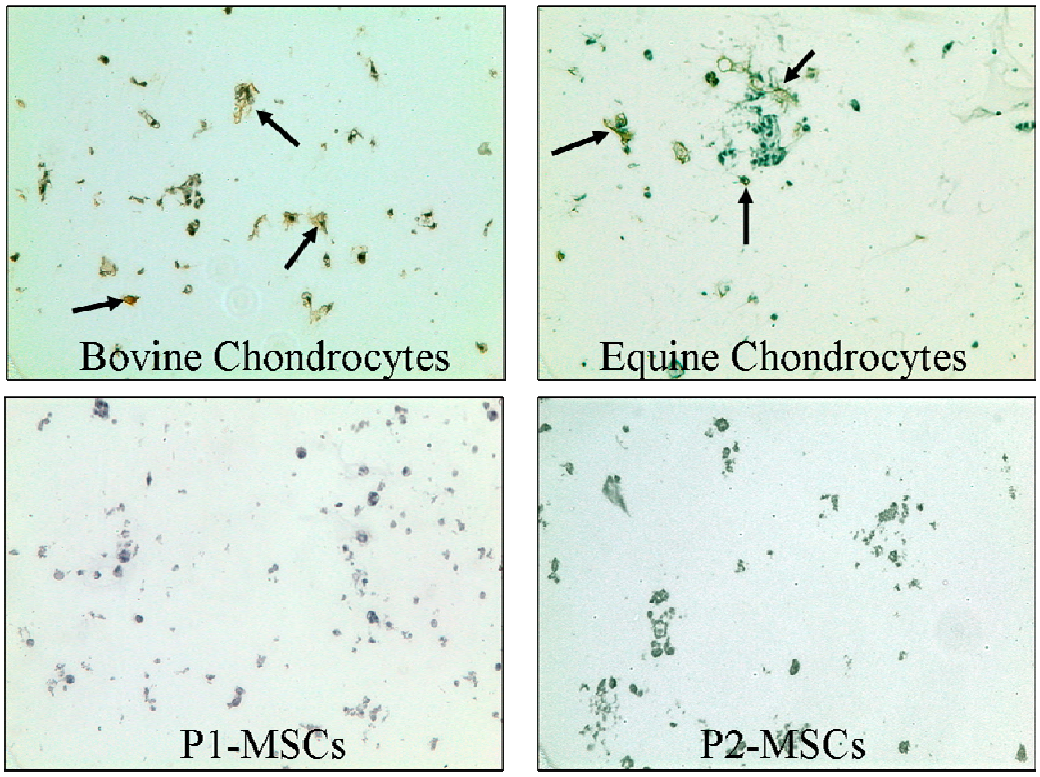

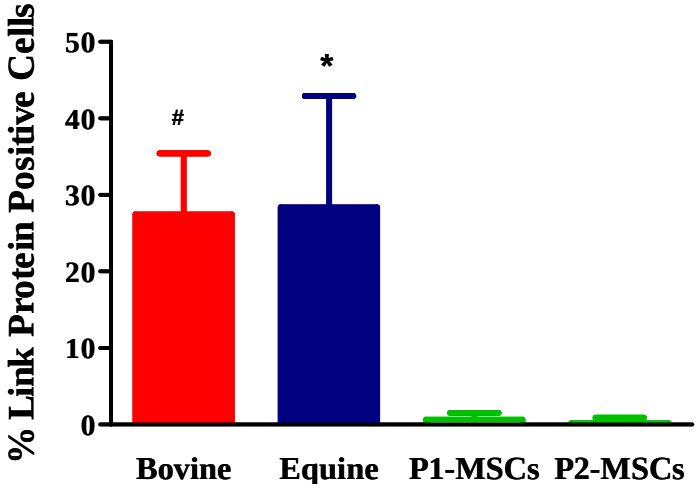

Figure 2.8: Sample images of gels analyzed for link protein localization (arrows) using IHC within gels at 6wks (images at 200x) and average percent (± st. dev.) of cells stained positive for link protein (n=10). * and # indicates significant difference between bovine or equine samples and both P1 and P2-MSC samples.

We can only postulate that the GAG content within any of the gels at 0wks correlates to cell density.

The fraction of synthesized GAG retained by MSCs was strikingly low, dropping from <20% at 2 weeks to <10% at 6 weeks. This lack of retention may be attributed to either the absence of other ECM components (e.g. link protein or hyaluronan) necessary to build proteoglycan aggregates or a high level of activity of proteases (e.g. MMPs, ADAMTS) that degrade proteoglycans. Higher GAG retention during early culture times followed by less retention at later times also may collectively suggest that high protease activity could be the cause of the low retention rates observed in this study. The deficiency in MSCs to retain cartilage-specific matrix components was also noted previously in a study (96) in which MSCs produced more but retained less lubricin than articular cartilage.

Collectively, these studies underscore the complexity of the process of ECM assembly in tissue engineered cartilage. For functional tissue assembly to occur, proteoglycans must be expressed, synthesized and secreted, then must stably aggregate. In this study, tracking the factors that relate only to proteoglycan production (e.g. aggrecan mRNA or ^{35}S incorporation) would have lead to the false conclusion that proteoglycan assembly was similar between AC and MSC. Alternatively, tracking only GAG accumulation in gels might have lead to the incorrect conclusion that proteoglycan production by MSCs was dramatically lower than AC. As such, this study has highlighted a key deficit in the ability of MSCs to assemble and retain proteoglycan.

This study showed a 2.5 – 7 fold increase in the average modulus of bovine chondrocyte seeded gels with time. Although statistically significant only at 6 weeks, these increases are consistent with the magnitude in changes observed in other studies. For examples, bovine chondrocyte seeded alginate gels have been reported to have an

aggregate modulus of either 30kPa (96), 1kPa (43) or 20kPa (141) by 6wks. This range in aggregate modulus is similar to the range found in our study (2-25kPa). Although no obvious signs of degradation were observed, this cannot be dismissed as a possibility that may affect GAG retention. If degradation affected retention more than expected, it would have affected all conditions similarly, and hence the conclusion of this study still remains the same.

This study found that the effect of increasing cell density was more prominent in AC seeded gels, with an increase from 10- to 25 x 10^6 cells/ml yielding a 2 - 4 fold increase in gel GAG content. An increase from 25- to 50 x 10^6 cells/ml, on the other hand, had no effect, indicating that a plateau exists after which increasing cell density has no effect. The effects of cell density on chondrocyte matrix assembly have been studied more extensively (120, 129, 142-145) than for chondrogenically differentiated stem cells. The lack of information on the effect of seeding density on stem cell cartilage tissue formation is especially prominent with respect to three dimensional cultures. Cell density has been shown to be a variable both in previous studies (120, 143), with differences seen with both cell type and species, as well as this study. As expected, gels seeded at higher densities produce more GAG, however, GAG retention was similar for gels seeded at 25-, and 50 x 10^6cells/ml, showing no benefit in doubling the initial seeding density. Although the bovine cells used in this study were neonatal and the equine cells used where from older but still skeletally immature animals, Tran-Khanh et al have shown that little difference exists between the metabolic capacity of bovine AC across this age range (146). This is also supported by both the chondrogenically differentiated equine MSCs and chondrocytes producing higher amount of GAG (gel + media) than the bovine chondrocytes (gels seeded at 25 x 10^6 cells/ml). However, the difference in the ability of MSCs and primary cells to retain synthesized proteoglycans may be age dependent.

This study reports important differences in how chondrocytes and differentiated passaged MSCs synthesize and assemble proteoglycan. First passage MSCs were found to be the most metabolically active cell type, producing the most amounts of GAG, but had one of the lowest retention rates. This is consistent with previous findings (80), where decreases in collagen type II and aggrecan gene expression were seen to occur as early as the first passage of the cells and with the decrease in production increasing with cell passage. These findings suggest that although earlier passage MSCs have the ability to produce a sufficient amount of GAG, they lack the ability to make a functional matrix. The deficiency of MSCs in proteoglycan assembly may be linked to their inability to make or retain link protein (Fig. 9). In addition, poor matrix assembly by MSCs may also be due to higher than normal enzymatic activity during matrix remodeling.

This study also demonstrated that the most biosynthetically active cells do not necessarily have the most functional matrix, as evident by the higher ranges of aggregate moduli within the bovine chondrocyte groups and the low ranges within the equine chondrocyte groups studied. Further studies will seek to further investigate the mechanism of GAG loss from the gels in order to determine whether loss to media is due to a lack of link protein production or aggregation due to lack of hyaluronan. In an effort to begin to address this lack of retention, a recent study by Nicodemus et al showed scaffolds functionalized with link protein successfully serving as anchors which increased retention of ECM molecules made by cells encapsulated within the scaffold (147). As such, this study and our data presented here points to optimizing proteoglycan retention as an important area of study for the advancement of MSC-based cartilage tissue engineering.

CHAPTER 3

Parametric Finite Element Analysis of Physical Stimuli Resulting from Mechanical Stimulation of Tissue Engineered Cartilage*

Abstract

Background: While mechanical stimulation of cells seeded within scaffolds is widely thought to be beneficial, the amount of benefit observed is highly variable between experimental systems. Although studies have investigated specific experimental loading protocols thought to be advantageous for cartilage growth, less is known about the physical stimuli (e.g. pressures, velocities, and local strains) cells experience during these experiments. This study used results of a literature survey, which looked for patterns in the efficacy of mechanical stimulation of chondrocyte seeded scaffolds, to inform the modeling of spatial patterns of physical stimuli present in mechanically stimulated constructs.

Method of approach: The literature survey revealed a large variation in conditions used in mechanical loading studies, with a peak to peak strain of 10% (i.e. the maximum amount of deformation experienced by the scaffold) at 1Hz on agarose scaffolds being the most frequently studied parameters and scaffold. This loading frequency was then used as the basis for simulation in the finite element analyses. 2D axisymmetric FE models of 2mm x 4mm scaffolds with 360 modulus/permeability combinations were constructed using COMSOL multiphysics software. A time dependant coupled pore pressure/effective stress analysis was used to model

* Babalola, O.M. and Bonassar, L.J. "Parametric Finite Element Analysis of Physical Stimuli Resulting from Mechanical Stimulation of Tissue Engineered Cartilage," J Biomech Eng, June 2009, vol. 131(6): 061014

fluid/solid interactions in the scaffolds upon loading. Loading was simulated using an impermeable, frictionless loader on the top boundary with fluid and solid displacement confined to the radial axis.

Results: As expected, all scaffold materials exhibited classic poroelastic behavior; having pressurized cores with low fluid flow and edges with high radial fluid velocities. Under the simulation parameters of this study, PEG scaffolds had the highest pressure and radial fluid velocity, but also the lowest shear stress and radial strain. Chitosan and KLD-12 simulated scaffold materials had the lowest radial strains and fluid velocities, with collagen scaffolds having the lowest pressures. Parametric analysis showed maximum peak pressures within the scaffold to be more dependent on scaffold modulus than on permeability, and velocities to depend on both scaffold properties similarly. The dependence of radial strain on permeability or modulus was more complex: maximum strains occurred at lower permeabilities and moduli, and the lowest strain at the stiffest, most permeable scaffold. Shear stresses within all scaffolds were negligible.

Conclusions: These results give insight into the large variations in metabolic response seen in studies involving mechanical stimulation of cell-seeded constructs, where the same loading conditions produce very different results due to the differences in material properties.

Introduction

The avascular nature of cartilage results in its limited ability to repair itself after injury. As a result, numerous approaches have been investigated as potential therapies, including tissue engineering strategies. Due to the low density of chondrocytes and the characteristic de-differentiation of the cells when expanded in monolayer (130), other cell types are being investigated for cartilage repair. In particular, mesenchymal stem cells (MSCs), which have been shown to differentiate into cells of several lineages including chondrocytes, osteoblasts and adipocytes (86), have been investigated as a potential source for cartilage repair (132, 133).

In an effort to augment such regeneration, several studies point to the importance of mechanical forces on the development and maintenance of the musculoskeletal system (55, 57, 62, 148). Muscle contraction during skeletogenesis has been found to be necessary for proper joint cavitation (55, 57) and lack of continuous skeletal loading has been associated with bone resorption (148, 149) and cartilage degradation (21, 150, 151). Previous mechanobiology and tissue engineering studies focused primarily on relating operational variables (e.g. strain, frequency) to cell and tissue scale outcomes. As such, experimental studies on cartilage tissue engineering incorporate different modes of mechanical stimulation in an attempt to mimic the events observed in skeletal development during embryogenesis (54-56). In addition to the different loading parameters used in these mechanical stimulation studies (strains ranging from 1.4 to 40%, frequencies from 0.01 to 3 Hz and various combinations of duty cycles), a variety of scaffold materials have been used to deliver cells in vitro and in vivo. The combination of large numbers of loading conditions and scaffold materials resulted in large variations in the metabolic response of cells seeded within the scaffolds. Although these studies have attempted to determine the loading conditions that are most advantageous for cartilage tissue growth, less is known about

the physical environment (e.g. pressures, velocities, local strains) that cells experience as a result of particular loading regimens imposed on these scaffolds. These studies have generally related loading strains and frequencies to cell activity or tissue development (Fig. 3.1). In actuality, the mechanical environment sensed by seeded cells under loading will not only depend on the mechanical loading conditions, but also on the material properties of the scaffold. It is likely that the resultant pressures, fluid velocities, strains and shear stresses are important regulatory factors for controlling differentiation and extracellular matrix biosynthesis. In a study by Kim et al. (152), physical stimuli gradients (fluid velocity and streaming potential) due to dynamic compression of cartilage disks was correlated to proteoglycan synthesis. Proteoglycan synthesis increased with dynamic loading, but markedly so at the outer 0.5mm region of their 1.5mm radius disks. The study also suggested that the stimulation of chondrocyte biosynthesis by dynamic compression is primarily related to changes in fluid flow and streaming potential, which would be more drastic at the outer radius of such geometries. The current work used dynamic loading variables in combination with scaffold material properties to predict the local mechanical environment that gives rise to cell and tissue scale responses.

To understand the effect of scaffold properties and loading conditions on a variety of cells undergoing mechanical stimulation, finite element models have been utilized as assessment tools to investigate the magnitudes of stresses, pressures and fluid velocities the cells may experience during loading (122, 123, 153, 154).
We conducted a comprehensive literature review that revealed a large variation in loading parameters used in mechanical loading studies (Fig. 3.2), with a peak to peak strain of 10% and frequency of 1Hz being the most utilized and studied parameters. With agarose hydrogels found to be the most studied scaffold materials, sinusoidal peak strains reported in literature ranged from 1.4 to 40%, with frequencies ranging

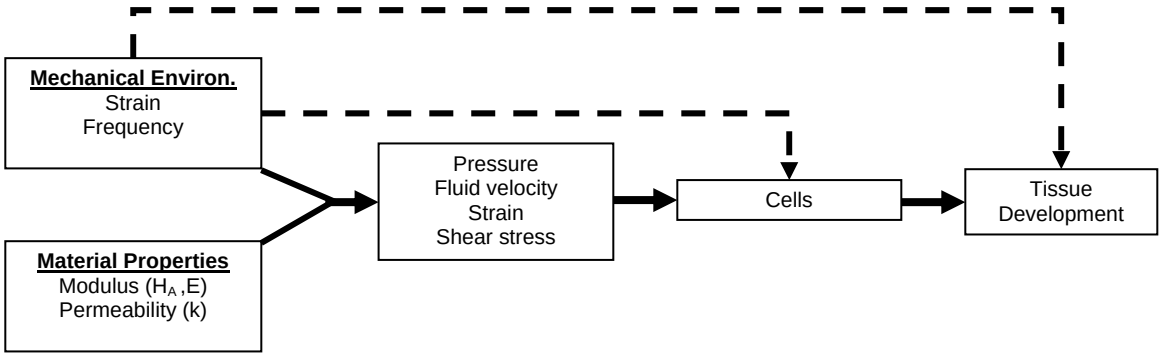

Figure 3.1: Flow chart of experimental approaches used to study mechanical influences on cartilage or chondrocyte metabolism.

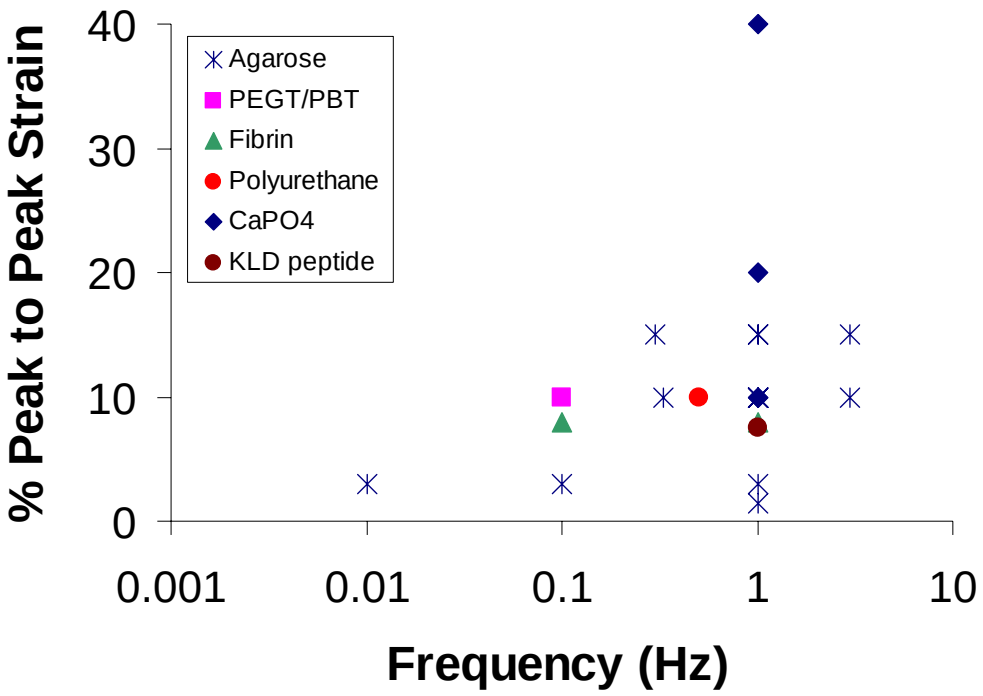

Figure 3.2: Results of the survey of the strain amplitudes and frequencies used for the cyclic axial compression of chondrocytes-seeded scaffolds displaying the wide range of strains and frequencies studied to date.

from 0.01 to 3Hz. Therefore, to analyze the stimuli within various dynamically loaded scaffolds, an estimate of the mechanical environment resulting from an applied uniaxial unconfined sinusoidal compressive strain with a 5% offset and 5% strain amplitude at frequency of 1 Hz was performed.

Analysis of the efficacy of loading parameters on GAG synthesis showed large variations, even for a particular strain or frequency studied (Fig. 3.3). GAG synthesis was found to range from an 11 fold decrease to a 4 fold increase due to loading frequencies spanning across 4 orders of magnitude (Fig. 3.3a) and % peak to peak strain across an order of magnitude (Fig. 3.3b). Variable effects on GAG synthesis were also found in studies using scaffolds with similar materials properties (Fig. 3.4), e.g. studies using agarose hydrogels demonstrated GAG synthesis ranging from a 60% decrease to a 350% increase when compared to controls.

Given the large variation in cell response to mechanical loading, the objective of this study was to use the results of the survey reported above to inform a finite element (FE) modeling study examining the effects of physical stimuli present within cyclically compressed typical scaffold materials used in cartilage tissue engineering. This study sought to elucidate some of the factors that may play a role in cell response to loading by estimating the magnitudes of pressures, shear stresses and fluid velocities that may exist within scaffolds used for tissue regeneration.

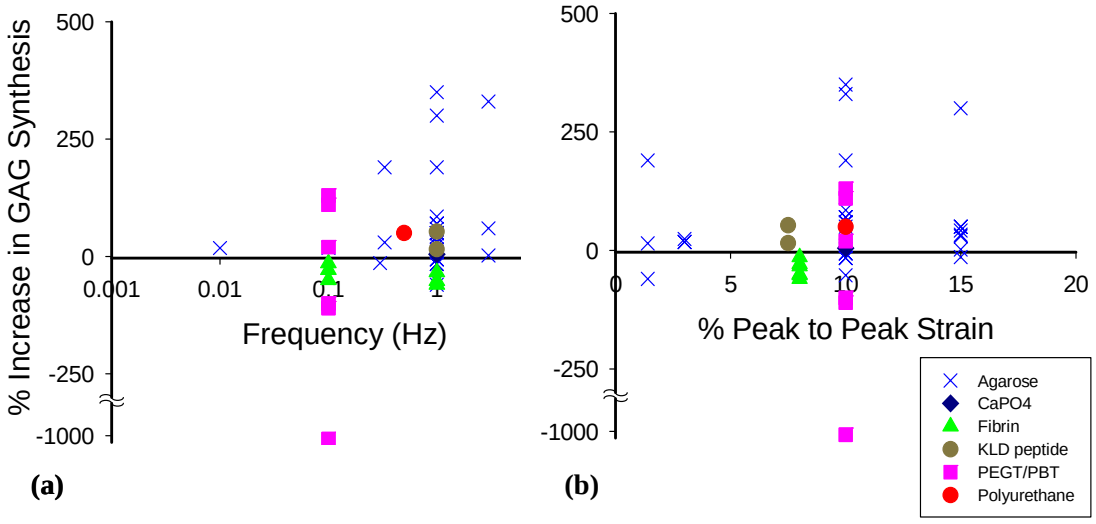

Figure 3.3: Compilation of the data from surveyed studies demonstrating the effect of loading parameters (frequency (a) and % peak to peak strain (b)) on glycosaminoglycan (GAG) synthesis.

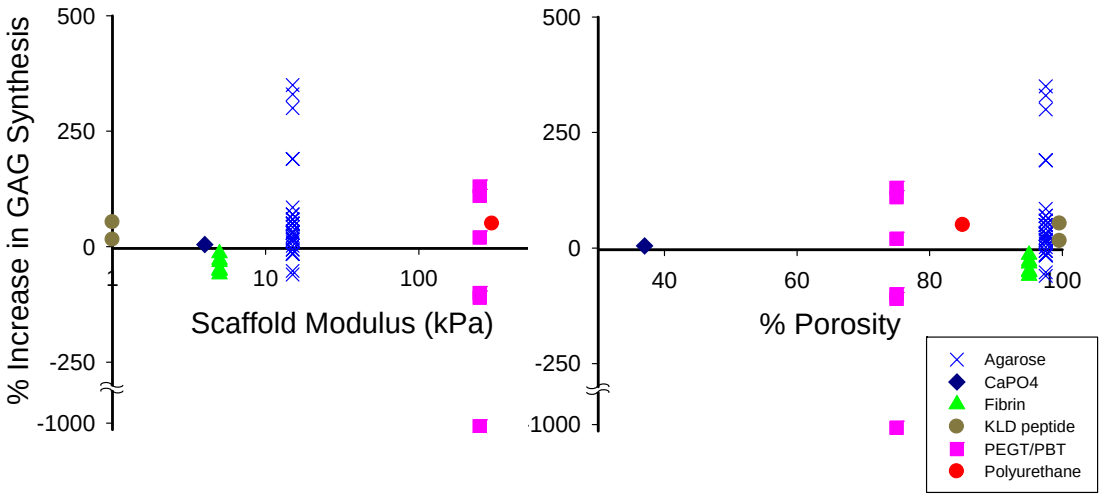

Figure 3.4: Compilation of the data from surveyed studies demonstrating the effect of loading parameters (scaffold modulus (a) and % porosity (b)) on glycosaminoglycan (GAG) synthesis.

Methods

Finite element analysis of loading scaffolds (Fig. 3.5)

A finite element models of scaffolds undergoing uniaxial unconfined compression were created using COMSOL multiphysics software (Burlington, MA). The models were of a two dimensional axisymmetric scaffolds and contained 320 quadrilateral elements each that were exponentially biased to the edges and yielded a total of 3063 degrees of freedom. The scaffold materials were assumed to be homogenous and isotropic with strain dependent permeability. All scaffolds were assumed to be 98% porous with Poisson's ratio of 0.167 and average solid density of 1240 Kg/m^3 (155-158). The scaffolds were simulated to be fully hydrated with the fluid having an assumed viscosity of 0.001 Pa·s and density of 1000 Kg/m^3.

Finite element model formulation

To model fluid/solid interactions in the loading scaffolds, a time dependent coupled pore pressure/effective stress analysis (121, 159) was implemented using the structural mechanics and chemical engineering modules of COMSOL multiphysics software package (COMSOL, Burlington, MA). Darcy's law in the chemical engineering module (Eq. 1 and 2) and solid mechanics governing equations in the structural mechanics module (Eq. 3) were used. The governing equation for steady-state Darcy flow was set to depend on fluid density ρ_f, solid fraction θ_s, and fluid velocity v; the latter which was dependent on the solid permeability κ, fluid viscosity η and pressure gradient ∇p. The equations are

$$\frac{\partial}{\partial t}\left(\rho_f \theta_s\right) + \nabla \bullet \rho_f v = \rho_f F, \quad (1)$$

$$v = -\frac{\kappa}{\eta}\left(\nabla p\right), \quad (2)$$

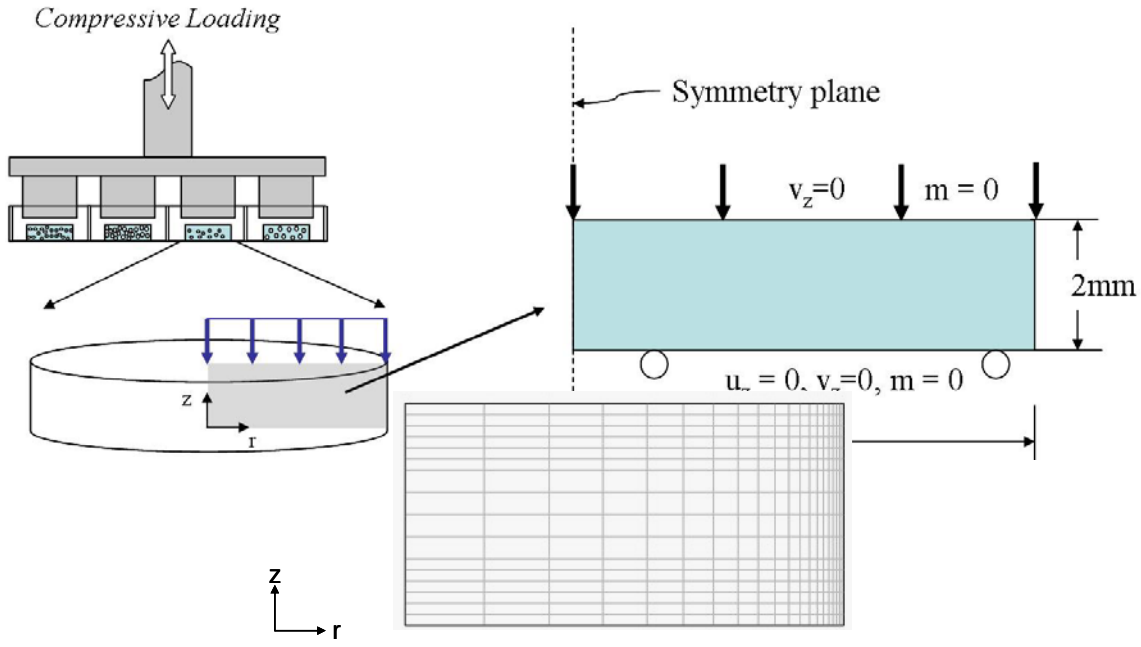

Figure 3.5: Schematic of the device geometry commonly used for mechanical stimulation studies and the resultant free body diagram of the dynamic compression of an axi-symmetric model of a scaffold used in such a device. Image below shows mesh density that are exponentially biased in the radial (r) direction. (NB: Images not drawn to scale).

Scaffold solid deformation depended on the normal σ & shear τ stresses and strains ε imposed on the models as a result of the cyclic load, with the governing equations given by

$$\frac{\partial \sigma_r}{\partial r}+\frac{\partial \tau_{rz}}{\partial z}+\frac{\sigma_r - \sigma_\theta}{r}+\mathrm{F}_r=0, \qquad \frac{\partial \tau_{rz}}{\partial r}+\frac{\partial \sigma_z}{\partial z}+\frac{\tau_{rz}}{r}+\mathrm{F}_z=0,$$
$$\varepsilon_r=\frac{\partial u}{\partial r}, \qquad \varepsilon = \frac{u}{r}, \qquad \varepsilon_z=\frac{\partial w}{\partial z}, \qquad \gamma_{rz}=\frac{\partial u}{\partial z}+\frac{\partial w}{\partial r}, \tag{3}$$

A source term, given as *F* in equations 1 and 3, was implemented to define the fluid/solid interaction, coupling plane strain deformation to Darcy flow, and was imposed as

$$- \frac{\partial \varepsilon_r}{\partial t}+\frac{\partial \varepsilon_z}{\partial t}, \tag{4}$$

Parametric Analysis

The model was used to estimate the mechanical environment resulting from an applied uniaxial unconfined sinusoidal load with 5% strain amplitude superimposed on a 5% strain offset at frequency of 1 Hz. The boundary conditions (Fig. 3.5) allowed displacement to occur freely at the top (loaded) surface and along the radial direction, but fixed along the axial direction at the bottom surface. Loading was simulated using an impermeable, frictionless loader with fluid movement confined to the radial edge. Scaffolds with moduli ranging from 0.5 to 512 kPa and hydraulic permeabilities ranging from 5e-14 to 1.0e-10 m^4/N.s were analyzed (Fig. 3.6). This range of modulus and permeability encompasses the reported material properties of several common scaffold materials used for chondrocyte three dimensional culture, and includes alginate (96), agarose (33, 136, 160-163), polyglycolic acid (PGA) (164), calcium phosphate (165), collagen (166), chitosan (167), fibrin (48), poly(ethylene glycol) (36) and KLD-12 self assembling peptide (37). The finite element simulations were run for 300s, at which time steady state was achieved for all physical stimuli. Analysis was performed at the maxima and minima of each cycle (every t=0.25s) during the

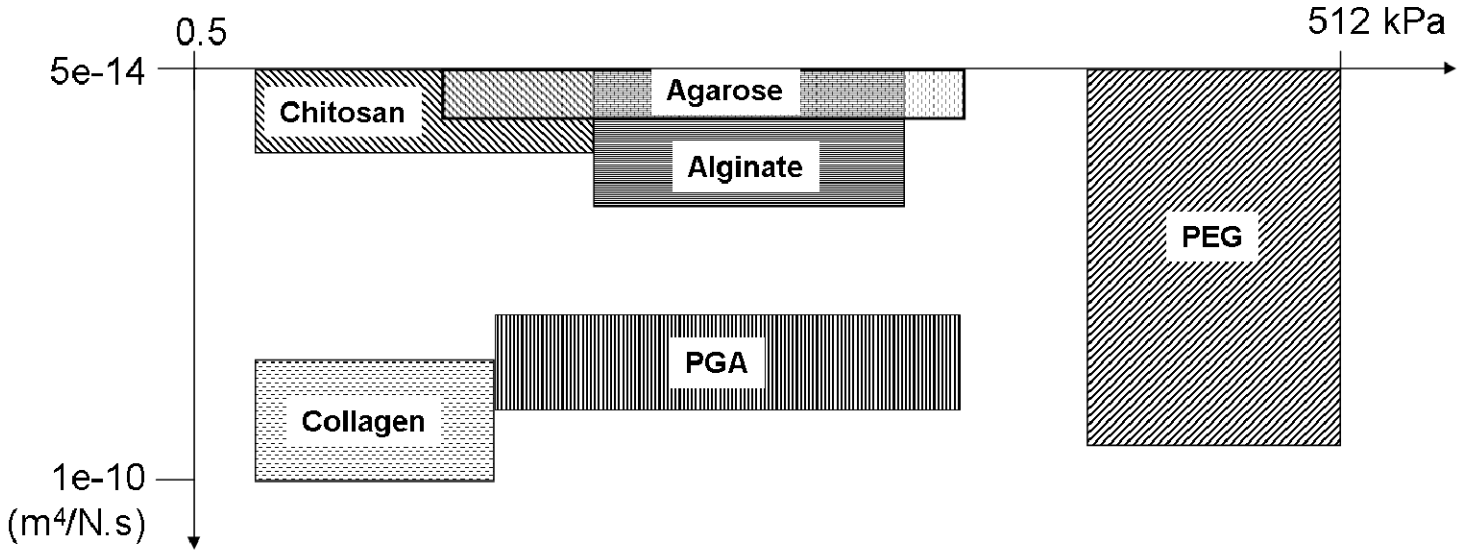

Figure 3.6: Map of scaffold materials depicting the range of modulus (horizontal)and hydraulic permeability (vertical) used in cartilage tissue engineering studies.

dynamic deformational loading. The maximum steady state peak pressures, shear stresses, radial fluid velocities and radial strains at equilibrium were analyzed. Analysis of a cartilage plug with the above mentioned dimensions and loading conditions was conducted for comparison with the loaded scaffolds, with an assumed modulus of 700kPa, hydraulic permeability of 7.6e-15 m^4/N.s, solid density of 7850 kg/m^3, poisson's ratio of 0.125, and a porosity of 70% (159).

Results

Simulated dynamic compression of the models resulted in a rise in pressure within the samples, which, depending on the permeability of the materials, was allowed or prevented fluid from escaping from the pore network of the material. This resulted in the models displaying classic poroelastic behavior upon loading. Peak pressures in the simulated model of loading cartilage showed pressures as high as 60kPa (Fig. 3.7a). By comparison, the models of PEG, alginate and collagen showed peak pressures of 13kPa, 1kPa and 0.025kPa, respectively (Fig. 3.7b – d). For the 360 combinations of modulus and permeability studied, both maximum peak pressures and radial fluid velocities were found to span 3 orders of magnitude, with the lowest values found in materials such as chitosan and the highest values found in materials like PEG (Fig. 3.8a and 3.9b). Pressures were found to be more dependent on scaffold modulus than on permeability and radial fluid velocities were found to depend on both scaffold properties similarly. The highest peak pressure of 37kPa was found in scaffolds with materials properties similar to PEG (E = 512Pa, k = 6.4e-12m^4/N.s), with the lowest value of 0.025kPa in scaffolds similar to collagen (E = 0.5kPa, k = 7.68e-11m^4/N.s). PEG-like scaffolds also had the highest radial fluid velocities

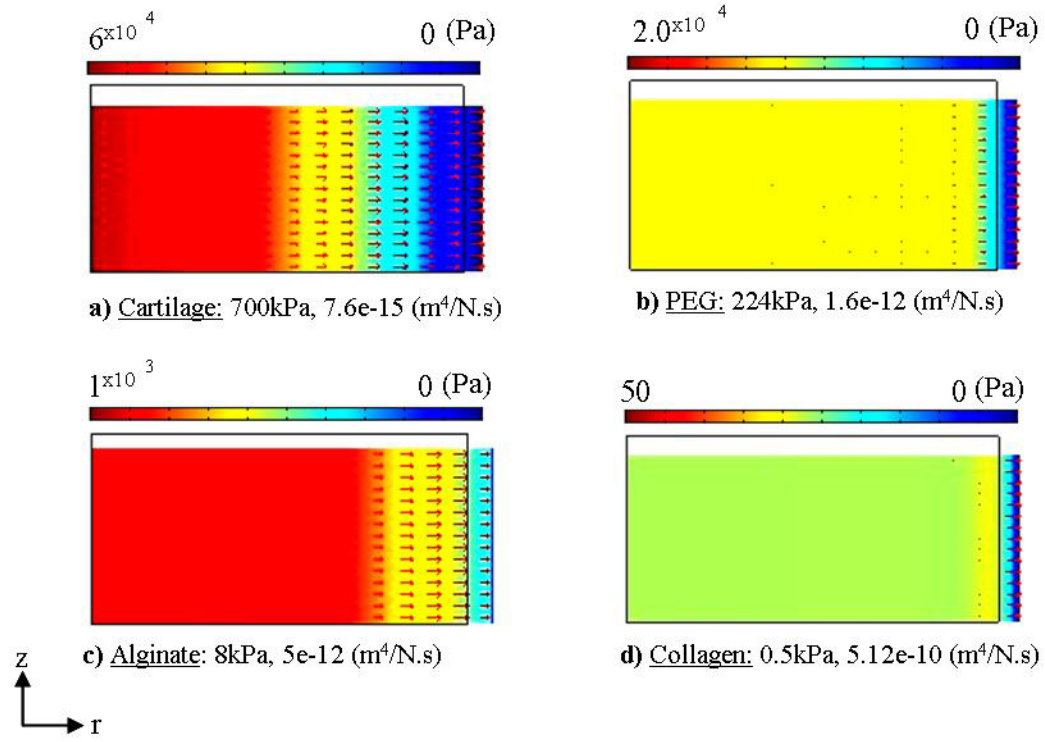

Figure 3.7: Surface plots of pressure (Pa) (color) and radial velocity (arrows) of dynamically loaded cartilage (a), polyethylene glycol (PEG) (b), alginate (c) and collagen models at steady state (t = 299.75s) and their assumed modulus (kPa) and permeability (m^4/N.s). NB: Note scale changes for each image.

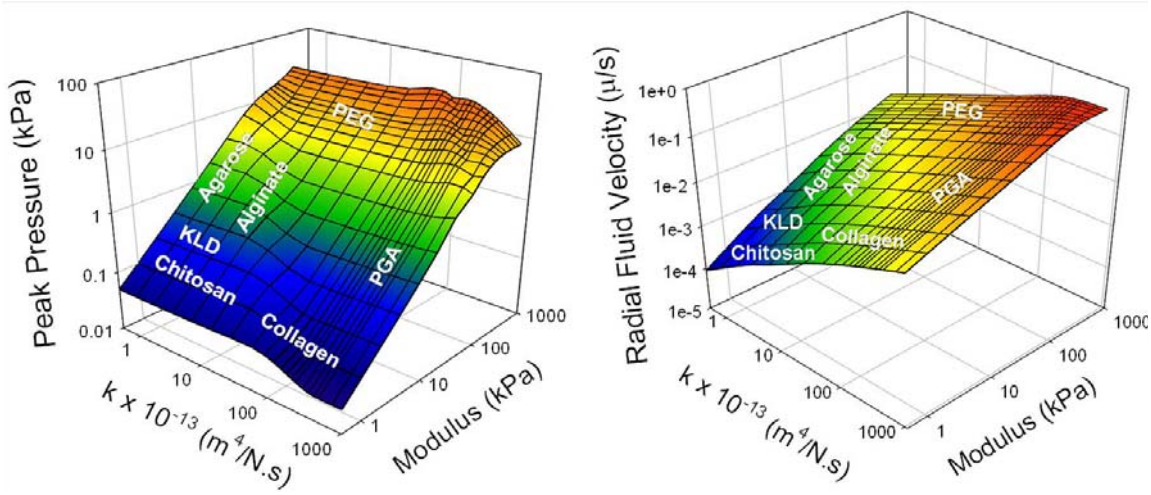

Figure 3.8: Maximum peak pressure and radial fluid velocity as a function of permeability and modulus, showing sample scaffolds with related material properties with labels for scaffolds superimposed over appropriate regions of material properties.

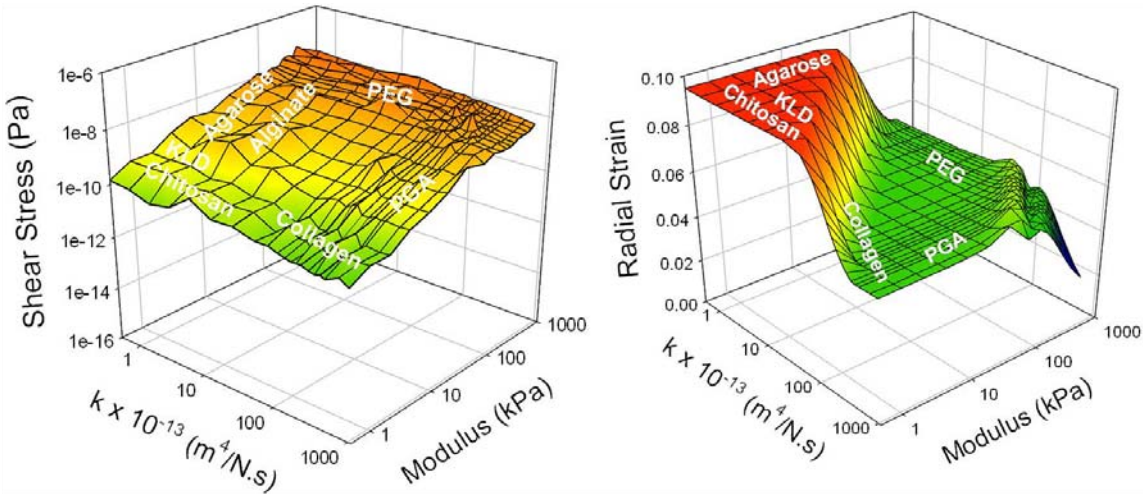

Figure 3.9: Plots of maximum shear stress and radial strain as a function of permeability and modulus, showing sample scaffolds with related material properties with labels for scaffold materials superimposed over appropriate regions of materials.

(maximum = 0.52μ/s), while materials such as chitosan (E = 0.5Pa, k = 0.5m^4/N s) had the lowest value of 8.8e-05μ/s.

Though analysis of shear stresses within all scaffolds showed negligible differences (Fig. 3.9a), radial strain analysis showed a complex dependence on permeability. In lower modulus and lower permeability scaffolds (e.g. alginate, agarose, chitosan) radial strains (Fig. 3.9b) peaked at 0.095 and decreased with increasing permeability and modulus, and dropped even further by the highest permeability and modulus combination studied (E = 512kPa, k = 1e-10m^4/N.s) to a value of 0.023.

Discussion

In this study, we first sought to survey the literature for the efficacy of mechanical stimulation for cartilage tissue engineering and regeneration. The results of the survey revealed a wide range in response from seeded cells, with no clear pattern of efficacy discernable. Effects on glycosaminoglycan metabolism were found to span orders of magnitude, with a particular loading strain and frequency combination found to be stimulatory in some cases and inhibitory in others. In attempting to determine the benefits of mechanical stimulation on chondrogenesis, studies have generally not considered the extent to which the scaffold material affects the physical stimuli sensed by seeded cells. Clearly the properties and characteristics of the scaffold would be expected to play a major role in the stimuli imposed on cells. Scaffolds used in cartilage tissue engineering can have moduli spanning 3 orders of magnitude and permeabilites spanning 4 orders of magnitude (Fig. 3.6). Such scaffolds are subjected to similar loading conditions which, due to the large variation

in properties, lead to drastic differences in response from cells seeded within such scaffolds.

Using our findings from the literature survey, we implemented a poroelastic model to analyze the physical stimuli present within mechanically loaded scaffolds typically used in cartilage tissue engineering. As expected, all scaffold materials exhibited classic poroelastic behavior, having pressurized cores with low fluid flow and edges with high radial fluid velocities (Fig. 3.8). The scaffolds simulated ranged from stiff impermeable materials such as polyethylene glycol to compliant materials such as collagen. The results of the literature study revealed that a peak to peak strain of 10% at frequency of 1Hz was the most utilized mechanical loading condition for the unconfined cyclic compression of cell-laden constructs, and as such was selected for the modeling studies. The model for this frequency and strain condition, involving the wide range in scaffold material properties studied, reveals one of the potential causes for the large variations in metabolic responses observed in studies involving the mechanical stimulation of cells seeded within scaffolds. The same loading condition was found to generate different pressures, strains and fluid velocities profiles within all materials modeled indicating that cells are subjected to different gradients of physical stimuli which are dependent on the scaffold used.

The maximum peak pressures found within the scaffold simulations were strikingly lower than simulated loading articular cartilage. In the extreme case for a material like collagen gel, the difference in peak pressures and velocities was as high as 2000 fold. For the parameters simulated in this study, PEG scaffolds had the highest pressure and radial fluid velocity, but also the lowest shear stress and radial strain. This may be due to the method of fabrication of PEG scaffolds which can be tuned across a wide range of moduli and permeabilities. Chitosan and KLD-12 simulated

scaffold materials had the lowest radial strains and fluid velocities, with collagen scaffolds having the lowest pressures.

A number of finite element models of scaffold materials have been conducted to analyze the physical stimuli imparted on cells within specific scaffolds (40, 122, 123, 168). In the study by Lima et al (122), finite element models were used to predict the spatial and temporal stress, strain, and fluid flow fields within agarose gels subjected to dynamic deformational loading. They found flux flow to be directed radially towards the circumferential boundary of their disk gels and was greatest at the edges of the gel construct. Silva et al (123) sought to characterize the spatial variation in solid stress/pore pressure and fluid velocity within loaded scaffolds for intervertebral disc (IVD) tissue engineering. They found spatial variations in strain, solid stress/pore pressure and fluid velocity within their composite polyvinyl alcohol IVD gels upon loading, which were comparable to the profiles that would be observed in loading biological IVD tissues. Although the analysis generated in the aforementioned studies generally agree with the present work, as well as those done on the unconfined compression of cartilage (159), this study is the first to expand the analysis to 360 modulus/permeability combinations which include up to 10 different scaffold materials in over 30 different studies reviewed. It begins to map out the large variations possible within dynamically loaded cartilage tissue engineering scaffolds and highlights the drastic differences in physical stimuli within these materials even under similar loading conditions.

These results may give insight into the large variations in metabolic response seen in studies involving mechanical stimulation of cell-seeded constructs, where the same loading conditions produce very different results due to the differences in material properties. The findings of this study do not attempt to highlight the benefits of one scaffold versus another, but instead highlights reasons for the large variations in

responses seen in the field. Our results of the literature survey on cell response to scaffold and loading parameters shows that though a frequency of 1Hz at a percent peak to peak strain of 10% is the most studied a higher frequency (e.g. 3Hz) at a slightly higher percent peak to peak strain of 15% yields more consistently positive results.

This study also shows that the pressures seen within loading cartilage plugs (similar to conditions that may be observed in vivo) are still much higher than those being produced in scaffolds. This approach will give insight into scaffold design and the selection of loading regimens for stimulation of tissue engineered cartilage. From our parametric analysis, though maximum levels of stimuli were found in poly(ethylene) glycol type scaffolds, combing this analysis with the results of the literature survey point to the use of highly porous (>97% porosity) scaffolds with compressive moduli within the 10 – 15kPa. A scaffold with this porosity and modulus combination will impose pressure of about 1-10kPa, velocities of 0.001 – 0.1μ/s and strains of about 0.1 on cells seeded within them.

CHAPTER 4

Effect of Scaffold Composition on the Response of Chondrocytes to Dynamic Compression

Abstract

Mechanical loading has been used to enhance the functionality of engineered tissues, but with large variations in efficacy evident in different scaffold materials. We have previously shown that this metabolic response spans orders of magnitude in different scaffold materials when loaded under the same mechanical conditions. To eliminate variation in response due to material chemistry, we studied the effects of scaffold composition on the response to mechanical loading using a single material. Articular chondrocytes were encapsulated in 1, 2 or 3 wt% alginate hydrogels at 25 x 10^6cells/ml. These constructs were either left under free swell conditions, or statically or dynamically loaded in a custom designed bioreactor. Constructs under static loading received a 2.5% static strain for 2 hrs (1hr on, 1hr off, 1hr on) every other day. Those being dynamically loaded received a 2.5% static off set strain and a 2.5% dynamic sinusoidal strain, with similar duty cycles as the static condition. Finite element analysis of the physical stimuli within the dynamically loading scaffolds predicted pressures ranging from 194 to 442 kPa and radial fluid velocities from 3.5 to 7.1 μ/s. The constructs and surrounding media were harvested at times up to 2 weeks and were assessed biochemically and histologically for DNA and glycosaminoglycan (GAG) content. Subsets of samples were mechanically tested for aggregate modulus and permeability. GAG production increased with time for all scaffold compositions. Although cells seeded in 1wt% gels produced the most, they retained the least amounts of GAG within their constructs by 2 weeks. Two and three weight percent

alginate constructs had similar GAG accumulation, but the small amount produced by 3wt% gels had a more drastic effect on the mechanical integrity of the resulting scaffold. The data presented here shows a clear dependence of chondrocyte metabolism on scaffold composition and begins to address one of the reasons for the differences in cells response seen between studies utilizing mechanical loading devices.

Introduction

The use of dynamic mechanical stimulation to improve the functionality of tissue engineered cartilage has been of great interest recently (31, 33, 34, 36, 37, 48, 169, 170). Several scaffold materials have been used within such systems, although the magnitude of enhancement has been found to be highly variable between the systems (171). For example, in the study by Lima et al. (161) , chondrocytes seeded in 2wt% agarose gels produced similar amounts of glycosaminoglycan when dynamically loaded compared to free swell cultured gels, while the study by Waldman et al. (170) reported almost twice the increase in GAG produced by chondrocytes seeded in porous calcium polyphosphate substrate after 4 weeks dynamic loading compared to their free swell constructs.

A recent study published on the finite element (FE) analyses of dynamically loading scaffolds (171) suggests that this variation in response may be due to similar loading conditions producing varied effects when imposed on different scaffold materials. Using the FE models to analyze the stimuli present within scaffolds with over 300 combinations of modulus and permeability, we showed that the same loading parameters applied to various scaffold material properties results in physical stimuli spanning orders of magnitudes. This study highlights the complexity of comparing the

efficacy of such systems and the loading parameters used. Hence, the extent to which the variations in the material properties of scaffolds affect cell response to mechanical loading is not well understood. This understanding is further confounded by the fact that scaffold chemistry (e.g. charge, hydrophobicity, backbone chemistry) may also affect cell metabolism and response to physical stimuli. To date, there has not been a thorough study on how scaffold materials properties affect the response of chondrocytes to mechanical loading.

Therefore, to elucidate the physical stimuli driving cell response to loading, the objective of this study was first to use FE analysis to estimate the spatial distribution of physical stimuli within engineered constructs of a similar material but with different material properties. The second objective was to characterize the effect the simulated stimuli would have on matrix metabolism and assembly by chondrocytes seeded within such constructs. We hypothesize that 1) chondrocyte metabolism is dependent on scaffold composition and 2) scaffold response affects the response of chondrocytes to mechanical loading.

Methods

Cell culture experiments

Chondrocyte harvest and isolation

Bovine articular chondrocytes (AC) were harvested using previously described protocols (74). Briefly, articular cartilage tissue was harvested from the patellofemoral grooves and femoral condyles of 1 to 3 day-old calves. The harvested tissues were chopped into smaller pieces and digested overnight at 37°C and 5% CO_2 in Dulbecco's modified Eagle medium (DMEM) containing 0.3% collagenase (Worthington Biochemicals, Lakewood, NJ) and 100 U/mL penicillin G sodium, 100

μg/mL streptomycin sulfate, 25 μg/mL amphoterocin B. The digest solution was filtered with a 100 μm cell strainer and primary articular chondrocytes were isolated from the strained digest solution by centrifugation at 338 x g for 7 min. Cells were washed twice with Dulbecco's phosphate-buffered saline (PBS) and viability was determined using trypan blue. Only cells solution with viabilities of 85% or higher were used for these studies. Primary chondrocytes from were seeded at density of 25 million cells per ml in 6mm diameter, 1mm height alginate disks of different weight percents as described below.

Gel formation and culture

Cell and alginate solutions of one, two and three weight percent purified alginate (10/60) alginate (FMC Biopolymers, Drammen, Norway) were crosslinked with sterilized 2wt % calcium sulfate (Sigma Aldrich, St. Louis, MO.) using an established injection molding technique (79). Briefly, cell pellets were resuspended in sterile 10 (C1), 20 (C2) or 30mg/ml (C3) alginate in PBS at a density of 25 million cells per ml and crosslinked with 20mg/ml $CaSO_4$ in PBS at a 2:1 ratio. The crosslinked solution was molded into a 1mm thick sheet, from which 6mm diameter disks were acquired using a biopsy punch. The chondrocyte encapsulated disks were cultured in an incubator at 5% CO_2, 95% humidity, and 37°C in DMEM supplemented with 10% fetal bovine serum, 100 μg/ml penicillin, 100 U/ml streptomycin and 50 μg/ml ascorbic acid.

Scaffold Loading (Fig. 4.1)

The cultured gels were maintained as either free swell, static (at 0-2.5% strain) or dynamically loaded. The dynamically loaded gels underwent a 2.5% static offset and 2.5% sinusoidal dynamic compression for 1hr on, 1hr off, 1hr on, every other day

(37). All gels (free swell (FS), static (S) and loaded (L)) were then cultured for 0, 1 and 2 weeks, with media changed every two days (after loading was completed); the disks (n=20-24 per condition and time point) and used media were frozen at -20°C for analysis.

Finite element analyses of scaffolds under loading

Finite element (FE) models of the dynamically compressing scaffold (one for each weight percent experimentally tested) was created using COMSOL multiphysics software (Burlington, MA), as previously described (171). Briefly, two dimensional models of 1 mm x 3 mm axisymmetric scaffolds, containing 320 quadrilateral elements exponentially biased to the edges, yielding a total of 3063 degrees of freedom, were created. The scaffold materials were assumed to be homogenous and isotropic with strain dependent permeability. All scaffolds were assumed to have a poisson's ratio of 0.167 and a density of 1240 Kg/m^3.

The scaffold moduli and permeabilities used for FE analysis were acquired from the mechanical analysis of the experimental samples prior to culture. The scaffolds were assumed to be fully hydrated, with the fluid having an assumed viscosity of 0.001 Pa·s and density of 1000 Kg/m^3. To model the fluid/solid interactions in the scaffolds under loading, a time dependent coupled pore pressure/effective stress analysis was performed using the structural mechanics application mode and Darcy's flow pressure model of the chemical engineering module of COMSOL. Maximum pressure, radial fluid velocity and radial strain were calculated for each model after equilibrium was achieve, which occurred at 300 seconds.

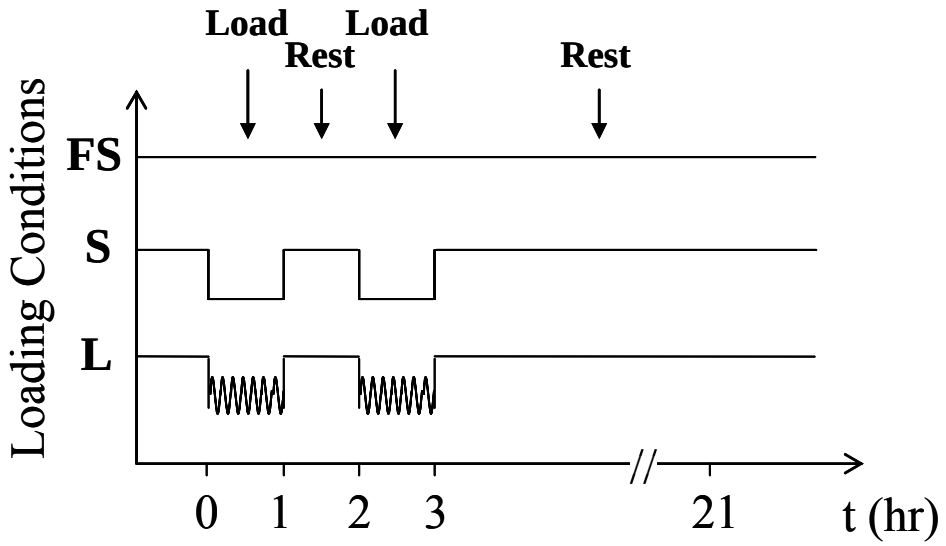

Figure 4.1: Time history of applied free swell (FS), static (S) or dynamic (L) loading on cultured samples. Static loading consisted of a 5% static strain and the dynamic loading consisted of a 2.5% sinusoidal strain super-imposed on a 2.5% static offset.

Biochemical Analysis

Gel samples were weighed upon removal from culture, lyophilized, and weighed again, before digestion in 1 ml of 0.125 mg/ml papain in phosphate buffer with EDTA at 60°C for 18hrs. Papain digests and frozen media samples were treated with 1µl of a 10 unit alginate lyase (Sigma Aldrich, St. Louis, MO) solution in PBS, to further reduce the effect of cross reaction of DMB with macromolecular alginate. Both the collected media (n=8) and disks (n=7-10) were assayed for glycosaminoglycan (GAG) content, with serial dilutions of chondroitin-6-sulfate (Sigma) from shark cartilage in papain digest buffer (for gel samples) or medium (for collected media samples) used as standards (137). DMB-GAG binding was observed at 525 nm.

DNA content within the constructs (n=7-10) was quantified using a Hoechst 33258 dye based assay following standard protocol (138). Briefly, papain digested samples were reacted with Hoechst 33258 dye excited at 358 nm and emission observed at 458 nm. Calf thymus DNA at serial dilutions was used as standards.

Mechanical Analysis

Confined compression tests were used to assess the mechanical integrity of the gels at the different time points according to established protocols (79, 172) (n=5-10 per condition). A uniaxial testing system (EnduraTec, Bose, IN) was used to determine the aggregate modulus. Harvested and frozen samples were thawed in 0.5 ml of an EDTA-free protease inhibitor cocktail (Sigma Aldrich, St. Louis, MO) in PBS solution in a 37°C water bath. Thawed samples were then placed in a confined compression chamber and loaded with a porous platen to 40% strain in sequential 50µm increments, with relaxation loads recorded with each strain step. Constructs were allowed to relax till equilibrium (approx. 7mins) before the next strain step was

imposed. The stress relaxation data was fit to a poroelastic model of material behavior that yielded the aggregate modulus (H_A) of the constructs (139, 140).

Histological Assessment

Samples reserved for histology (n = 4-6 per condition) were fixed in 10% formalin supplemented with 1% calcium sulfate to help maintain gel integrity. Samples were then dehydrated in increasing concentrations of ethanol to 100% ethanol, embedded in paraffin, sectioned (5μm thick circular en face slices) and mounted onto slides. Sections were stained with Safranin O (0.1% in DI water) for glycosaminoglycan deposition and localization and Hematoxylin and eosin (H&E) for nuclei and general matrix distribution. Slides were imaged using a Spot Jr Digital camera attached to an inverted Nikon TS 200 microscope (MicroVideo Instruments, Avon, MA), and photomicrographs were obtained of stained regions.

Statistical analysis

Data in all graphs were reported as means +/- standard deviation for all conditions. Statistical comparisons of total GAG, μg GAG/mg wet weight (WW), cumulative media GAG, GAG retention, H_A and cell density between all groups was performed on the data from all groups using a two way ANOVA by proc mixed analysis ($p<0.001$) on SAS 9.1 (Cary, NC). The proc analysis, which uses standard linear models, allows for both fixed and random effects in our study. Tukey's HSD post hoc test was carried out to make pairwise comparisons between groups with calculated *p* values considered significant for $p<0.05$.

The data for static and dynamically loaded samples were then normalized to the averages of the data of free swell samples to analyze changes due to loading

condition. A multiple ANOVA on the normalized data set with a Bonferroni correction was done to assess effects with time, compare means of the different scaffold compositions as a result of either dynamic or static loading and to compare the effects of both static and dynamic loading on scaffold composition. To compare normalized values to the free swell conditions, analysis of the confidence intervals of the least square means was done with $p<0.05$.

Results

Finite Element Analysis

Finite element analysis of the loading gels showed uniform physical stimuli in the majority of the bulk of all models (Fig. 4.2), with low pressures and high fluid velocities at the radial edges. The analysis of the 3wt% gel showed twice the amount of pressure (p=442Pa) and radial fluid velocity (v=7.1μ/s) than 1wt% (p=194Pa, v=3.5μ/s) and 2wt% (p=217.6Pa, v=3.7μ/s) gels. No difference in radial strains was found for any of the weight percents (not shown).

DNA Analysis

Gels in all conditions studied showed a significant decrease in DNA ($p<0.003$) after the first week of culture (Fig. 4.3). By the second week, 1wt% gels had significantly higher DNA content than 2 and 3wt% gels ($p\leq0.003$), regardless of the culture conditions. Static and dynamic loading had no effect on all but 1wt% gels, where at 2 weeks, statically loaded gels had higher DNA content than either free swell (p=0.03) or dynamically loaded gels (p=0.001).

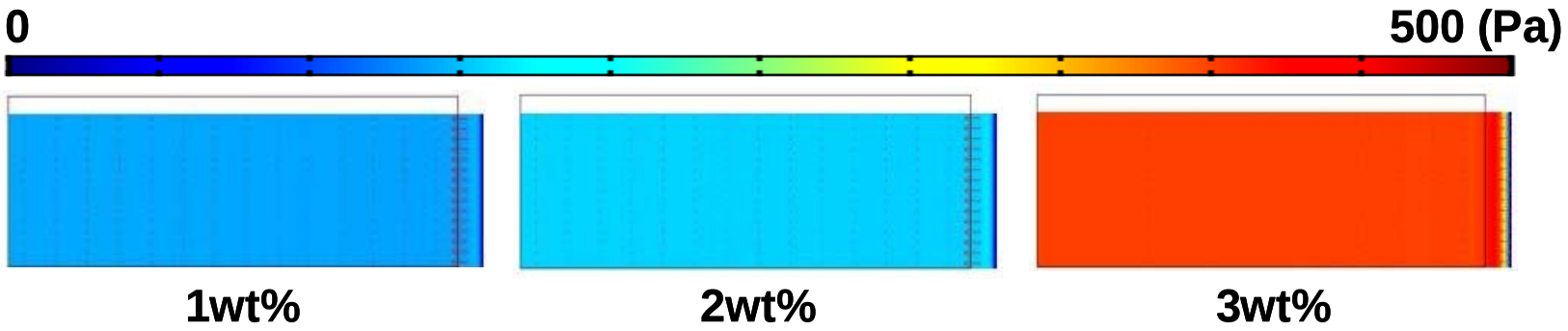

Figure 4.2: Surface plots of pressure (color) and radial fluid velocity (arrows) of dynamically loading 1, 2 and 3wt% alginate scaffolds at steady state (t = 299.75s)

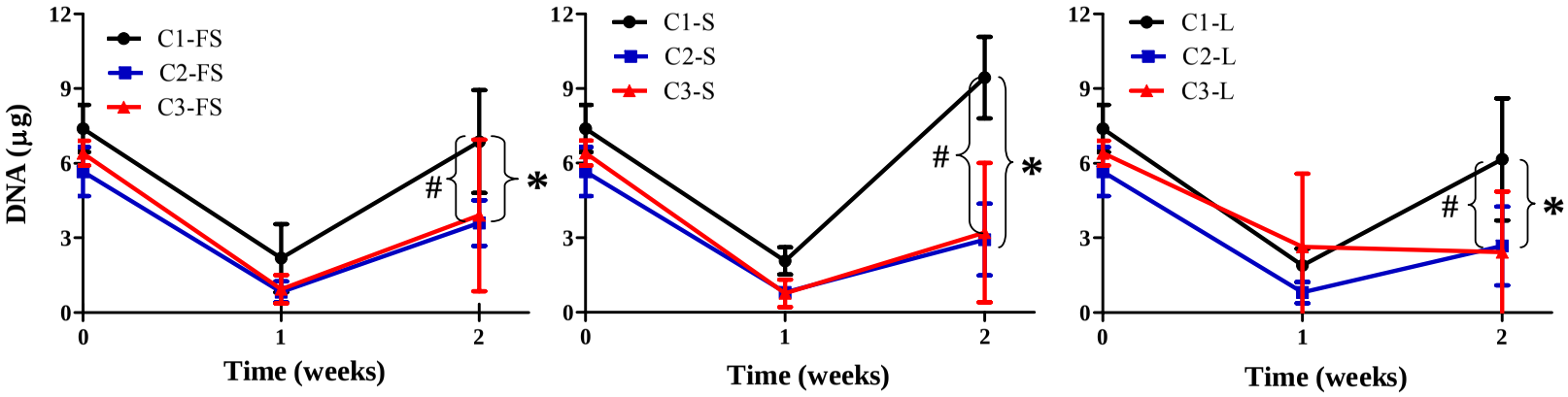

Figure 4.3: Average microgram of DNA per chondrocyte seeded gel as a function of scaffold composition and loading condition (mean ± stdev.; n = 7-10). Free swell, static, and dynamic are represented as FS, S and L, respectively and 1-, 2-, and 3wt% gels are represented by C1, C2 and C3 respectively. # and * represent significant differences between 1wt% gels and 2 and 3wt% gels, respectively (all with $p<0.05$)

GAG Analysis

Glycosaminoglycan content in the gels increased with time for all groups ($p<0.05$), with the most rapid accumulation in 1 wt% gels (Fig. 4.4, $p=0.006$). When 2wt% gels were subjected to dynamic loading, a significant increase in gel GAG content was found by 2 weeks when compared to static loading ($p=0.04$). When normalized to free swells, the gel GAG content of statically loaded 3wt% gels and dynamically loaded 2 and 3wt% gels were significantly higher by two weeks of culture ($p<0.05$ for all comparisons). Dynamic loading also significantly increased the gel GAG content in 3wt% gels with time ($p<0.0001$) (Fig. 4.4b).

The amount of glycosaminoglycans released to the surrounding medium increased with time, with 1wt% gels releasing at a much higher rates than either 2 or 3wt% gels (data not shown). At 2 weeks, the cumulative amount released by 1wt% gels was significantly higher than amounts released by either 2 or 3wt% gels ($p<0.0001$), with most of the release occurring after the first week of culture. Neither static nor dynamic loading enhanced GAG release to the surrounding medium. In addition, GAG retention decreased with time only for cells encapsulated in 1wt% gels ($p\leq0.003$), regardless of loading condition (Fig. 4.5a). Retention by 1wt% gels at 2 weeks was significantly lower than 3wt% gels under free swell ($p=0.0003$) (Fig. 4.5a) and 2 and 3wt% gels when statically or dynamic loaded ($p\leq0.02$) (data not shown). Lastly, static loading had no effect on GAG retention and dynamic loading significantly increased retention only in 2wt% gels at 2 weeks ($p<0.05$), both when compared to free swell values.

Total GAG production increased with time for all groups studied (data not shown), although this increase was highest for 1wt% gels by 2 weeks ($p<0.0001$). The total amount produced was more sensitive to scaffold composition than loading condition, with cells seeded in 1wt% gels producing more than twice the amount

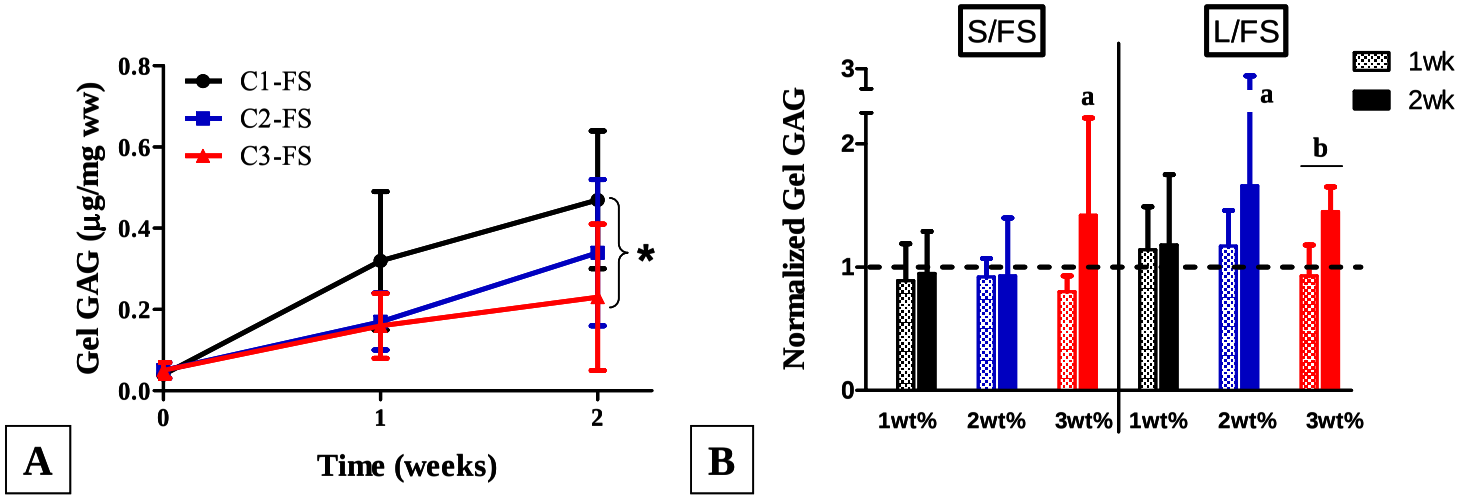

Figure 4.4: Average amount of GAG per chondrocyte seeded gel normalized to weight wet, as a function of scaffold composition and loading condition (mean ± stdev.; n = 8) displayed as raw data (Fig. 4.4a) or loaded conditions (Fig. 4.4b) normalized to free swell values. Free swell, static, and dynamic are represented as FS, S and L, respectively and 1-, 2-, and 3wt% gels are represented by C1, C2 and C3 respectively. # and * represent significant differences between 1wt% gels, and 2 and 3wt% gels, respectively (all with $p<0.05$). 'a' represents significantly different values from free swell and 'b', significant increase with time, when normalized to free swell conditions.

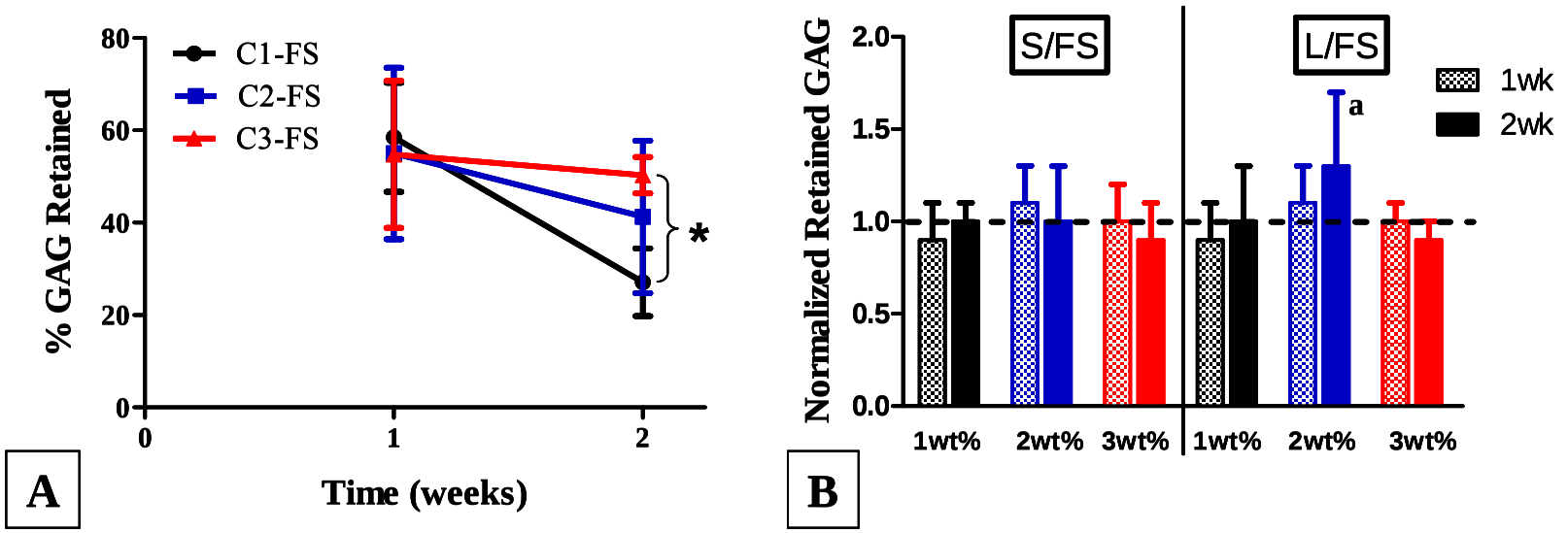

Figure 4.5: Average percentage of GAG retained within chondrocyte seeded constructs, as a function of scaffold composition and loading condition (mean ± stdev.; n = 8) displayed as raw data (Fig. 4.5a) or loaded conditions (Fig. 4.5b) normalized to free swell values. Free swell, static, and dynamic are represented as FS, S and L, respectively and 1-, 2-, and 3wt% gels are represented by C1, C2 and C3 respectively. # and * represent significant differences between 1wt% gels and 2 and 3wt% gels, respectively (all with $p<0.05$) and 'a' represents significantly different from free swell values.

produced by those seeded in 2 or 3wt% gels ($p \leq 0.005$ and $p \leq 0.0006$, respectively). Although loading had no statistically significant effect on total GAG produced, on average, dynamically loaded 2 and 3wt% gels produced higher amounts of GAG than statically loaded gels by 2 weeks.

In comparing the results of the finite element analysis to the resulting effects on chondrocyte behavior, increasing physical stimuli resulted in increase in total GAG produced and amount retained (Table 4.1). This increase with increase stimuli was more drastic between 1 and 2 or 3wt% gels, than between 2 and 3wt% gels. For example, in 3wt% gels, FE analysis demonstrated twice the increase in pressure and fluid velocity (at 442 kPa and 3.1 μ/s, respectively), when compared to 1wt% gels that resulted in 1.2 total GAG produced (loaded/free swell).

Histological Assessment

Gels cultured under free swell and static loading conditions had more GAG and collagen staining as evident by histological analysis (data not shown). This difference was more pronounced in 1wt% gels and less so in 3wt% gels. In 1wt% gels, GAG and general collagen staining, although predominantly localized to the circumference of the gels was diffusely evident within the body of the construct. GAG and Collagen staining was similar in 2 and 3wt% gels, with few localized areas of large matrix deposits found at the circumference of 2wt% gels and fewer in 3wt% gels.

Aggregate Modulus (H_A)

Loading had no effect on the aggregate moduli of 1 and 2wt% gels throughout the culture period (Fig. 4.6a and 4.6b). In 3wt% gels, dynamic loading increased the

Table 4.1: Comparisons of finite element analyzed physical stimuli to gel GAG amounts (normalized to free swell culture values) produced by 2 weeks for all scaffold compositions studied.

	Pressure (kPa)	**Radial Velocity (μm/s)**	**Total GAG (Loaded/Free Swell)**
C1	194	3.5	0.9 ± 0.2
C2	217	3.7	1.5 ± 0.8
C3	442	7.1	1.2 ± 0.5

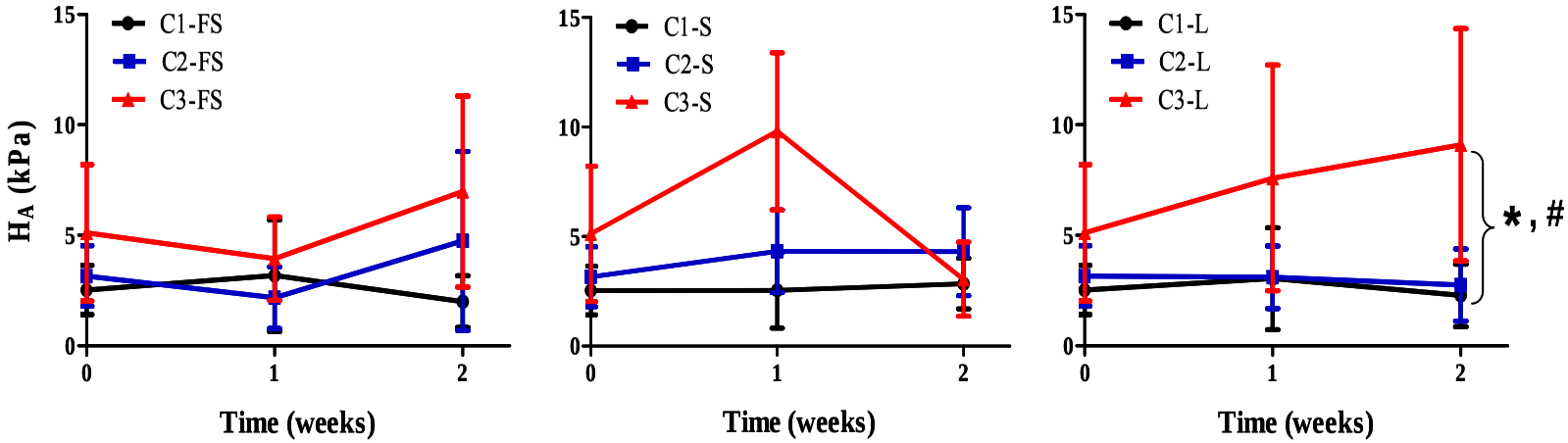

Figure 4.6: Aggregate moduli of chondrocyte seeded gels per time, as a function of scaffold composition and loading condition (mean ± stdev.; n = 8). Free swell, static, and dynamic are represented as FS, S and L, respectively and 1-, 2-, and 3wt% gels are represented by C1, C2 and C3 respectively.

aggregate modulus up to 80% by 2 weeks ($p \leq 0.04$) and static loading decreased the moduli of these constructs by the second week ($p=0.007$) when compared to dynamic loading (Fig. 4.6c).

Discussion

This study demonstrates that scaffold composition (and the resulting mechanical properties) affects articular chondrocyte proteoglycan assembly and response to mechanical loading. The least compliant and most permeable constructs (1wt% alginate) produced the largest amounts of glycosaminoglycan and released the most to the surrounding medium. In addition, dynamic loading increased GAG content in 2- and 3wt% gels at 2 weeks. Convective flow within the gels due to either static or dynamic loading did not increase GAG loss over the culture period studied in 2 or 2wt% gels, but did limit GAG retention in 1wt% gels.

Finite element analysis showed different levels of physical stimuli present within the loading gels and this pattern was consistent with the differences in GAG accumulation within them. Few studies have sought to correlate physical stimuli present within loading tissues or constructs with matrix metabolism (40, 122, 123, 152, 168). In a study we recently published on finite element analysis of loading scaffolds, differences in physical stimuli (pressures, fluid velocities and strains) were found to span orders of magnitude when loaded with the same loading regimen (171). This large variation is due to scaffold composition and hence material properties; the repercussions of which has been highlighted in this study. Presently, we've shown that dynamic loading of 3wt% gels, which experienced the highest amounts of pressure and radial fluid velocity, produced the most functional matrix as evidenced by a 80% increase in aggregate modulus. Although the amounts produced by these gels were

smaller than that produced by 1wt% gels, this small amount was sufficient enough to have a profound effect on the resulting mechanical integrity of engineered construct (Fig. 4.6). This suggests that proteoglycans may interact mechanically with alginate scaffolds.

Although several studies have highlighted the dependence of cell metabolic activity on scaffold composition (33, 112, 173-176), few have assessed the effects of scaffold composition on GAG assembly by chondrocytes when dynamically loaded. In a study assess the effects of scaffold composition on cell behavior, Buschmann et al. (33) showed no significant difference in the GAG or DNA content of 2 and 3wt% agarose seeded constructs, which is consistent with the findings of our study. In our study, scaffold composition played a major role on GAG assembly by chondrocytes. Cells seeded in 1wt% gels produced on average, more than twice the amounts produced by those seeded in 2 or 3wt% gels. This may be attributed to increased scaffold permeability which increases nutrient and waste transport in and out of the constructs. Interestingly, the decreased permeability of 3wt% gels didn't enhance GAG retention, although 2 weeks of culture may be too short a time for significant changes to occur.

The behavior of cells and their interaction with scaffolds becomes more complex with the application of dynamic loading. Even still, fewer studies have tried to relate the physical stimuli present within loading constructs to the behavior of cells encapsulated within them. In a study by Stops et al. (177), a finite element model was developed to analyze the mechanical influence of the host environment (i.e. scaffold) on cell-seeded collagen-GAG scaffold. Their results demonstrated that a very wide range of microscopic strains act at the cellular level, when a sample value of macroscopic strain was imposed on the cell-seeded scaffold. This variation in strain is made larger by the use of scaffold of different compositions, as found in our study,

and creates even larger variations with loading. The reduced response to mechanical loading found in our study is consistent with published data (33, 42, 170) and can be attributed to the short culture period used. These published studies have shown that cell response to mechanical loading increases with increased matrix deposition within the scaffold which comes with longer culture times. And increasing culture time and loading cycles can be expected to affect our engineered constructs similarly.

In this study, we have highlighted the important roles scaffold composition play in cell metabolic activity and the complex effect it has when dynamically loaded. We hypothesize that the actual physical stimuli present within loading scaffolds (pressures, strains and fluid velocity gradients) are better predictors of cell response and should thus be used as the metric of choice when assessing the benefits of a scaffold or mechanical loading parameters.

CHAPTER 5

Mesenchymal Stem Cell response to Dynamic Compression is Modulated by Scaffold Composition in Engineered Cartilage Constructs

Abstract

Dynamic compression is increasingly being used on cell-seeded constructs to enhance tissue formation and the functionality of engineered cartilage tissues. Its use has resulted in large variations in cell response that has been attributed to large variations in scaffold properties and loading parameters. To date, the effects of scaffold composition and the resulting scaffold property on mesenchymal stem cell matrix metabolism has yet to be elucidated. Using a specific loading regimen, we studied the effects of different scaffold compositions on cartilage tissue engineered constructs. Second passage mesenchymal stem cells were encapsulated in 1, 2 or 3wt% alginate hydrogels at 25 x 10^6cells/ml. The constructs were either left under free swell conditions, or statically or dynamically loaded in a custom designed bioreactor. Constructs under static loading received a 2.5% static strain for 2 hrs (1hr on, 1hr off, 1hr on) every other day. Those being dynamically loaded received a 2.5% static off set strain and a 2.5% dynamic sinusoidal strain, with similar duty cycles as the static condition. Constructs and surrounding media harvested at up to 2 weeks were assessed biochemically and histologically for DNA and glycosaminoglycan (GAG) content. Immunohistochemistry of link protein was done, and subsets of samples were mechanically tested for aggregate modulus. Finite element analysis of the physical stimuli within the loading scaffolds showed differences with scaffold composition.

GAG production increased with time for all scaffold compositions studied, though cells seeded in 1wt% gels under free swell produced the most but retained the least amount of GAG within the constructs by 2 weeks. Two and three weight percent constructs had similar GAG metabolic activity, regardless of culture condition. Interestingly, extracellular matrix assembly did not differ for gels of all compositions when statically or dynamically loaded. The data presented here is consistent with trends found in MSC studies using different scaffold types and loading conditions. This study highlights how scaffold loading can modulate MSC response in scaffolds of different compositions.

Introduction

Mesenchymal stem cells (MSCs) can differentiate into cells of several lineages, including cartilage, bone and muscle cells (86). The use of these cells for cartilage tissue engineering and regeneration has increased recently (118, 169, 178), with the attraction stemming from their ability to retain their phenotype after serial passaging (80). As a result, tissue engineering strategies are increasingly focusing on their use in cartilage tissue engineered constructs. Several studies have shown that MSCs encapsulated in scaffolds can indeed produce cartilage matrix molecules with corresponding increases in mechanical integrity, although not to the same extent as chondrocyte seeded scaffolds (88, 96, 118, 133, 178).

To enhance the integrity and functionality of engineered cartilage, several studies have incorporated the use of mechanical loading devices to enhance matrix production by the encapsulated cells (31, 37, 40, 43, 45, 170, 179, 180). The use of mechanical stimulation to enhance construct formation in vitro stems from mechanical stimuli being present in developing musculoskeletal systems. In growing embryos,

physical stimuli in the form of muscle contractions acting on cartilage rudiments has been shown to be crucial for joint cavitation and subsequent articular cartilage development (51, 55, 60, 61). Mechanical loading has also been shown to be crucial for maintaining cartilage homeostasis (21, 58, 150, 151). Findings such as these have resulted in the use of mechanical loading devices for cartilage tissue engineering whereby pertinent stimuli applied to engineered constructs are used to improve tissue formation in vitro.

In addition to the different combinations of parameters being used for dynamic loading, several scaffold materials have been formulated for use within such systems (43, 95, 96, 106, 113, 173, 181). Unfortunately, the magnitude of enhancement found is highly variable amongst systems. For example, in a study by Lima et al (161), chondrocytes seeded in two weight percent agarose gels produced similar amounts of glycosaminoglycan when dynamically loaded compared to free swell cultured gels, while a study by Waldman et al (165) reported almost twice the increase in GAG produced by chondrocytes seeded in porous calcium polyphosphate substrate after 4 weeks of dynamic loading compared to their free swell constructs. In a recent study (171), we showed that variations in response can be found in mechanical loading studies due largely to similar loading conditions producing varied effects when imposed on different scaffold materials. As a result, assessment of the efficacy of mechanical loading systems and the loading parameters used has proven difficult.

Finite element (FE) analyses have been employed to quantify the physical stimuli present within dynamically loaded scaffolds (121-123, 154, 171). Using such a method, we have previously shown that loading applied to scaffolds of various material properties result in physical stimuli spanning orders of magnitudes. However, the extent to which the variations in the material properties of scaffolds affect cell response to mechanical loading is not well understood. To begin to elucidate the

physical stimuli driving cell response to loading, we used FE analysis to estimate the spatial distribution of physical stimuli present within cyclically compressing engineered constructs. The analysis was done on alginate gels of varying scaffold composition, and hence varying mechanical properties. The effects the simulated stimuli would have on matrix assembly by mesenchymal stem cells seeded within such constructs were then characterized. We hypothesized that 1) MSC proteoglycan assembly is dependent on scaffold composition and 2) the difference in proteoglycan assembly by MSCs seeded in varying scaffold composition is more pronounced with static or dynamic scaffold loading; with glycosaminoglycan content being used as a marker of differential response.

Methods

Cell culture experiments

Mesenchymal Stem cell harvest and Isolation

Equine sternal MSCs were harvested and passaged using established protocols (79, 88). Bone marrow aspirates were obtained aseptically from the sternum of the horses within two hours of euthanasia. Aspirates were collected in 60 cc syringes containing 8 ml of 10,000 USP units of chilled heparin sodium solution (Baxter Healthcare corp., Deerfield, IL). Four to six 60cc syringes were obtained per animal. Under sterile conditions, 30 ml of aspirate was resuspended in 15 ml of PBS and centrifuged at 338 x g for 10 min to remove red blood cells. The cell pellet was resuspended in 30 ml of DMEM containing 4.5 g/L sodium pyruvate supplemented with 10% Fetalplex (Gemini Bioproducts, West Sacramento, CA), 100 μg/ml penicillin G sodium, 100 U/ml streptomycin sulfate, 25 μg/mL amphoterocin B, 4.5 g/L L-glutamine, 25 mM HEPES buffer (Sigma Aldrich, St. Louis, MO.) and 1 ng/ml

basic fibroblast growth factor (PeproTech, Rocky Hill, NJ),) and plated in 175 cm^2 flasks at 5% CO_2, 95% humidity, and 37°C. Twenty-four hours after incubation, half the volume in each flask was transferred to a new flask and the media level was supplemented up to 30 ml/flask. The medium was changed twice a week until 80% confluency was achieved to attain first passage cells (P1). Second passage cells (P2) were obtained by replating P1 cells at a concentration of 10,000 cells/cm^2 in T-175cm^2 flasks and treated as above until they formed 80% confluent monolayer. Each flask yielded 6-8 million cells and the resulting monolayer cultures appeared homogeneous and morphologically resembled cells commonly described as MSCs (86). Some cell heterogeneity may have persisted, despite phenotypic similarities. Trypsinized P2 cells were encapsulated in 6 mm alginate gel disks by injection molding as described below.

Gel formation

Cell and alginate solutions of one, two and three weight percent purified alginate (10/60) alginate (FMC Biopolymers, Drammen, Norway) were crosslinked with sterilized 2wt % calcium sulfate (Sigma Aldrich, St. Louis, MO) using established injection molding techniques (79). Briefly, cell pellets were resuspended in sterile 10, 20 or 30 mg/ml alginate in PBS at a density of 25e6 per ml and crosslinked with 20 mg/ml $CaSO_4$ in PBS at a 2:1 ratio. The crosslinked solution was molded into a 1 mm thick sheet, from which 6 mm diameter disks were acquired using a biopsy punch.

Gel disk culture

The cell encapsulated alginate disks were cultured in an incubator for 0, 1 or 2 weeks at 5% CO_2, 95% humidity, and 37°C. The MSC seeded disks were cultured in

chondrogenic medium consisting of DMEM, 4.5 g/L sodium pyruvate, 10% fetalplex, 100 μg/ml penicillin G sodium, 100 U/ml streptomycin sulfate, 25 μg/mL amphoterocin B, 4.5 g/L L-glutamine and 25 mM HEPES buffer and supplemented with 5 ng/ml transforming growth factor beta 1 (TGF-β1, − PeproTech, Rocky Hill, NJ) (88).

Dynamic compressive loading of scaffolds

Cultured gels were kept as either free swell, static (at 0% strain) or loaded. The loaded gels underwent a 2.5% static offset and 2.5% sinusoidal dynamic compression for 1hr on, 1hr off, 1hr on, every other day (37). Gels were then cultured for 0, 1 or 2 weeks, with media changed every two days after loading was completed; the disks and used media were frozen at -20°C for analysis.

Analysis

Finite element model of scaffolds under loading

Finite element (FE) analysis of the dynamically compressing scaffold (one for each weight percent experimentally tested) was done using COMSOL multiphysics software (Burlington, MA), as previously described (171). Briefly, two dimensional models of 1 mm x 3 mm axisymmetric scaffolds, containing 320 quadrilateral elements exponentially biased to the edges, yielding a total of 3063 degrees of freedom, were created. The scaffold materials were assumed to be homogenous and isotropic with strain dependent permeability. All scaffolds were assumed to have a poisson's ratio of 0.167 and a density of 1240 Kg/m^3. Scaffold moduli and permeabilities used for FE analysis were acquired from the mechanical analysis of the experimental samples. The scaffolds were assumed to be fully hydrated, with the fluid having an assumed viscosity of 0.001 Pa·s and density of 1000 Kg/m^3. To model the

fluid/solid interactions in the scaffolds under loading, a time dependent coupled pore pressure/effective stress analysis was performed using the structural mechanics application mode and Darcy's flow pressure model of the chemical engineering module of COMSOL. Maximum pressure, radial fluid velocity and radial strain were calculated for each model after equilibrium was achieve, which occurred at 300 seconds

Biochemical Analysis

A 1, 9-dimethylmethylene blue dye (DMB, Sigma) based assay (137) was used to quantify sulfated GAG content in papain digested disks and collected media samples. Gel samples were weighed upon removal from culture, lyophilized, and weighed again, before digestion in 1 ml of 0.125 mg/ml papain in phosphate buffer with EDTA at 60°C for 18hrs. Papain digests and frozen media samples were treated with 1 μl of a 10 unit alginate lyase (Sigma Aldrich, St. Louis, MO) solution in PBS, to further reduce the effect of cross reaction of DMB with macromolecular alginate. Both the collected media and disks were assayed for GAG content with serial dilutions of chondroitin-6-sulfate (Sigma) from shark cartilage in papain digest buffer (for gel samples) or medium (for collected media samples) used as standards. DMB-GAG binding was observed at 525 nm. DNA was quantified using a Hoechst 33258 dye based assay following standard protocol (138). Briefly, papain digested samples were reacted with Hoechst 33258 dye excited at 358 nm and emission observed at 458 nm. Calf thymus DNA at serial dilutions was used as standards.

Mechanical Analysis

Confined compression tests were used to assess the mechanical integrity of the gels at the different time points according to established protocols (79, 96) (n=3-5 samples

per condition). A uniaxial testing system (EnduraTec, Bose, IN) was used to determine the aggregate modulus. Harvested and frozen samples were thawed in 0.5 ml of an EDTA-free protease inhibitor cocktail (Sigma Aldrich, St. Louis, MO) in PBS solution in a 37°C water bath. Thawed samples were then placed in a confined compression chamber and loaded with a porous platen to 40% strain in sequential 50 μm increments, with relaxation loads recorded at each strain step. Constructs were allowed to relax until equilibrium (approx. 7mins) before the next strain step was imposed. The stress relaxation data was fit to a poroelastic model of material behavior that yielded the aggregate modulus (H_A) of the constructs (139, 140).

Histological Assessment

Samples reserved for histology (n=2 samples per group) were fixed in 10% formalin supplemented with 1% calcium sulfate to maintain gel integrity. Samples were then dehydrated in increasing concentrations of ethanol to 100% ethanol, embedded in paraffin, sectioned (5 μm thick slices) and mounted onto slides. Sections were stained with Safranin O (0.1% in DI water) for glycosaminoglycan deposition and localization and Hematoxylin and eosin (H&E) for nuclei and general matrix distribution. Samples with the highest GAG retention from each group, as indicated by biochemical analysis, were analyzed for link protein localization using an established immunohistochemistry protocol (182). Slides were imaged using a Spot Jr Digital camera attached to an inverted Nikon TS 200 microscope (MicroVideo Instruments, Avon, MA), and photomicrographs were obtained of stained regions.

Statistical analysis

Data in all graphs were reported as means +/- standard deviation for all conditions. Statistical comparisons of total GAG, μg GAG/mg ww, cumulative media

GAG, GAG retention, H_A and cell density between all groups was performed on the data from all groups using a two way ANOVA by proc mixed analysis ($p<0.001$) SAS 9.1, Cary, NC). The proc analysis, which uses standard linear models, allows for both fixed and random effects in our study. Tukey's HSD post hoc test was carried out to make pairwise comparisons between groups with calculated *p* values considered significant for $p<0.05$. Linear regression and Pearson's correlation analysis was performed on H_A per μg GAG/mg ww data sets.

The data for static and dynamically loaded samples were normalized to the averages of the data of free swell samples to analyze changes due to loading condition. A multiple ANOVA on the normalized data set with a Bonferroni correction was done to assess effects with time, compare means of the different scaffold compositions as a result of either dynamic or static loading, and to compare the effects of both static and dynamic loading on scaffold composition. To compare normalized values to the free swell conditions, analysis of the confidence intervals of the least square means was done with $p<0.05$.

Results

Finite Element Analysis

Finite element analysis of the loading gels showed uniform physical stimuli in the majority of the bulk of all models (data not shown), with low pressures and high fluid velocities at the radial surfaces. The analysis of the 3wt% gel showed twice the amount of pressure (p=442 Pa) and radial fluid velocity (v=7.1 μ/s) than 1wt% (p=194 Pa, v=3.5 μ/s) and 2wt% (p=217.6 Pa, v=3.7 μ/s) gels. No difference in radial strains was found for any of the weight percents.

DNA Analysis

All conditions showed an initial decrease in DNA at the first week of culture ($p \leq 0.0003$). Although gels in all conditions significantly increased in DNA content by the second week of culture, only 1wt% gels were able to rebound to initial DNA levels (Fig. 5.1a). At the second week of culture, 1wt% gels had significantly higher DNA content than either 2 or 3wt% gels ($p \leq 0.004$), only when cultured under free swell conditions. Two and three weight percent gels had similar DNA contents regardless of culture condition ($p > 0.05$). Dynamic loading significantly decreased DNA content only in 1 and 2wt% gels by the second week of culture ($p < 0.05$) when compared to free swell (Fig. 5.1b). Dynamic loading significantly decreased DNA content of 2wt% gels by 2 weeks ($p = 0.014$).

GAG Analysis

Total GAG production increased with time for all groups studied, though this increase was significantly higher for 1wt% gels cultured under free swell ($p < 0.0001$). Under free swell conditions at 2 weeks, the total amount of GAG produced in 1wt% gels was almost twice the amount produced by either 2 or 3wt% gels ($p < 0.002$ and $p < 0.004$, respectively) (Fig. 5.2a). Static loading significantly decreased the total GAG produced only in 1wt% gels ($p < 0.05$), while dynamic loading decreased the amounts produced by gels in all weight percents, when compared to free swell ($p < 0.05$) (Fig. 5.2b). Dynamic loading decreased the total GAG produced in 2 and 3wt% gels by the second week of culture.

Glycosaminoglycan content significantly increased by the second week of culture only for gels cultured under free swell conditions ($p < 0.05$). And under free swell, 1wt% gels had statistically larger amounts of GAG than 2wt% ($p < 0.0001$) (Fig.

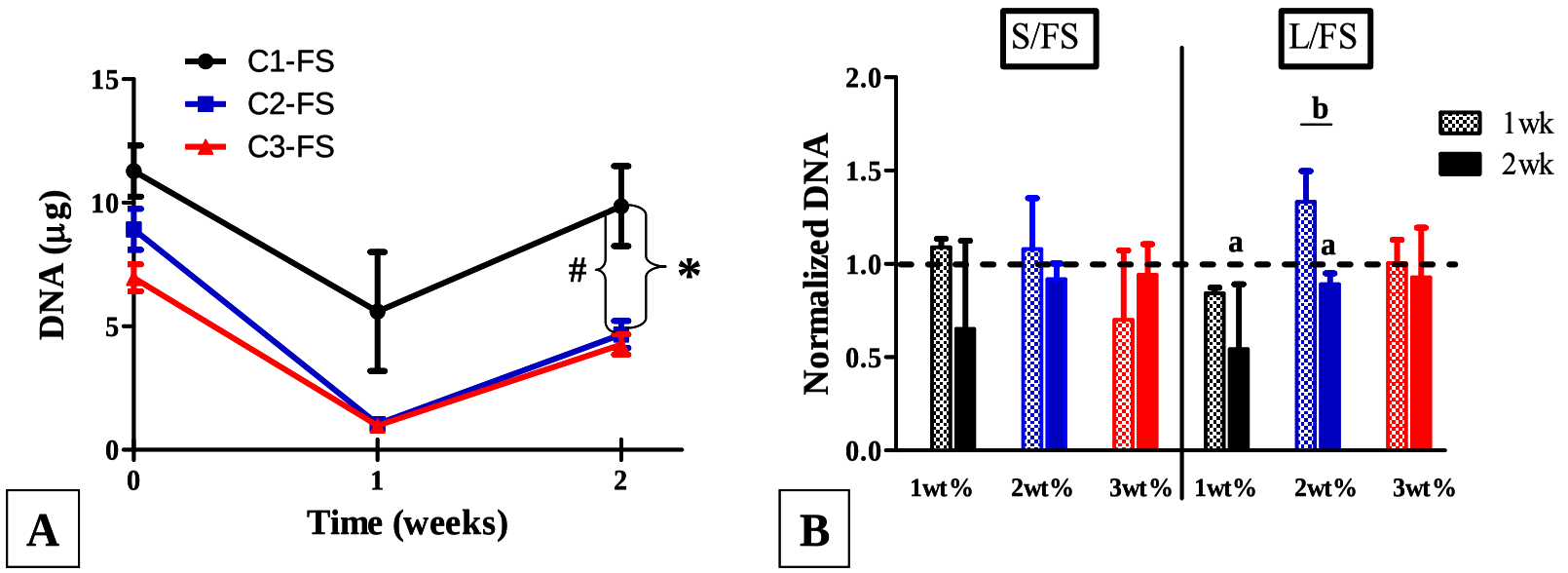

Figure 5.1: Average microgram of DNA per MSC seeded gel as a function of (a) scaffold composition and (b) loading condition (mean ± stdev.; n = 4-5). Free swell, static, and dynamic are represented as FS, S and L, respectively, and 1-, 2-, and 3wt% gels are represented by C1, C2 and C3 respectively. # and * represent significant differences between 1wt% gels and 2 and 3wt% gels, respectively. [a] indicates significant difference from free swell condition and [b] indicates significant difference with time

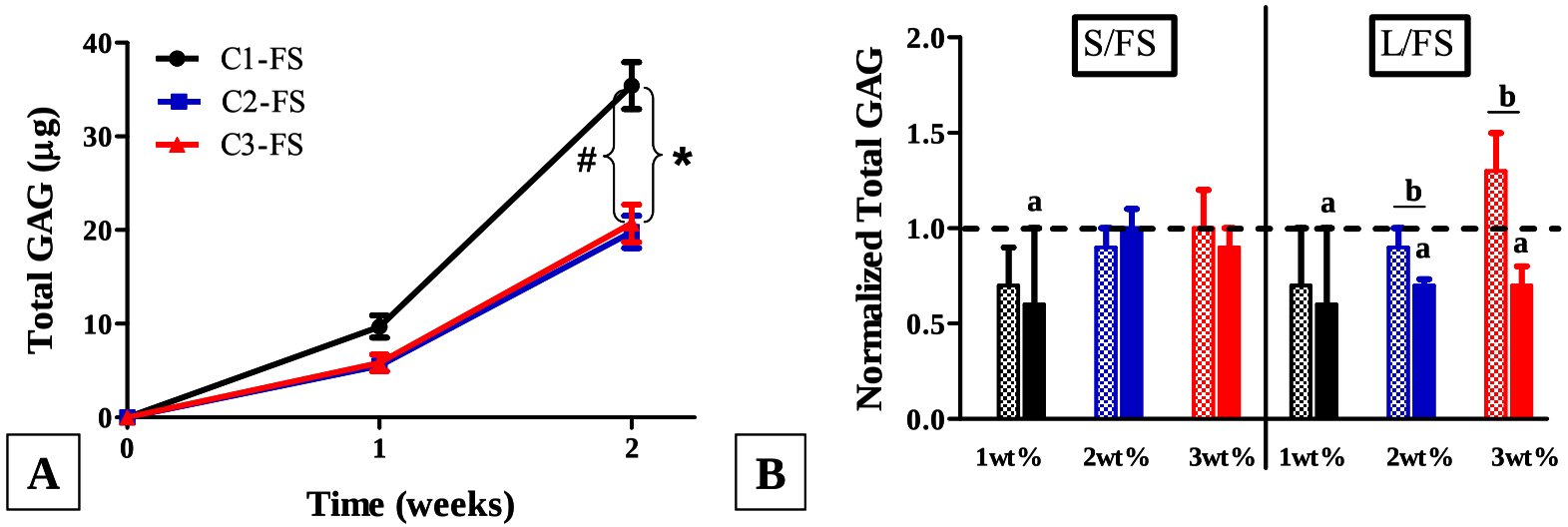

Figure 5.2: Average total GAG produced per MSC seeded gel as a function of scaffold composition and loading condition (MSC ± stdev.; n = 4) displayed as raw data (a) or loaded conditions (b) normalized to free swell. # and * represent significant differences between 1wt% gels and 2 and 3wt% gels, respectively. [a] indicates significant difference from free swell condition and [b] indicates significant difference with time

5.3a). Both static and dynamic loading decreased gel GAG content in gels of all weight percents, when compared to free swell gels ($p<0.05$) (Fig. 5.3b). And static loading decreased gel GAG content only in 2wt% gels ($p=0.047$), while dynamic loading decreased gel GAG in all gels of all weight percents ($p\leq0.0012$), by the second week in culture. In addition, the amount of glycosaminoglycans released to the surrounding medium increased with time ($p<0.05$). 1wt% gels released significantly larger amounts than either 2 or 3wt% gels when cultured under free swell (Fig. 5.4a), while no difference was found between 2 & 3wt% gels. Both static and dynamic loading significantly decreased the amounts released by 1wt% gels ($p<0.05$), while dynamic loading significantly increased by 3wt% gels during the first week of culture (Fig. 5.4b and 5.4c).

GAG retention decreased with time for all conditions and the drop in retention was more drastic for cells encapsulated in 1wt% gels (Fig. 5.5a). Retention by 1wt% gels was significantly lower than 2 and 3wt% gels ($p<0.02$) when cultured under free swell (Fig. 5.5a). Only statically loaded 1wt% gels at 1 week of culture had a significantly different amount of GAG retained, when compared to free swell ($p<0.05$) (Fig. 5.5b). And dynamic loading decreased retention only in 2wt% gels by the second week of culture ($p=0.014$).

Histology and Immunohistochemical Assessment

One weight percent gels had more diffuse GAG and collagen staining as evident by histological analysis (data not shown), although staining was predominantly localized to the circumference of the gels. GAG and Collagen staining was similar in 2 and 3wt% gels, with few localized areas of large matrix deposits

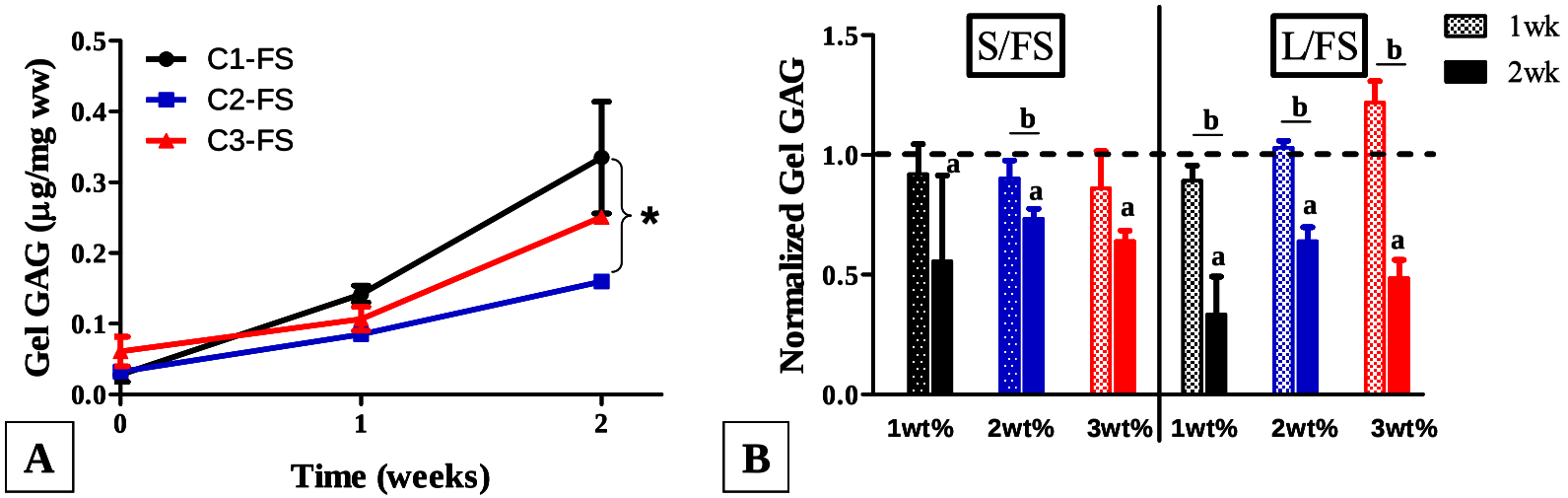

Figure 5.3: Average amount of GAG per MSC seeded gel normalized to weight wet, as a function of scaffold composition and loading condition (MSC ± stdev.; n = 4) displayed as raw data (a) or loaded conditions (b) normalized to free swell values. # and * represent significant differences between 1wt% gels and 2 and 3wt% gels, respectively. [a] indicates significant difference from free swell condition and [b] indicates significant difference with time

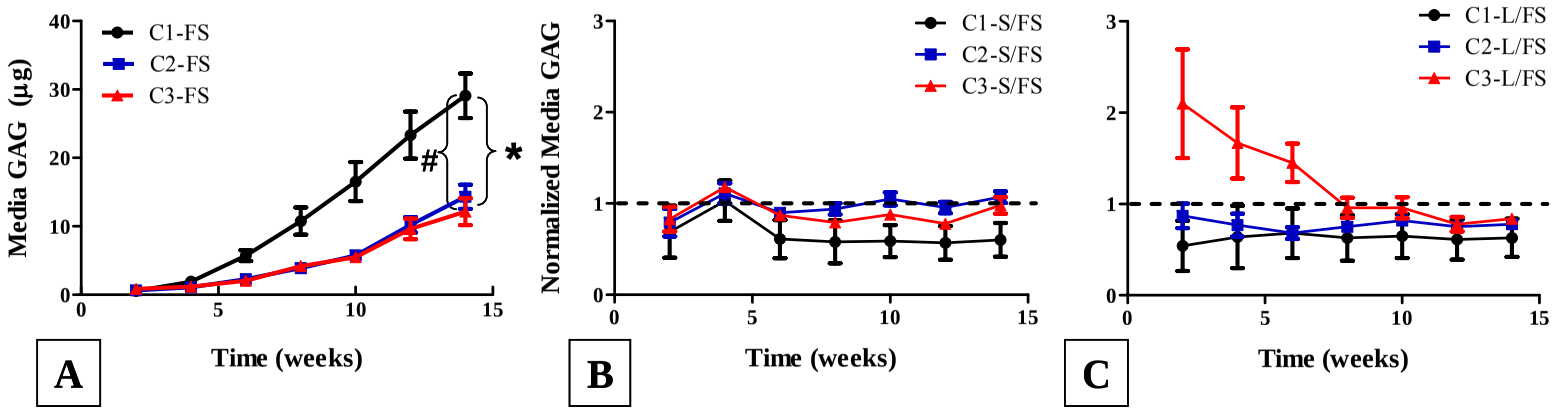

Figure 5.4: Average amount of GAG cumulatively released to the surrounding medium by MSC seeded gels, as a function of scaffold composition and loading condition (MSC ± stdev.; n = 4) displayed as raw data (a) or static (b) and dynamically loaded (c) conditions normalized to free swell values. # and * represent significant differences between 1wt% gels and 2 and 3wt% gels, respectively (all with $p<0.05$)

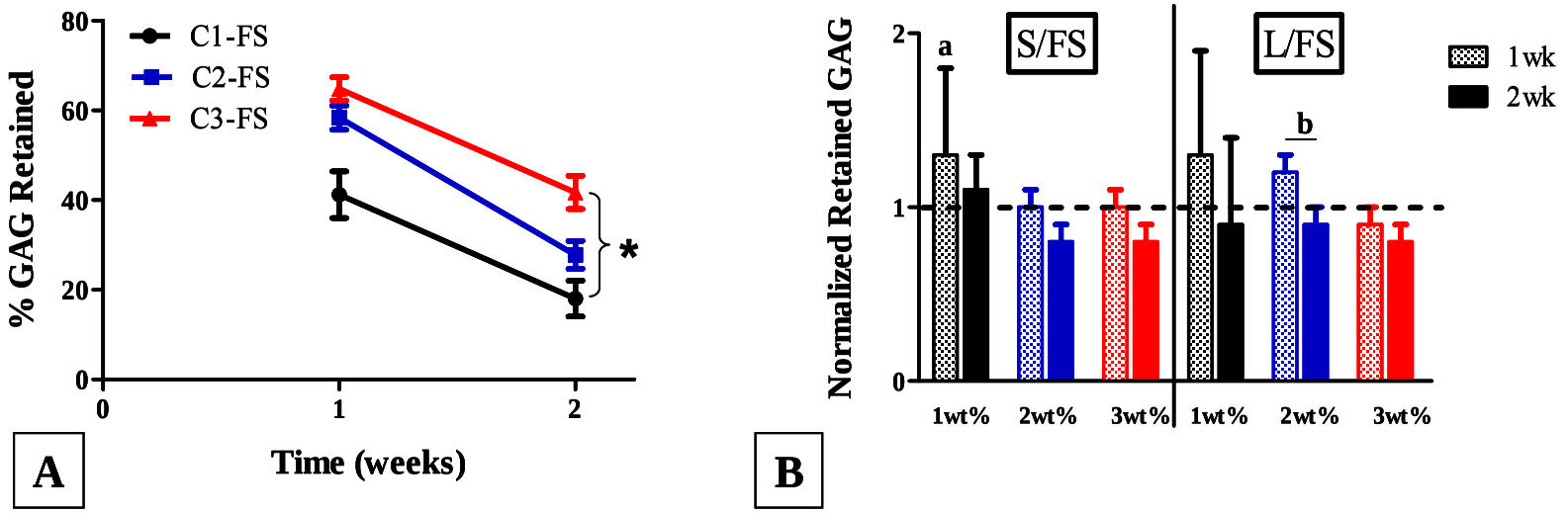

Figure 5.5: Average percentage of GAG retained within MSC seeded constructs, as a function of scaffold composition and loading condition (MSC ± stdev.; n = 4) displayed as raw data (a) or loaded conditions (b) normalized to free swell values. # and * represent significant differences between 1wt% gels and 2 and 3wt% gels, respectively. [a] indicates significant difference from free swell condition and [b] indicates significant difference with time (all with $p<0.05$)

found at the circumference of 2wt% gels and fewer in 3wt% gels. There was no difference in staining for gels statically or dynamically cultured.

Immunohistochemical analysis of link protein localization showed diffuse staining within the constructs of all conditions tested (Fig. 5.6). Gels cultured under free swell had more link protein stains, evident throughout the body of the construct. When statically or dynamically loaded, gels were found to have less link protein localization, and this was more evident in 2 and 3wt% gels.

Mechanical Assessment

No change in aggregate modulus was found regardless of time in culture, culture condition or scaffold composition (data not shown).

FE analysis vs Total GAG

In relating physical stimuli to total GAG produced, the range of pressures and fluid velocities produced within the different scaffold compositions scaled linearly with total GAG produced. The stimuli produced by dynamic loading of highest weight percent gel resulted in the largest increase in GAG production (Table 5.1).

Discussion

This study demonstrates that mesenchymal stem cells respond to scaffold composition under free swell conditions and respond minimally to scaffold composition when either statically or dynamically loaded. The least stiff and most permeable constructs studied (1wt% alginate) resulted in the production of significantly larger amounts of glycosaminoglycan when cultured under free swell conditions. One weight percent gels also released the largest amounts to their surrounding medium. Although lowest for 1wt% constructs, all gels had a significant

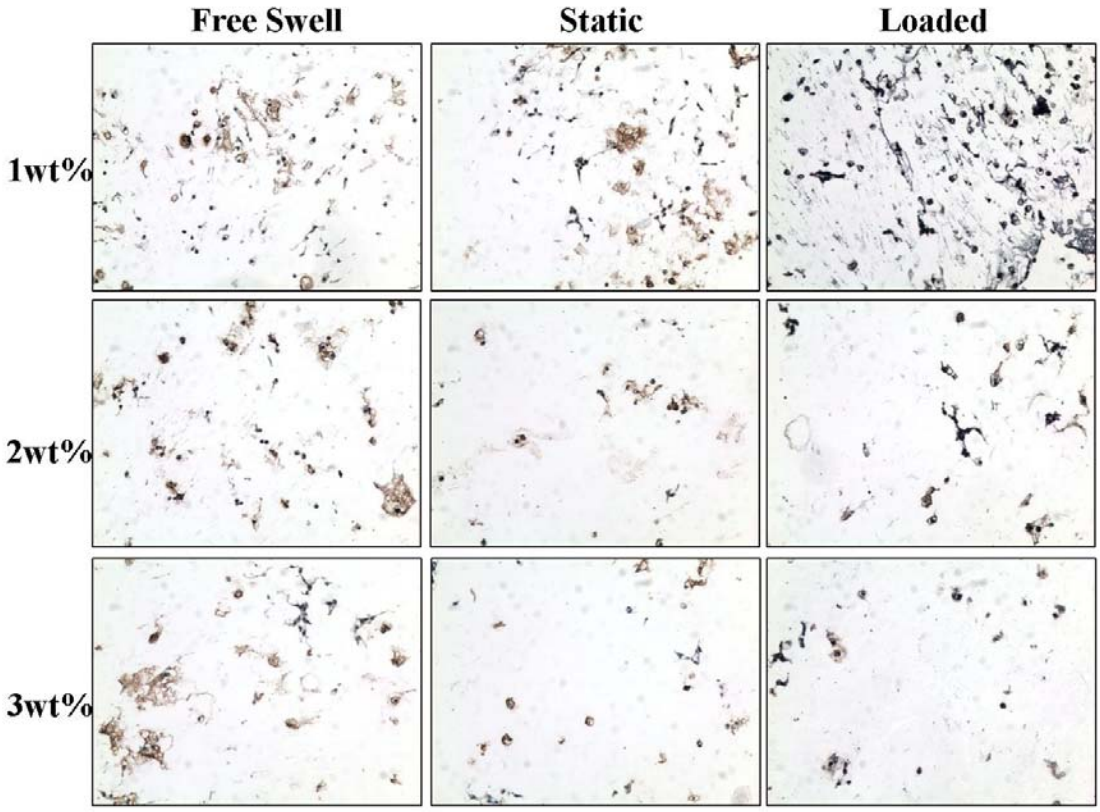

Figure 5.6: Representative sample images of MSC seeded gels analyzed for link protein using immunohistochemical analysis on gels at 2 weeks (images at 200X magnification). The images show samples staining positively for link protein (brown stains) that are mostly localized to areas surrounding the encapsulated cells (dark blue).

Table 5.1: Comparisons of finite element analyzed physical stimuli to total GAG produced (normalized to free swell) by 2 weeks for all scaffold compositions studied.

	Pressure (kPa)	**Radial Velocity (μm/s)**	**L/FS Total GAG**
C1	194	3.5	0.7
C2	217.6	3.7	0.9
C3	442	7.1	1.3

drop in retention from the first to second week of culture. Lastly, although static and dynamic loading had no effect on GAG loss in 1wt% gels, both loading conditions significantly decreased GAG retention in 2 and 3wt% gels.

Several studies have assessed chondrocyte to response to dynamic compression (33, 37, 43, 47, 174, 183). These studies have shown up-regulation of extracellular matrix production by chondrocytes with the application of dynamic stimulation. Mesenchymal stem cell response to dynamic loading has been less studied, with most studies assessing response over much shorter time periods and mostly using gene expression analysis (45, 136, 184-187). These studies have shown variable response to mechanical loading, which we have recently established to result from differences in loading conditions, and scaffold materials (171). As assessed by finite element analysis, different levels of physical stimuli were present in the loading constructs used in our study. However, the different mean levels of physical stimuli, present in either statically or dynamically loaded gels, did not elicit different responses. In fact, static and dynamical loading was found to have an adverse effect on MSC matrix metabolism.

The inability of intermittent dynamic compression to assist in the formation of a more functional cartilaginous tissue when compared to free swell controls was highlighted by Thorpe et al. (186). This reflects the finding of our study, where neither static nor dynamic loading was found to enhance matrix production. A possible explanation is that due to the early application of loading to the constructs, the chondrogenic effects of the stimuli may be muted since MSCs are still undergoing chondrogenesis. Indeed, as observed in a study by Mouw et al. (45), the response of bone marrow derived MSCs encapsulated in agarose to dynamic loading did not enhance matrix production until 16 days free swell culture with TGF-β1. This two week pre-culture allowed the chondrogenic process to take place, after which the

differentiated cells could response to the physical stimuli being applied. In addition, as shown by Buschmann et al. (33), chondrocyte respond to mechanical loading is greater at later time points and after the development of a matrix through which mechanotransduction signals can be better transferred.

Some of the dependence of cell metabolic activity on scaffold composition has been previously highlighted (33, 112, 173-176). For example, in the study by Buschmann et al (33), no significant difference was found in GAG and DNA content of 2 and 3wt% agarose seeded constructs, which is consistent with the findings of this study. Unfortunately, very few studies have sought to assess stem cell response to scaffold composition. In this study, we have shown that scaffold composition modulates stem cells' ability to produce and assembly an extracellular matrix. Their response to scaffold composition is muted with the application of loading, both static and dynamic. However, only a single combination of loading parameters was examined here, and scaffold composition may up-regulate matrix production by MSCs when loaded using different combinations of parameters. Although a peak to peak strain of 5% at a frequency of 1Hz is widely used in dynamic loading studies, larger and smaller combinations of strain and frequency have been used to show differential response of chondrocytes to those parameters (36, 48, 180, 188). MSCs are expected to respond differently to various combinations of strain and frequency as well.

In this study, we have highlighted the important roles scaffold composition play in mesenchymal stem cell metabolic activity and the important effect it has under static and dynamic loading. The data presented here suggest that the actual physical stimuli present within loading scaffolds (pressures, strains and fluid velocity gradients) are better predictors of cell response and that physical stimuli may compensate for differences in scaffold composition.

CHAPTER 6

Conclusions

This dissertation assessed the ability of chondrocytes and mesenchymal stem cells to produce and assemble extracellular matrix towards engineering cartilage tissue. To establish baseline behaviors of these cells under widely studied cartilage tissue engineering conditions, the effects of cell seeding density, type and species on tissue formation was first assessed (Chapter 2). Then to elucidate the complex environments cells might sense when encapsulated in scaffolds under loading, a finite element model of a dynamically loaded scaffold was developed using COMSOL multiphysics (Chapter 3). Finally, to relate the physical stimuli present in loaded scaffolds to cell behavior, studies were done to assess glycosaminoglycan production and assembly within dynamically loading scaffolds, using chondrocytes (Chapter 4) and mesenchymal stem cells (Chapter 5). This chapter discusses the main findings of this dissertation and proposes future studies that can build on this body of work.

In chapter 1, ECM assembly by chondrocytes was found to depend on cell density and was shown to be different between chondrocytes and chondrogenically differentiated MSCs. The most important result from this body of work was elucidating the limited ability of MSCs to assemble proteoglycan compared to chondrocytes, for which one of the causes may be reduced link protein production. Cartilage extracellular matrix production has been shown to be different for MSCs compared to chondrocytes (88, 133). But this differential response to chondrogenic culture has not been studied for varying cell densities or species. One of the consequences of the limitation in the use of MSCs was that GAG retention, although increasing with seeding density, was higher in chondrocyte seeded gels than MSC

encapsulated gels. Despite this disadvantage, chondrogenically differentiated first passage MSCs did produce the largest amounts of GAG. Although, unfortunately, much of the proteoglycan was subsequently lost to the surrounding culture medium. Finally, GAG production and retention by equine chondrocytes and MSCs was lower than that of the bovine chondrocytes, the cell type most commonly used to study cartilage matrix assembly.

Although the effects of the parameters studied in the first chapter have been studied independently (42, 81, 82, 101, 116, 142, 189), few studies have assessed loss of matrix components to the surrounding medium and fewer have sought to determine mechanisms of loss. The most biosynthetically active cells did not necessarily have the most functional matrices as evident by the higher ranges of aggregate moduli within the bovine chondrocyte seeded gels and the low ranges observed within the equine chondrocyte seeded gels. To begin to address this lack of retention, a recent study by Nicodemus et al (147) detailed the functionalization of polyethylene glycol scaffolds with link protein to served as anchors for proteoglycans produced. This scaffold modification resulted in increased retention of ECM components made by cells encapsulated within the scaffold. Optimizing proteoglycan retention should be an important area of study for the advancement of MSC-based cartilage tissue engineering.

With baseline behaviors of chondrocytes and MSCs using standard TE conditions established, the physical environments presented to cells was quantified when scaffolds are dynamically loaded. Knowing the important role mechanical loading plays in normal cartilage homeostasis (21, 22, 51, 52) has spurred the increase use of mechanical loading devices for TE construct stimulation (37, 42, 43, 45, 48, 165, 179, 190, 191). Detailed in chapter 3, a literature survey on the efficacy of mechanical stimulation for cartilage tissue engineering and regeneration was done.

The survey revealed a wide range in cell response with no clear pattern of efficacy discernable. Glycosaminoglycan production spanned orders of magnitude, with particular loading strain and frequency combinations stimulatory in some cases and inhibitory in others. The properties and characteristics of scaffolds will play a major role in the stimuli imposed on cells. With scaffolds used in cartilage tissue engineering having moduli spanning 3 orders of magnitude and permeabilites spanning 4 orders of magnitude, the large variations seen in cell response within such scaffolds when dynamically loaded are not surprising.

Next, to quantify the range in stimuli that responsible for the large variations in cell response, a poroelastic model was used to analyze the physical stimuli present within mechanically loaded scaffolds typically used in cartilage tissue engineering (chapter 3). Other studies have successfully used similar models to assess physical environments within loading tissues or scaffolds (121-123, 179, 192-194). As expected, all scaffold materials exhibited classic poroelastic behavior; i.e. pressurized cores with low fluid flow and edges with high radial fluid velocities. The simulated scaffolds ranged from stiff impermeable materials such as polyethylene glycol to complaint materials such as collagen. When modeling the dynamic compression of such scaffolds under the same loading condition, large variations in pressures, strains and fluid velocities profiles within the models indicated that cells are indeed subjected to different gradients of physical stimuli. This large variation is highly dependent on the scaffold used.

Although studies have utilized finite element analysis to quantify the stimuli present within loading scaffolds, direct correlation to cell behavior is rarely done. The patterns of stimuli present within our models are consistent with those published in few studies that do exist. In addition, this is the first study that expands the analysis to 360 modulus/permeability combinations, which included up to 10 different scaffold

materials in the over 30 different studies reviewed. As a result, it has enabled the creation of a map of the large variations possible within dynamically loading cartilage tissue engineering scaffolds and has highlighted the drastic differences in physical stimuli within these materials even when similarly loaded. This map can serve as a source for identifying key stimulatory factors that are critical for the formation of engineered tissue as well as for improving the functionality of the engineered constructs.

The results detailed in chapters 4 and 5 gives insight into the large variations in metabolic response seen in studies involving mechanical stimulation of cell-seeded constructs. Elucidated in these chapters, the same loading conditions were found to produce very different results due to differences in material properties. The data presented in chapter 3 has shown that the pressures seen within loading cartilage plugs (similar to conditions that may be observed in vivo) are still much higher than those being produced in scaffolds, but that the loads produced within scaffolds can be as complex. With the knowledge that scaffold properties play a major role in cell response to loading, ranges of physical stimuli present within loading scaffolds responsible for specific cell behaviors/response were then determined. Therefore, the experiments analyzed in chapter 4 sought to elucidate the physical stimuli driving chondrocyte response to loading. First, finite element analysis was used to estimate the spatial distribution of physical stimuli within engineered constructs of a similar material but with different compositions and mechanical properties. The effects these ranges in stimuli would have on matrix metabolism and assembly by chondrocytes seeded within such constructs was then characterized.

The results discussed in chapter 4 demonstrated that scaffold compositions (and the resulting mechanical properties) affect articular chondrocyte proteoglycan assembly and response to mechanical loading. The least compliant and most

permeable constructs (1wt% alginate) produced the largest amounts of glycosaminoglycan and released the most GAG to the surrounding medium. And although loading had no effect on the total GAG produced, dynamic loading increased gel GAG content in 2wt% and 3wt% gels with time. As previously shown (33, 136, 170), this response to loading would be expected to increase with increasing in culture period. The body of work in this chapter suggests a change in paradigm. It suggests that the actual physical stimuli present within loading scaffolds (pressures, strains and fluid velocity gradients) are better predictors of cell response.

In assessing MSC response to scaffold composition and dynamic compression, as observed in chapter 2, MSCs responded differently when compared to chondrocytes. Mesenchymal stem cells responded to scaffold composition only under free swell conditions. When cultured in free swell, 1wt% gels produced more total and had higher amounts of gel GAG than either 2 or 3wt% gels (for which there was no difference). No difference in total or gel GAG was found for constructs from all weight percents subjected to either static or dynamic loading, by 2 weeks of culture. Alternatively, compared to chondrocyte seeded gels, dynamic loading significantly decreased the total amount of GAG produced by 2 weeks in MSC seeded constructs. And both static and dynamic loading significantly decreased gel GAG content by 2 weeks of culture.

Analysis of GAG loss to the medium still showed large losses especially by 1wt% gels and, in this case, loss was enhanced by static loading in 1 and 3wt% gels and by dynamic loading in all compositions studied. Retention analysis showed a clear dependence on scaffold composition in free swell samples, with 3wt% gels retaining more than 2wt% and 2wt% retaining more than 1wt% gels. With static and dynamic loading, 3wt% gels retained more GAG than either 1 or 2wt% gels, for which there was no difference in retention either. Both static and dynamic loading decreased

retention when compared to free swell samples. This increased loss of GAG due to loading induced convection can once again be tied to reduced link protein production by MSCs.

To our knowledge, these studies are the first to systematically quantify cell response to specific stimuli presented within loading scaffolds. The results highlighted the significant role scaffold composition plays in determining cells response. Although differential scaffold response to loading was muted, response would be expected to change with increasing culture periods, after which varying amounts of retained matrix will begin to determine the physical environment.

Future work

Although this dissertation has highlighted a major difference between chondrocyte and MSC proteoglycan assembly, more analyses are still required before MSCs can be considered equal replacements for chondrocytes. This section presents potential extensions of the work detailed in this thesis that may strengthen the knowledge on chondrocyte and/or MSC response to tissue engineering conditions.

Further elucidate other mechanisms that may be responsible for GAG loss.

Immunohistochemical analysis has been used in this dissertation to show the presence or absence of link protein localization within engineered constructs, using either chondrocytes or mesenchymal stem cell. Due to the reduced ability to retain produced GAG, link protein analysis was a logical first step to determine mechanisms responsible for the reduction in retention seen in MSC seeded constructs. Although link protein is responsible for stabilizing proteoglycan molecules onto hyaluronan to form aggregates, reduced amount of hyaluronan may also be a reason for the reduced

retention. Further immunohistochemical analysis can be done to determine hyaluronan localization within the engineered constructs. The outcome of such an analysis may also highlight another difference between chondrocyte and MSC matrix production and assembly.

In addition to the presence or absence of key matrix molecules essential for glycosaminoglycan aggregation, higher than normal enzymatic activity may also be responsible for reduced GAG retention. There are normal levels of cartilage specific enzymes that are required for tissue homeostasis. The over expression and/or production of catabolic enzymes (e.g. aggrecanases, matrix metalloproteinases and other members of the ADAMTS family) will lead to increased matrix degradation, resulting in decreased retention. Analysis of fragments of proteoglycan within the gels and in the surrounding medium can help determine if increased enzymatic activity is another mechanism responsible for GAG loss. Determining the size of fragments of proteoglycan lost can be done using a number of techniques, including western blot analysis or liquid chromatography, which have been successful used to analyze by products of matrix degradation (195, 196). These methods use epitope antibodies (e.g. epitope 3B3(-) and 846) to analyze volumes of proteoglycans that have been cleaved as a result catabolic activity, which are smaller in size compared to full length proteoglycan molecules.

Analyzing production and assembly of other cartilage extracellular matrix molecules.

Although proteoglycan molecules make up a 15–40% and collagen fibers, 50-75% of the dry mass of cartilage tissue, this ratio is different for tissue engineered cartilage. The analysis presented in this dissertation has focused mainly on the assembly of proteoglycan. Collagen assessment should be a logical step for further

analysis of the effects of the parameters perturbed in this dissertation, on cartilage engineered constructs. The study of collagen production and assembly may further highlight differences in the ability of chondrocytes and MSCs to produce functional cartilage tissue.

To begin assess metabolism of other extracellular matrix components in tissue engineered constructs, histological analysis of the engineered gels were done. The results of this analysis have been included in the appendix sections, as supplemental data on cell behavior. Further analysis should include biochemical analysis of hydroxyproline, a major component of collagen, within the constructs or released to the surrounding medium.

Effects of larger ranges in physical stimuli and longer time points on cell behavior.

In chapter 3, a survey was done to assess the range of scaffolds types and properties and loading conditions responsible for a particular cell response. In this survey, cell response to these factors was found to range across four orders of magnitude. This range was as a result of the multi-factorial effects within each experiment, which lead to decreases or increases in matrix production. As determined in the chapter, highly variable and complex environments are generated within the scaffolds when subjected to dynamic compression. The experiments carried out in chapters 4 and 5 sought to assess cell response to a very narrow range of scaffold properties. To expand on this analysis cell response to larger ranges in scaffold properties need to be done. The parametric analysis of loading scaffold done in chapter 3 showed that the physical stimuli within the stiffest, least permeable scaffold was still orders of magnitude below the stimuli present in loading cartilage plugs. To assess the response of cells to physiologically relevant physical stimuli, further

analysis of cells encapsulated in stiffer, less permeable gels is required. To this end, finite element models of dynamically loading polyethylene glycol scaffolds have been developed, the results of which are detailed in the appendix. The analysis of the physical environment within these scaffolds may result in stimuli closer to those seen in loading cartilage.

In addition, as indicated in chapters 4 and 5, a limitation of this dissertation is the short time points studied in analyzing physical stimuli effects on cells. And as discussed in those chapters, larger cells response to mechanical loading is observed at longer time points. This increased response is possibly due to cells' ability to directly interact with their environment after their production of matrix molecules to which they can bind to. Increasing culture period may show increased response (stimulatory or inhibitory) to the loading conditions studied in chapters 4 and 5.

Incorporate the use of functionalized scaffolds.

Another alternative to increasing cell interaction with mechanically loaded scaffolds is the use of ligand-functionalized scaffolds. Several studies have successfully functionalized RGD, the specific region to which cells bind to on matrix components, onto scaffold materials (197-199). These studies have shown differential response of cells to modified versus un-modified scaffolds, although they have mostly been done under free swell cultures conditions. For example, in the study by Connelly et al., increasing concentrations of RGD in modified alginate was found to increasingly inhibit chondrogenesis of bone marrow stromal cells (198). Extending the use of RGD-modified scaffolds to dynamic compression studies may create a more physiologically relevant environment to which cells respond differently. This increase in cell-matrix interaction may have an opposite effect under loading conditions and

result in increased chondrogenic response, leading to matrix production and assembly that may make for more functional constructs (197).

In addition, scaffolds can also be functionalized with matrix constituents that aid in the aggregate of cell generated extracellular matrix to increase retention. For example, functionalizing alginate scaffolds with link protein may have resulted in a different outcome than that seen in chapters 2, 4 and 5 of this dissertation. And indeed, as previously mentioned, a recent study by Nicodemus et al. (147) showed scaffolds functionalized with link protein successfully serving as anchors which increased retention of ECM molecules made by cells encapsulated within the scaffold.

Appendices

APPENDIX A

Supplementary Data for Chapters 2

The first aim of this dissertation detailed the effects of cell density and species on extracellular matrix assembly by chondrocytes and chondrogenically differentiated MSCs. This appendix contains supplementary supporting data not included in the body of the chapters. Specifically, it includes data on the cummulative release of GAG to the surrounding medium by the cell seeded scaffolds. This data was used to estimate the percent GAG retained within the gels as a function of time in culture. The next set graph shows the amount of GAG produced by the seeded cells normalized to the dry weight of the constructs. The trends in this data set is similar to that found for the data on amount of GAG produced normalized to the wet weight of the constructs. In addition, on analyzing GAG produced by cells, the last set of data included shows glycosaminoglycan localization within the gels as indicated by Safranin O staining as well as link protein localized around chondrocytes and their limited or lack of localization within MSC seeded gels. The last analysis of proteoglycan produced was done using Western blot analysis. The analysis shows evidence of the G1 and G3 domains (which are present on aggrecan molecules) in the medium in which MSC seeded constructs were incubated, which partially confirms chondrogenesis of the MSCs. Unfortunately, the results of the analysis produced a very murky result due the interference by alginate molecules.

Following the additional data on proteoglycan analysis are graphs and figures showing results of collagen assessment done via biochemical analysis of hydroxyproline and immunohistochemical analysis of both type I and II collagen. The biochemical analysis for hydroxyproline shows that the data on hydroxyproline gel

content was inconclusive due to large variations which we attribute to the possibility of alginate macromolecules interfering with the hydroxyproline assays of the gel samples. Alternatively, the trends of total hydroxyproline produced and amount retained were similar to that found for total GAG produced and retained. Although there was less of a dependence on cell density. Analysis of the type of collagen produced by the differentiated MSCs showed positive stained via immunohistochemistry for both type I and II collagen. Although there was more staining for type I collagen, the positive staining for type II collagen further confirms that the MSCs underwent chondrogenesis due to the culture conditions used for the experiments.

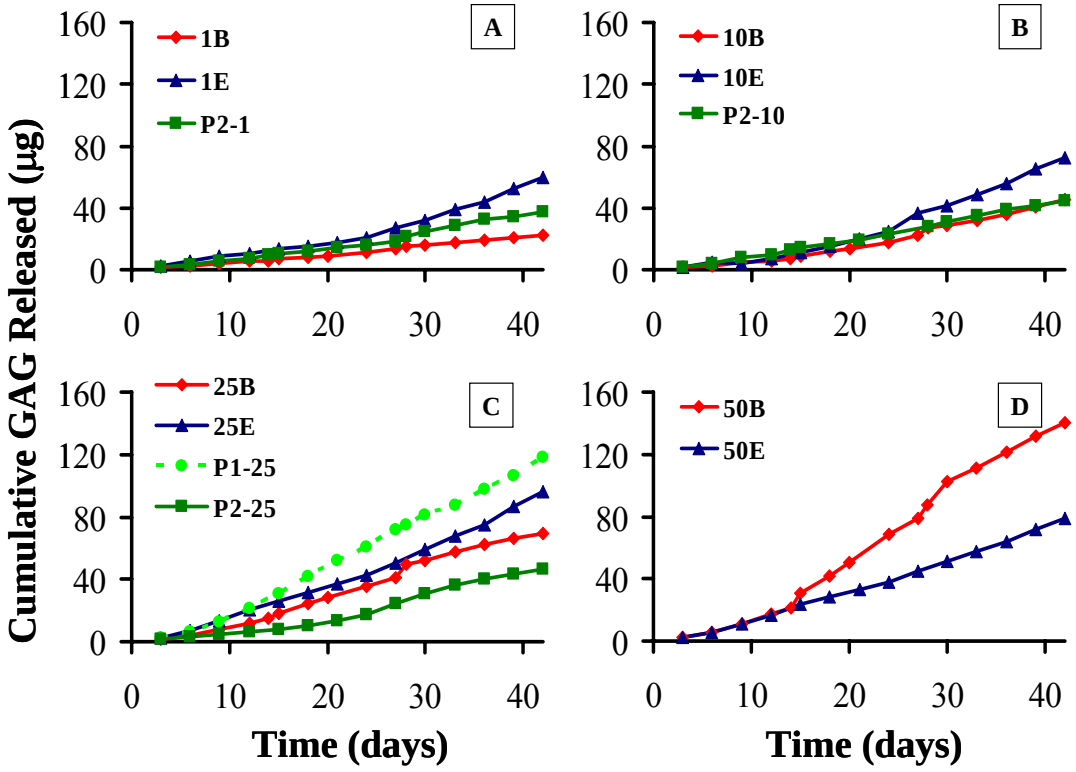

Cumulative release of GAG into media with time for gels seeded at 1 x 10^6 cells/ml (A), 10 x 10^6 cells/ml (B), 25 x 10^6 cells/ml (C), and 50 x 10^6 cells/ml (D). Release was quantified from pooled media from 7-8 disks for bovine AC, equine AC, P1 and P2 MSCs.

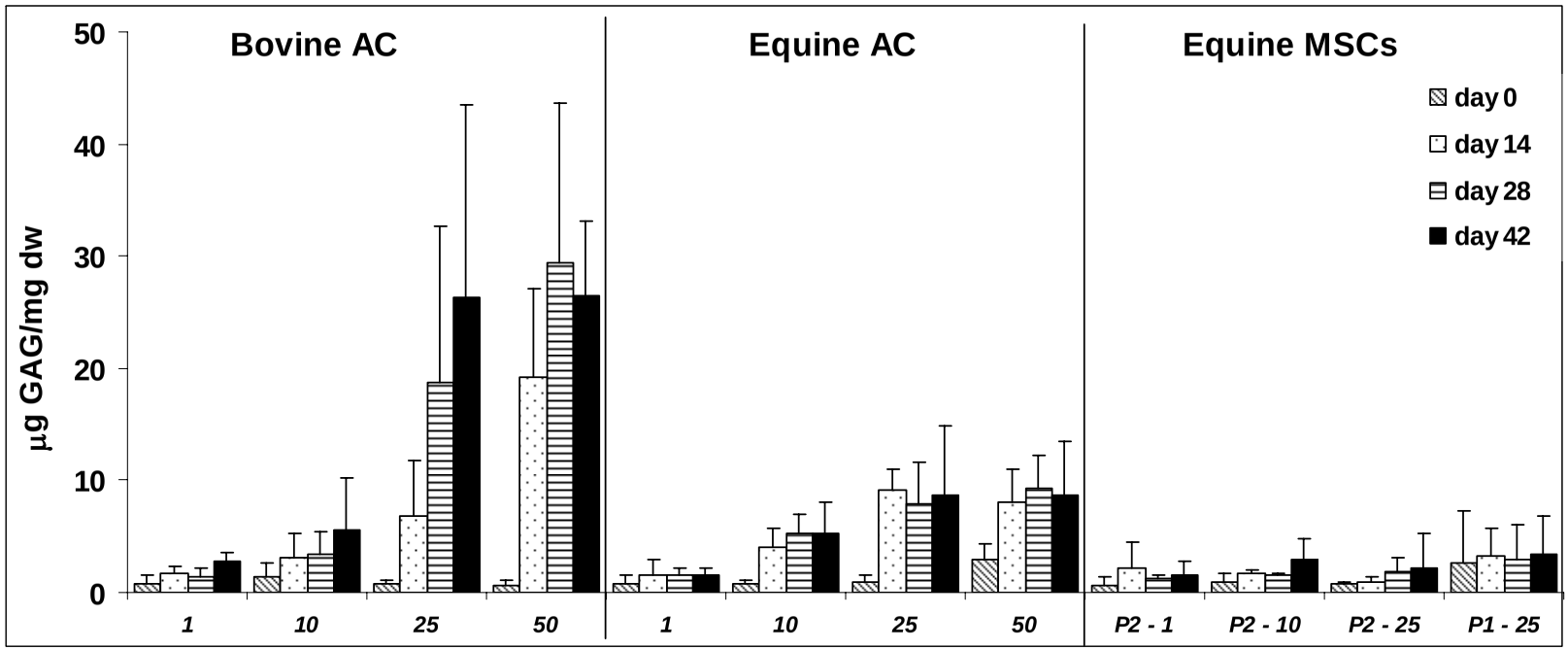

Average concentration of GAG in gels normalized to dry weight for bovine and equine AC and equine MSCs

(n = 7–9 ± st. dev.)

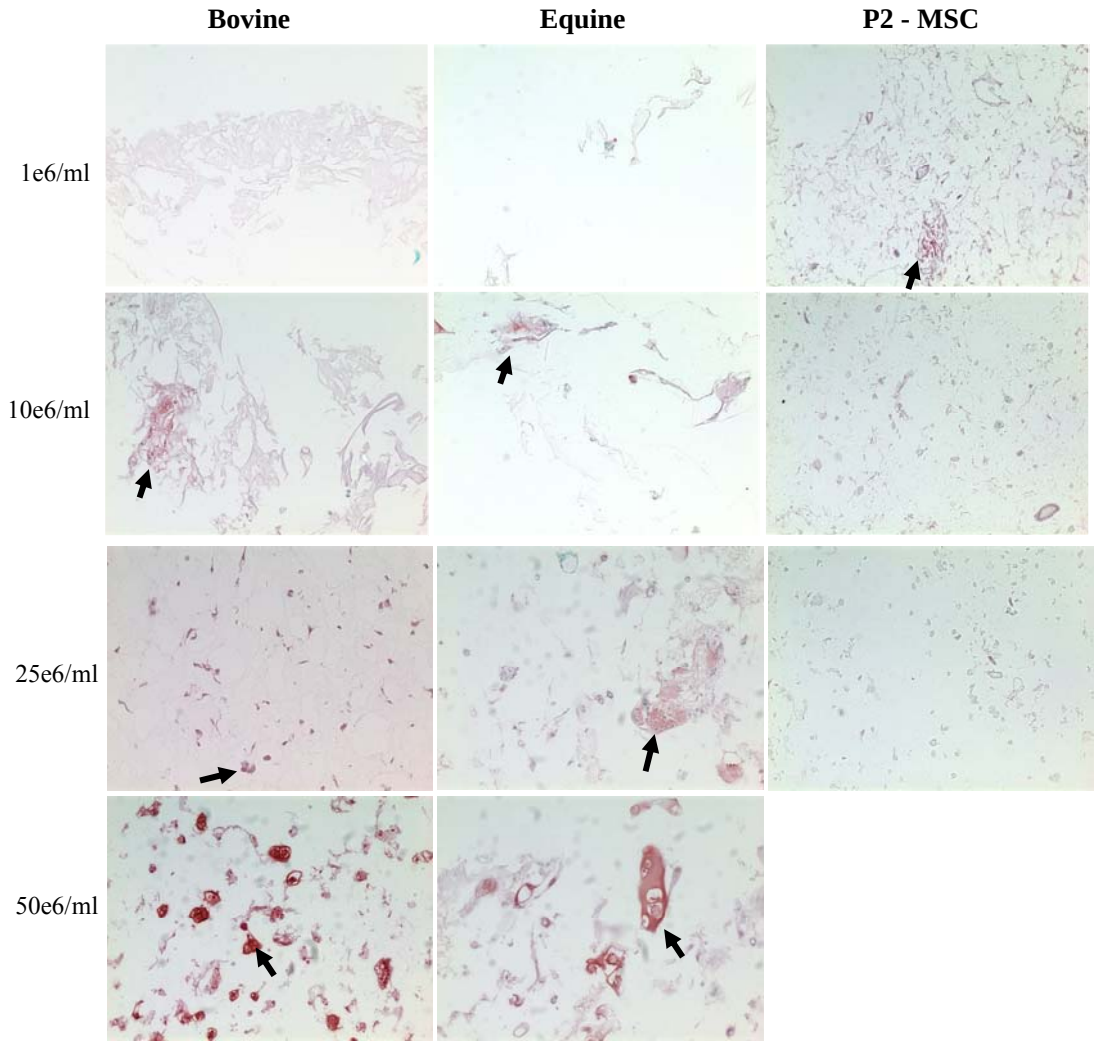

Sample images of gels stained for glycosaminoglycan via Safranin O by histological analysis on 6 week gels (images at 200X magnification)

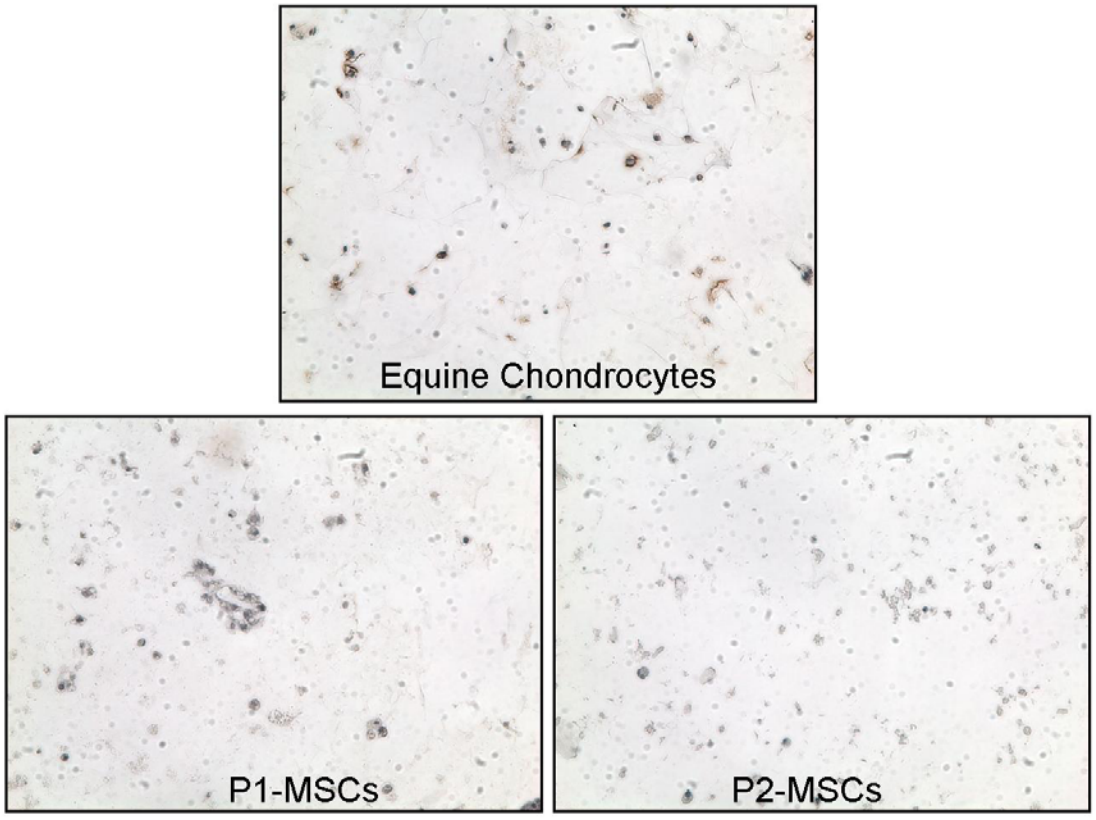

Representative sample images of chondrocyte and MSC seeded gels analyzed for link protein using immunohistochemical analysis on gels at 2 weeks (images at 200X magnification). The images show samples staining positively for link protein (brown stains) that are mostly localized to areas surrounding the encapsulated cells (dark blue).

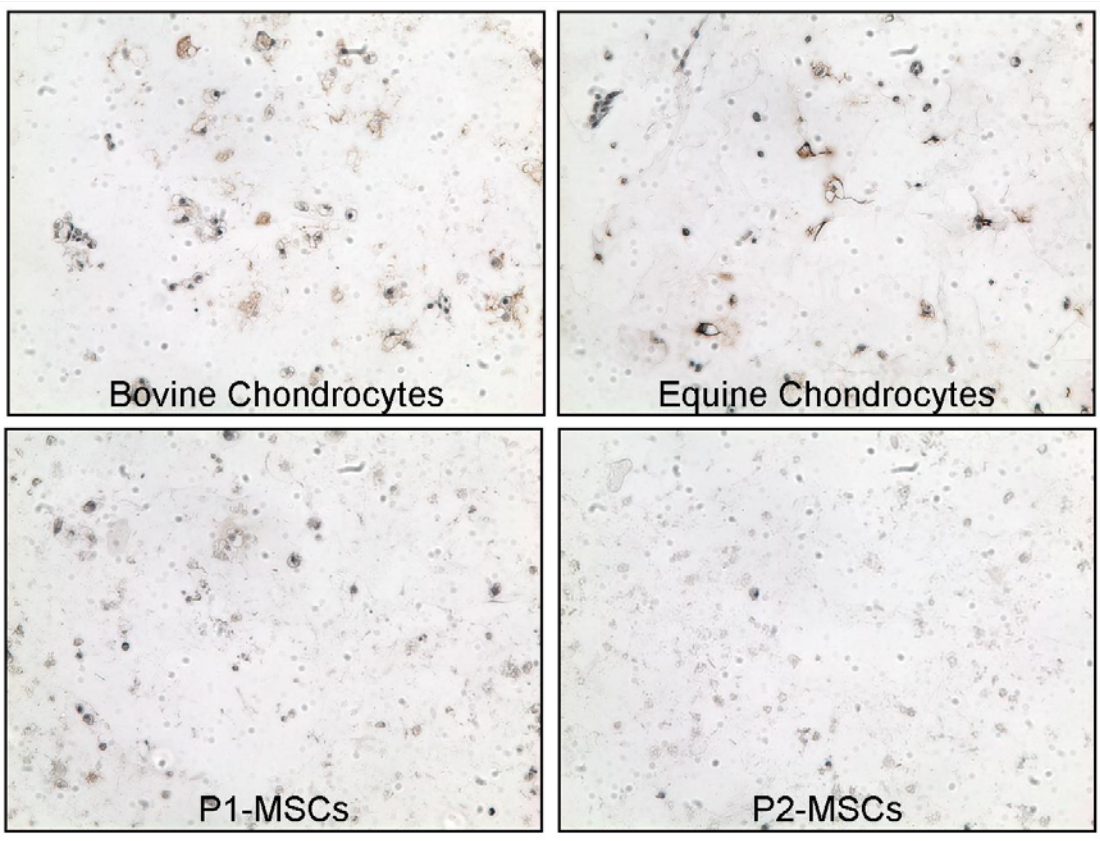

Representative sample images of chondrocyte and MSC seeded gels analyzed for link protein using immunohistochemical analysis on gels at 4 weeks (images at 200X magnification). The images show samples staining positively for link protein (brown stains) that are mostly localized to areas surrounding the encapsulated cells (dark blue).

Western Analysis

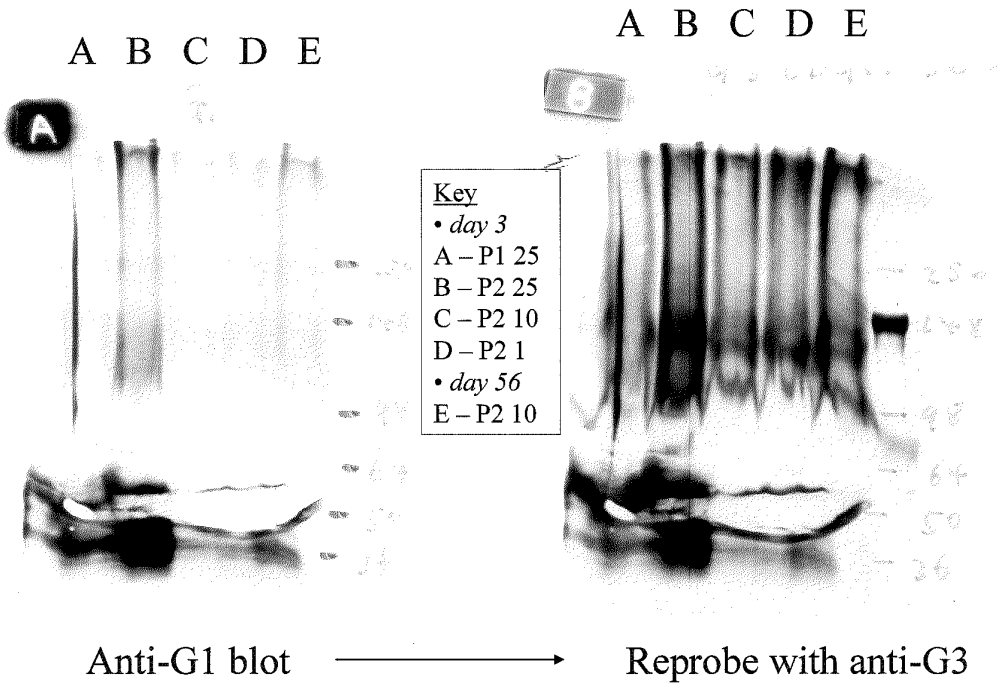

Western blot analysis of media collected for the presence and size of Aggrecan molecules using probes of the G1 and G3 domain. Samples are from first and second passage mesenchymal stem cell seeded constructs cultured for either 3 or 56 days.

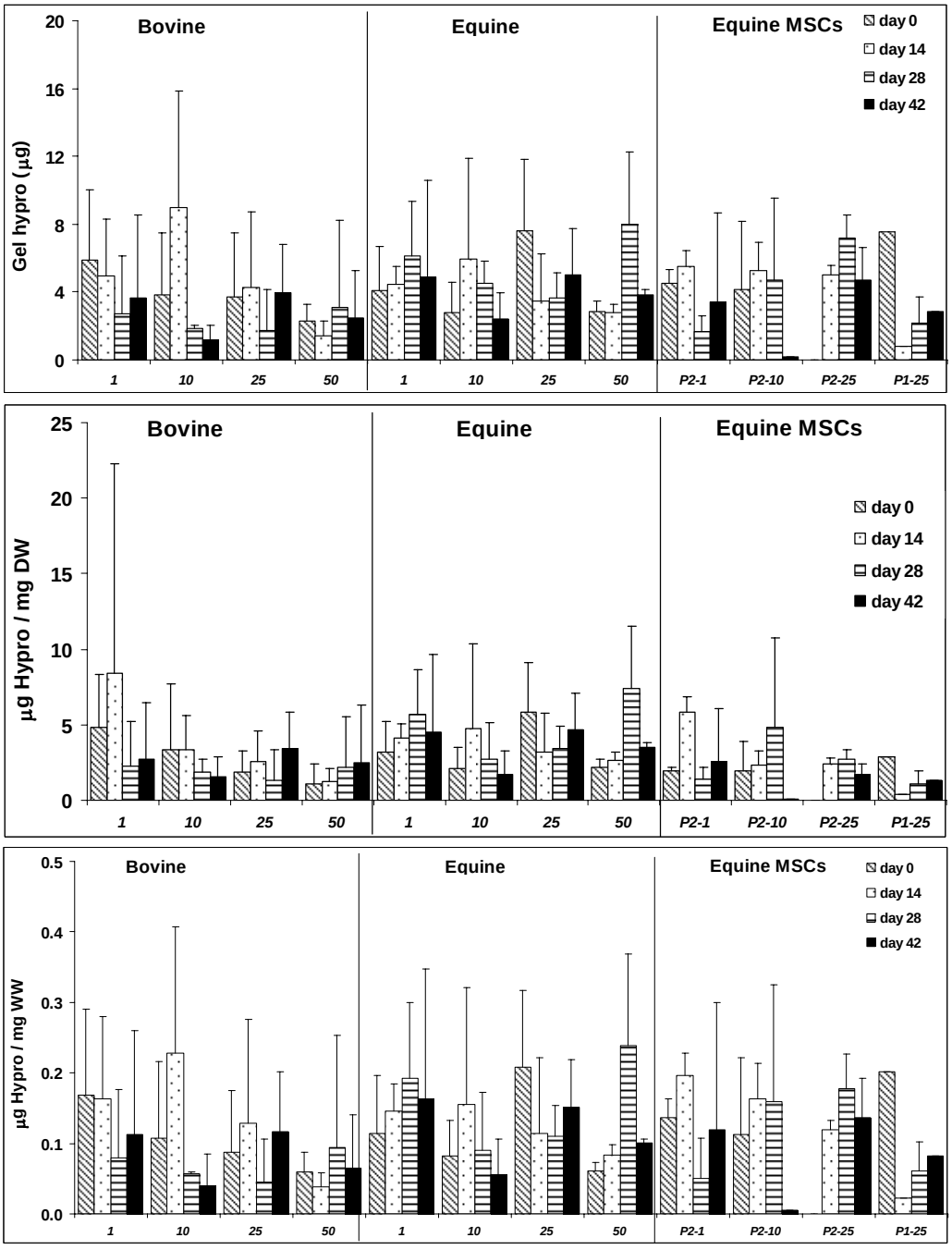

Average amount of hydroxyproline in gels in micrograms (top), normalized to dry weight (middle) and wet weight (bottom) for bovine and equine articular chondrocytes (AC) and equine MSCs (n = 7–9 ± stdev.) as a function of seeding density (x 10^6)

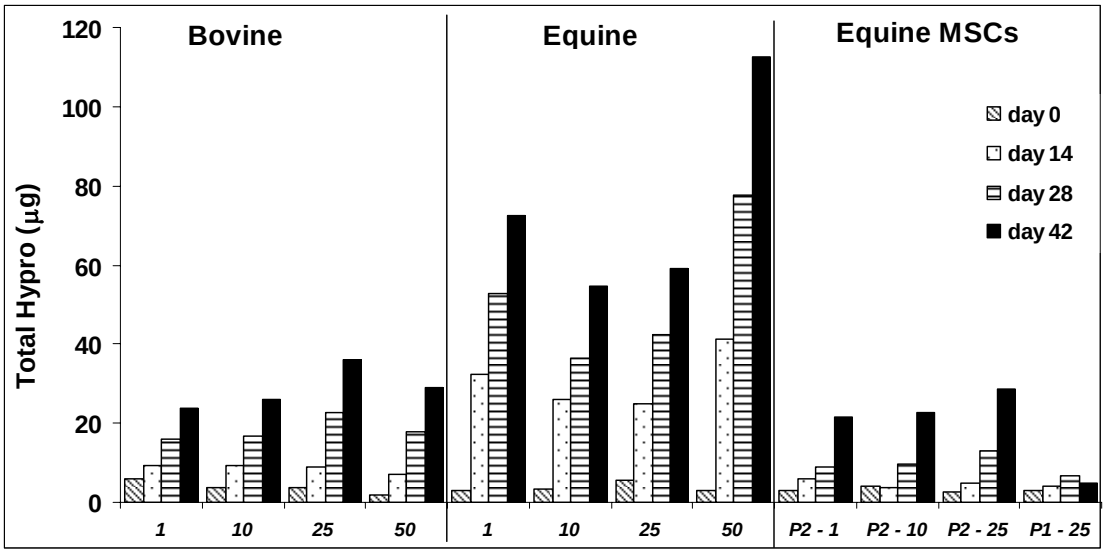

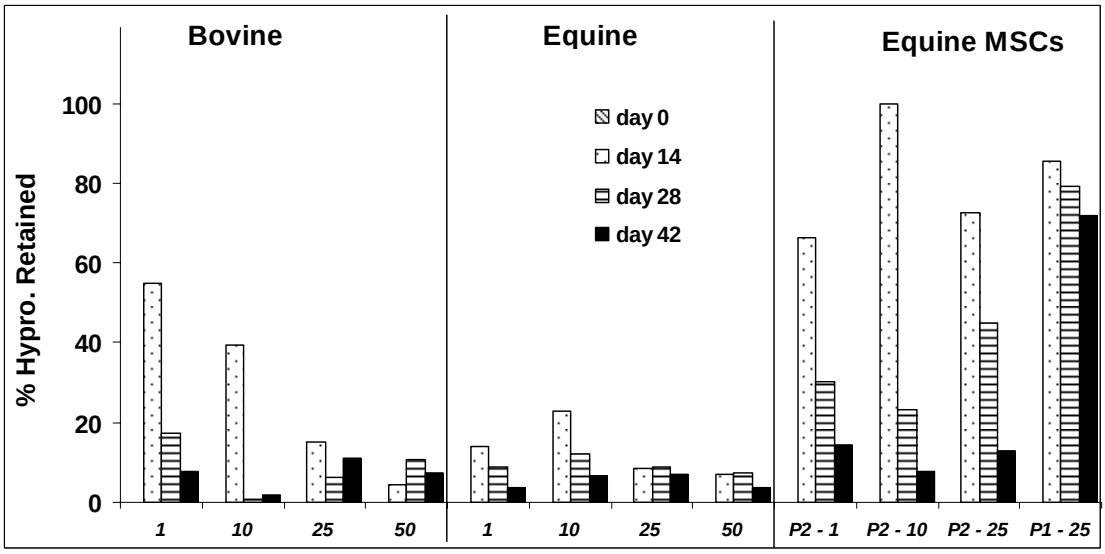

Average amount of total hydroxyproline produced by cell seeded constructs in micrograms (top) and percent retained within gels with time (bottom) for bovine and equine articular chondrocytes (AC) and equine MSCs (n = 7–9 ± stdev.) as a function of seeding density (x 10^6)

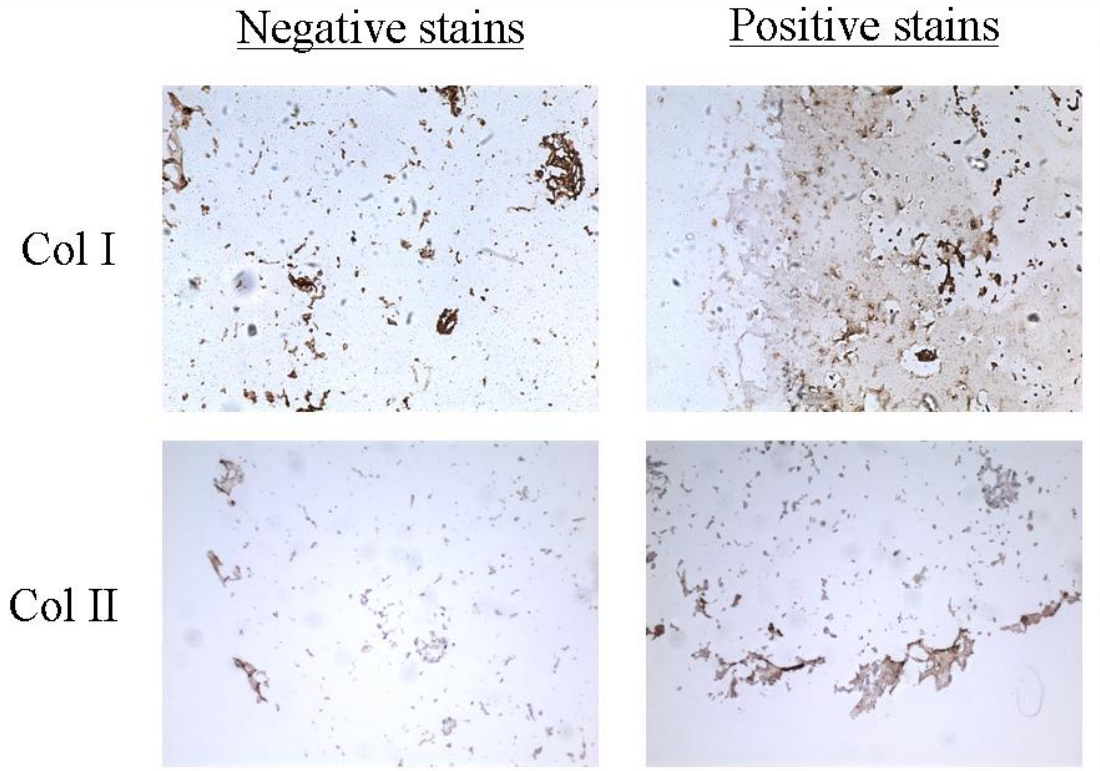

Representative sample images of MSC seeded gels analyzed for collagen I and II using immunohistochemical analysis on gels at 6 weeks (images at 100X magnification). The images show samples staining positively for collagen I and II (brown stains in "positive stains" panel).

APPENDIX B

Immunohistological Analysis of Link Protein

Introduction

The first, third, and fourth aims of this thesis qualifies the ability of chondrocytes and mesenchymal stem cells to produce link protein when subjected to conditions detailed in the body of this dissertation. This appendix details the steps of the protocol used on staining paraffin imbedded and sectioned slide for link protein using immunohistological analysis. It relies on the use of hyaluronidase for epitope recovery and the binding of link protein specific antibodies for the visualization of link protein localization. This protocol was adapted from the article by Caterson EJ, Nesti LJ, Li W, Danielson KG, Albert TJ, Vaccaro AR and Tuan RS, titled "Three dimensional cartilage formation by bone marrow-derived cells seeded in polylactide/alginate amalgam" (published in J Biomed Mater Res. 2001 Dec 5;57(3):394-403).

Materials

All chemicals were purchased from Sigma-Aldrich unless otherwise specified.

Tris-HCl – Cat. # T6666-250G

Sodium acetate – Cat. # S8750-500G

Bovine serum albumin – Cat. # A3803-100G

N-ethymaleimide – Cat. # E1271-1G

Hyaluronidase – Cat. # H3506

Methanol – Cat. # M1775

DAB histochemistry kit 1 (contained goat anti-mouse IgG-HRP): Invitrogen #D22185

Purified rat chondrosarcoma link protein-2 immunogen (monoclonal): Hybridoma bank #8-A-4

*NB: Final working solution of DAB should be made fresh and immediately before use on slides

Solutions to make before day of staining

Solution A (masses in parenthesis are for a 100ml volume), pH-ed to 8.0

50mM Tris-HCl (788mg)

30mM Sodium Acetate (246.09mg)

0.5mg/ml Bovine serum albumin (50mg)

10mM N-ethymaleimide (125.13mg)

Solutions to make on day of staining

Hyaluronidase solution

- 300U/ml hyaluronidase in solution A

3% hydrogen peroxide in methanol

Blocking solution

- 1% (10mg/ml) blocking reagent in PBS

Primary antibodies

- Link protein antibody solution (1:125 dilution) diluted in 1% blocking solution

HRP conjugate working solution

- prepare 1ug/ml working solution by diluting HRP-conjugate (1:500) in 1% blocking solution

Methodology

1. De-paraffinize and hydrate slides to distilled water
2. During hydration in distilled water, prepare enzyme solution if needed (i.e. hyaluronidase solution for link protein)
3. Predigest sections for 30mins at 37°C with enzyme solution to expose protein of interest
4. Rinse extensively in PBS
    - i.e. rinse with 3 changes of PBS for 5mins each
5. Treat with 3% hydrogen peroxide in methanol for 30mins to inactivate endogenous peroxidases at room temperature
6. Block with blocking serum solution for 30mins at room temperature
7. Incubate with primary antibody solution for 60mins at room temp.
    - check and hydrate samples periodically prevent sample dehydration
8. Rinse 3X with PBS
9. Prepare working solution of the HRP conjugate
10. Apply HRP-conjugate working solution to samples and incubate for 30-60mins at room temperature
11. Rinse 3X with PBS
12. Apply DAB/H_2O_2 solution to specimen and visualize under microscope to assess the degree of color development (10sec to 5mins)
13. Counter stain with Hematoxylin and eosin

Conclusion

The protocol outline above successfully shows localization of link protein on fixed and sectioned samples. Images showing the results of this protocol can be seen

in micrographs of stained slides from experiments detailed in above chapters, shown in appendix c.

APPENDIX C

Development of a Finite Element Model of a Dynamically Compressing Scaffold

Introduction

The second aim of this chapter focused on the development of a finite element model of a dynamically loading cartilage tissue engineering scaffold. This aim sought to quantify the physical stimuli present within loading scaffolds that may be imposed on cells seeded within them. In this aim, the parametric analysis of 16 scaffolds encompassing 360 different combinations of scaffold modulus and permeability was also reported. This appendix details the development of the model, analysis of its finite element model output and the code used for the parametric study.

Methods

Model Development

To analyze the physical stimuli (i.e. pressures, stresses, velocities and strains) present within a dynamically compressing scaffold, a time dependant coupled pore pressure/effective stress analysis was implemented using the structural mechanics and chemical engineering modules of COMSOL multiphysics software package (COMSOL, Burlington, MA). This was used to model fluid/solid interactions within the loading scaffolds. Darcy's law in the chemical engineering module (Eq. 1 and 2) and solid mechanics governing equations in the structural mechanics module (Eq. 3) were used. The governing equation for steady-state Darcy flow was set to depend on fluid density ρ_f, solid fraction θ_s, and fluid velocity v; the latter which was dependent

on the solid permeability κ, fluid viscosity η and pressure gradient ∇p. The equations are

$$\frac{\partial}{\partial t}\left(\rho_f \theta_s\right) + \nabla \bullet \rho_f v = \rho_f F, \tag{1}$$

$$v = -\frac{\kappa}{\eta}\left(\nabla p\right), \tag{2}$$

Scaffold solid deformation depended on the normal σ & shear τ stresses and strains ε imposed on the models as a result of the cyclic load, with the governing equations given by

$$\frac{\partial \sigma_r}{\partial r} + \frac{\partial \tau_{rz}}{\partial z} + \frac{\sigma_r - \sigma_\theta}{r} + F_r = 0, \qquad \frac{\partial \tau_{rz}}{\partial r} + \frac{\partial \sigma_z}{\partial z} + \frac{\tau_{rz}}{r} + F_z = 0,$$
$$\varepsilon_r = \frac{\partial u}{\partial r}, \qquad \varepsilon = \frac{u}{r}, \qquad \varepsilon_z = \frac{\partial w}{\partial z}, \qquad \gamma_{rz} = \frac{\partial u}{\partial z} + \frac{\partial w}{\partial r}, \tag{3}$$

A source term, given as *F* in equations 1 and 3, was implemented to define the fluid/solid interaction, coupling plane strain deformation to Darcy flow, and was imposed as

$$- \frac{\partial \varepsilon_r}{\partial t} + \frac{\partial \varepsilon_z}{\partial t}, \tag{4}$$

The model was assumed to be axi-symmetric in response and incompressible solid and fluid conditions were also assumed.

FE analysis of loading scaffolds

The finite element model a of scaffold undergoing uniaxial unconfined compression were created using COMSOL multiphysics software (Burlington, MA). The models were of a two dimensional axisymmetric scaffolds and contained 320 quadrilateral elements each which were exponentially biased to the edges and yielded a total of 3063 degrees of freedom. The scaffold materials were assumed to be homogenous and isotropic with strain dependent permeability. All scaffolds were assumed to be 98% porous with poisson's ratio of 0.167 and average solid density of 1240 Kg/m^3. The scaffolds were simulated to be fully hydrated with the fluid having an assumed viscosity of 0.001 Pa·s and density of 1000 Kg/m^3.

```
% COMSOL Multiphysics Model M-file
% Generated by COMSOL 3.3a (COMSOL 3.3.0.511, $Date: 2007/02/02 19:05:58 $)

flclear fem

% COMSOL version
clear vrsn
vrsn.name = 'COMSOL 3.3';
vrsn.ext = 'a';
vrsn.major = 0;
vrsn.build = 511;
vrsn.rcs = '$Name:  $';
vrsn.date = '$Date: 2007/02/02 19:05:58 $';
fem.version = vrsn;

% Geometry
g1=rect2(1,0.4,'base','corner','pos',[0,0]);
g2=rect2('0.005','0.0015','base','corner','pos',{'0','0'},'rot','0');

% Analyzed geometry
clear s
s.objs=;
s.name={'R1'};
s.tags={'g2'};

fem.draw=struct('s',s);
```

```
fem.geom=geomcsg(fem);
% COMSOL Multiphysics Model M-file
% Generated by COMSOL 3.3a (COMSOL 3.3.0.511, $Date: 2007/02/02 19:05:58 $)

% Geometry
g1=rect2('0.00125','0.001','base','corner','pos',{'0','0'},'rot','0');

% Analyzed geometry
clear s
s.objs={g1};
s.name={'R1'};
s.tags={'g1'};

fem.draw=struct('s',s);
fem.geom=geomcsg(fem);
% COMSOL Multiphysics Model M-file
% Generated by COMSOL 3.3a (COMSOL 3.3.0.511, $Date: 2007/02/02 19:05:58 $)

% Initialize mesh
fem.mesh=meshinit(fem, ...
                  'hauto',5);

% Refine mesh
fem.mesh=meshrefine(fem, ...
                    'mcase',0, ...
                    'rmethod','regular');
```

```
% Refine mesh
fem.mesh=meshrefine(fem, ...
                    'mcase',0, ...
                    'rmethod','regular');

% (Default values are not included)

% Application mode 1
clear appl
appl.mode.class = 'SmeAxialSolid';
appl.mode.type = 'axi';
appl.module = 'SME';
appl.gporder = 4;
appl.cporder = 2;
appl.assignsuffix = '_smaxi';
clear prop
prop.analysis='quasi';
appl.prop = prop;
clear bnd
bnd.Rz = {0,0,0,'-0.00005*flc1hs(t-250,250)'};
bnd.Hz = (200);
bnd.constrcond = {'free','sym','roller','displacement'};
bnd.ind = [2,3,4,1];
appl.bnd = bnd;
clear equ
equ.nu = 0.125;
```

```
equ.E = 0.700e6;
equ.Fz = '-p2z';
equ.Fr = '-p2r';
equ.ind = [1];
appl.equ = equ;
fem.appl{1} = appl;

% Application mode 2
clear appl
appl.mode.class = 'DarcysLaw';
appl.mode.type = 'axi';
appl.dim = {'p2'};
appl.module = 'CHEM';
appl.shape = {'shlag(1,"p2")'};
appl.gporder = 2;
appl.cporder = 1;
appl.assignsuffix = '_chdl';
clear prop
clear weakconstr
weakconstr.value = 'off';
weakconstr.dim = {'lm3'};
prop.weakconstr = weakconstr;
appl.prop = prop;
clear bnd
bnd.p0 = {0,'p2',0,0};
bnd.type = {'ax','N0','N0','P'};
```

```
bnd.ind = [1,2,3,4];
appl.bnd = bnd;
clear equ
equ.eta = 0.83;
equ.F = '(-(diff(uaxir_smaxi,t)+diff(wz,t)))*1e3';
equ.epsilon = 0.83;
equ.init = 0;
equ.k = 7.6e-15;
equ.rho = 1e3;
equ.ind = [1];
appl.equ = equ;
fem.appl{2} = appl;
fem.sdim = {'r','z'};
fem.frame = {'ref'};
fem.border = 1;
fem.outform = 'general';
clear units;
units.basesystem = 'SI';
fem.units = units;

% Multiphysics
fem=multiphysics(fem);

% Extend mesh
fem.xmesh=meshextend(fem);
```

```
% Solve problem
fem.sol=femtime(fem, ...
                'solcomp',{'w','p2','uor'}, ...
                'outcomp',{'w','p2','uor'}, ...
                'tlist',[0:50.0:2000.0], ...
                'tout','tlist');

% Save current fem structure for restart purposes
fem0=fem;

% Plot solution
postplot(fem, ...
        'tridata',{'p2','cont','internal','unit','Pa'}, ...
        'trimap','jet(1024)', ...
        'deformsub',{'uaxi_smaxi','w'}, ...
        'arrowdata',{'u_chdl','v_chdl'}, ...
        'arrowxspacing',15, ...
        'arrowyspacing',15, ...
        'arrowtype','arrow', ...
        'arrowstyle','proportional', ...
        'arrowcolor',[1.0,0.0,0.0], ...
        'solnum','end', ...
        'title','Time=2000    Surface: Pressure [Pa]   Arrow: Velocity field [m/s]
Deformation: Displacement [m]', ...
        'axis',[-6.451517874866485E-4,0.0022013390400076865,-
5.528143240131765E-4,0.0017220451487794273,-1,1]);
```

Model Validation

The implementation of the code outlined below results in the analysis of articular cartilage with a modulus of 0.675MPa, hydraulic conductivity of 7.6e-15 m^4/N.s., poisson's ratio of 0.125, solid density of 1.373g/ml, viscosity of 0.83 N.s/m^2 and porosity of 70%. First, the geometry is created and meshes applied. The modules defining the physics of the analysis implemented in application mode 1 (solid mechanics) and application mode 2 (Darcy law). Meshes are then extended to the application modes. This model was validated by comparison to data published by Spilker, Suh and Mow in the Journal of Biomechanical Engineering May 1990, vol. 112. The results of this validation are consistent with those reported in the Spilker, Suh and Mow paper. The plot below shows the results of the validation which is consistent with the results published by Spilker et al. for the conditions detailed for geometry B. And the subsequent table shows parameters translated from the models developed by Spilker et al, for use in the model developed here.

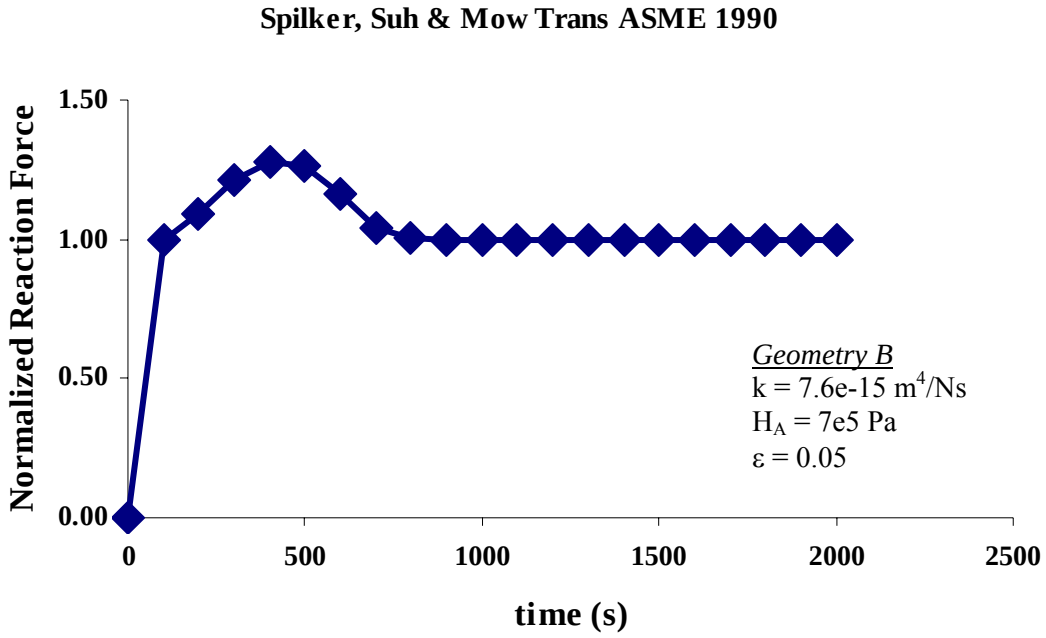

Spilker model - Earth Science Module in Comsol (provided by Dr. Spilker)

Solid mechanics

Subdomain	*values*	*units*	*Boundary condition*
E	2.25E+05	Pa	1
ν	0.125		2
α	1.20E-05	1/K	3
ρ	7850	Kg/m3	4

Load		*Loading function*
Fr	-p2r	displ. Control
Fz	-p2z	= -0.007e-3*(t/500)*flc1hs(t-5,5)

Damping		
Raleigh α_{dm}	1	1/s
Raleigh β_{dk}	0.001	s

Darcy

Subdomain	*values*	*units*	*Boundary condition*	
S	0	1/Pa	1	symmetry plane
k_s	7.60E-15		2	zero flux/symmetry plane
p_f	0		3	zero flux/symmetry plane
η	0.83		4	atm./gauge
Q_s	-(diff(uaxir_smaxi,t) + diff(wz,t)			

Scaling	
δ_s	0
δ_k	0.83
δ_Q	1

Spilker model - modified for the Chem Eng. Module for validation

Geometry B
Permeability 3

Solid mechanics

Subdomain	*values*	*units*	*Boundary condition*
E	700000	Pa	1
ν	0.125		2
α	0.000012	1/K	3
ρ	1000	Kg/m3	4

Load		*Loading function*
Fr	-p2r	displ. Control
Fz	-p2z	= -0.007e-3*(t/500)*flc1hs(t-5,5)

Damping		
Raleigh α_{dm}	1	1/s
Raleigh β_{dk}	0.001	s

Darcy

Subdomain	*values*	*units*	*Boundary condition*	
k	7.60E-15		1	symmetry plane
p_f	1.E+03		2	insulation/symmetry plane
ε	0.83		3	insulation/symmetry plane
η	0.83		4	pressure (p = 0)
F	(-(diff(uaxir_smaxi,t) + diff(wz,t))*1e3			

Time scaling factor	
δ_{ts}	1

Parametric Analysis

This developed model was used to estimate the mechanical environment resulting from an applied uniaxial unconfined sinusoidal load with 5% strain amplitude superimposed on a 5% strain offset at frequency of 1 Hz. The boundary conditions allowed displacement to occur freely at the top (loaded) surface and along the radial direction, but fixed along the axial direction at the bottom surface. Loading was simulated using an impermeable, frictionless loader with fluid movement confined to the radial edge. Scaffolds with moduli ranging from 0.5 to 512 kPa and hydraulic permeabilities ranging from 5e-14 to 1.0e-10 m^4/N.s were analyzed. The finite element simulations were run for 300s, at which time steady state was achieved for all physical stimuli. Analysis was performed at the maxima and minima of each cycle (every t=0.25s) during the dynamic deformational loading. The maximum steady state peak pressures, shear stresses, radial fluid velocities and radial strains at equilibrium were analyzed. Analysis of a cartilage plug with the above mentioned dimensions and loading conditions was conducted for comparison with the loaded scaffolds, with an assumed modulus of 700kPa, hydraulic permeability of 7.6e-15 m^4/N.s, solid density of 7850 kg/m^3, poisson's ratio of 0.125, and a porosity of 70%.

Code

The implementation of the code outlined below results in the parametric analysis of scaffolds with moduli ranging from 0.5 to 512 kPa and hydraulic permeabilities ranging from 5e-14 to 1.0e-10 m^4/N.s. Increments of theses ranges are as listed in the modarray and perarray matrices in the extended mesh routine. First, the geometry is created and meshes applied. The modules defining the physics of the analysis implemented in application mode 1 (solid mechanics) and application mode 2 (Darcy law). Meshes are then extended to the application modes. The equations specified in

the application modes are then solved for pressure, strain, shear stress and radial fluid velocity, implemented within a series of while loops. The solutions for each modulus and permeability pair is saved in a text file created and saved as the “Press Ex_Ky” where E represents the modulus constant and x the value that constant in pascals and K represents the permeability constant and y, the value of the constant in m^2.

```
flclear fem

% COMSOL version
clear vrsnb
vrsn.name = 'COMSOL 3.3';
vrsn.ext = 'a';
vrsn.major = 0;
vrsn.build = 511;
vrsn.rcs = '$Name:  $';
vrsn.date = '$Date: 2007/02/02 19:05:58 $';
fem.version = vrsn;

% Geometry
g1=rect2(1,0.4,'base','corner','pos',[0,0]);
g2=rect2('0.005','0.0015','base','corner','pos',{'0','0'},'rot','0');

% Analyzed geometry
clear s
s.objs={g2};
s.name={'R1'};
```

```
s.tags={'g2'};

fem.draw=struct('s',s);
fem.geom=geomcsg(fem);
% COMSOL Multiphysics Model M-file
% Generated by COMSOL 3.3a (COMSOL 3.3.0.511, $Date: 2007/02/02 19:05:58 $)

% Geometry
g1=rect2('0.00125','0.001','base','corner','pos',{'0','0'},'rot','0');

% Analyzed geometry
clear s
s.objs={g1};
s.name={'R1'};
s.tags={'g1'};

fem.draw=struct('s',s);
fem.geom=geomcsg(fem);
% COMSOL Multiphysics Model M-file
% Generated by COMSOL 3.3a (COMSOL 3.3.0.511, $Date: 2007/02/02 19:05:58 $)

% Geometry
g2=rect2('0.004','0.0020','base','corner','pos',{'0','0'},'rot','0');

% Analyzed geometry
clear s
```

```
s.objs={g2};
s.name={'R1'};
s.tags={'g2'};

fem.draw=struct('s',s);
fem.geom=geomcsg(fem);
% COMSOL Multiphysics Model M-file
% Generated by COMSOL 3.3a (COMSOL 3.3.0.511, $Date: 2007/02/02 19:05:58 $)

% Geometry
g1=rect2(0.0040,0.0010,'base','corner','pos',[0,0]);
g3=rect2('0.0040','0.0008','base','corner','pos',{'0','0'},'rot','0');
g4=rect2('0.0040','0.0007','base','corner','pos',{'0','0'},'rot','0');
g5=rect2('0.0040','0.0005','base','corner','pos',{'0','0'},'rot','0');
[g6]=geomcopy({g5});
g6=move(g6,[0,7.5E-4]);
g6=move(g6,[0,7.5E-4]);
g7=rect2(0.0010,0.0020,'base','corner','pos',[0.0030,0]);
g8=rect2('0.0005','0.0020','base','corner','pos',{'0.0030','0'},'rot','0');
g8=move(g8,[7.499999999999998E-4,0]);
g8=move(g8,[-0.0010,0]);
g9=rect2('5.0E-4','0.0020','base','corner','pos',{'0.004','0'},'rot','0');
g10=rect2('5.0E-4','0.0020','base','corner','pos',{'0.0005','0'},'rot','0');
g11=rect2('5.0E-4','0.0020','base','corner','pos',{'0.005','0'},'rot','0');
g12=rect2('5.0E-4','0.0020','base','corner','pos',{'0.05','0'},'rot','0');
g13=rect2('5.0E-4','0.0020','base','corner','pos',{'0.005','0'},'rot','0');
```

```
g14=rect2('5.0E-4','0.0020','base','corner','pos',{'0.004','0'},'rot','0');
g15=rect2('5.0E-4','0.0020','base','corner','pos',{'0.0045','0'},'rot','0');
g16=rect2('5.0E-4','0.0020','base','corner','pos',{'0.0035','0'},'rot','0');

% Analyzed geometry
clear s
s.objs={g2,g5,g6,g16};
s.name={'R1','R2','R3','R4'};
s.tags={'g2','g5','g6','g16'};

fem.draw=struct('s',s);
fem.geom=geomcsg(fem);
% COMSOL Multiphysics Model M-file
% Generated by COMSOL 3.3a (COMSOL 3.3.0.511, $Date: 2007/02/02 19:05:58 $)

% Geometry

% Geometry objects
clear s
s.objs={g2};
s.name={'R1'};
s.tags={'g2'};

fem.draw=struct('s',s);
% COMSOL Multiphysics Model M-file
% Generated by COMSOL 3.3a (COMSOL 3.3.0.511, $Date: 2007/02/02 19:05:58 $)
```

```
% Geometry

% Analyzed geometry
clear s
s.objs={g2};
s.name={'R1'};
s.tags={'g2'};

fem.draw=struct('s',s);
fem.geom=geomcsg(fem);

% COMSOL Multiphysics Model M-file
% Generated by COMSOL 3.3a (COMSOL 3.3.0.511, $Date: 2007/02/02 19:05:58 $)

% (Default values are not included)

% COMSOL Multiphysics Model M-file
   % Generated by COMSOL 3.3a (COMSOL 3.3.0.511, $Date: 2007/02/02 19:05:58
$)

   % Create mapped quad mesh
   fem.mesh=meshmap(fem, ...
         'edgegroups',{{[2],[4],[3],[1]}}, ...
         'edgelem',{1,[0:0.5:2.5 3:1:7 7.5:0.5:10],2,[0 0.1801764433778299
0.32855770621241176 0.4507545858245572 0.5513877594590998
0.6342625077170205 0.7025126050830863 0.7587188185364379
```

```
0.8050064950773133 0.8431259282843007 0.874518542833419
0.9003713996395082 0.921662082643639 0.9391956645677698
0.9536351494368349 0.9655265430029726 0.9753194990694128
0.983384322421347 0.9900259713020967 0.9954955889155542 1],3,[0
0.1801764433778299 0.32855770621241176 0.4507545858245572
0.5513877594590998 0.6342625077170205 0.7025126050830863
0.7587188185364379 0.8050064950773133 0.8431259282843007
0.874518542833419 0.9003713996395082 0.921662082643639 0.9391956645677698
0.9536351494368349 0.9655265430029726 0.9753194990694128
0.983384322421347 0.9900259713020967 0.9954955889155542 1],4,[0:0.5:2.5 3:1:7
7.5:0.5:10]}, ...
        'hauto',5);

% Application mode 1
clear appl
appl.mode.class = 'SmeAxialSolid';
appl.mode.type = 'axi';
appl.module = 'SME';
appl.gporder = 4;
appl.cporder = 2;
appl.assignsuffix = '_smaxi';
clear prop
prop.analysis='quasi';
appl.prop = prop;
clear bnd
bnd.Rz = {0,0,0,'-0.0002+0.0002*sin(2*pi*t)'};
```

```
bnd.Hz = {0,0,0,1};
bnd.constrcond = {'free','sym','roller','displacement'};
bnd.ind = [2,3,4,1];
appl.bnd = bnd;
clear equ
equ.nu = 0.125;
equ.rho = 1240;
equ.betadK = 0.01;

equ.Fz = '-p2z';
equ.Fr = '-p2r';
equ.ind = [1];
appl.equ = equ;
fem.appl{1} = appl;

% Application mode 2
clear appl
appl.mode.class = 'DarcysLaw';
appl.mode.type = 'axi';
appl.dim = {'p2'};
appl.module = 'CHEM';
appl.shape = {'shlag(1,"p2")'};
appl.gporder = 2;
appl.cporder = 1;
appl.assignsuffix = '_chdl';
clear prop
```

```
clear weakconstr
weakconstr.value = 'off';
weakconstr.dim = {'lm3'};
prop.weakconstr = weakconstr;
appl.prop = prop;
clear bnd
bnd.p0 = {0,'p2',0,0};
bnd.type = {'ax','N0','N0','P'};
bnd.ind = [1,2,3,4];
appl.bnd = bnd;
clear equ
equ.eta = 1e-3;
equ.F = '(-(diff(uaxir_smaxi,t)+diff(wz,t)))*1e3';
equ.epsilon = 0.98;
equ.init = 0;

equ.rho = 1e3;
equ.ind = [1];
appl.equ = equ;
fem.appl{2} = appl;
fem.sdim = {'r','z'};
fem.frame = {'ref'};
fem.border = 1;
fem.outform = 'general';
clear units;
units.basesystem = 'SI';
```

```
fem.units = units;

% Multiphysics
fem=multiphysics(fem);

% Extend mesh
fem.xmesh=meshextend(fem);

modarray = [500 1000 2000 4000 8000 16000 32000 64000 96000 128000 160000
192000 224000 256000 320000 384000 448000 512000];
perarray = [5e-17 1E-16 2E-16 4E-16 8E-16 1.6E-15 3.2E-15 6.4E-15 9.6E-15 1.28E-
14 1.6E-14 1.92E-14 2.24E-14 2.56E-14 3.2E-14 3.84E-14 4.48E-14 5.12E-14 7.68E-
14 1.024E-13];

l=11;
m=2;

while l<=length(modarray)
equ.E = modarray(l);


    while m<=length(perarray)
    equ.k = perarray(m);

    % Solve problem
    fem.sol=femtime(fem, ...
```

```
'solcomp',{'w','p2','uor'}, ...
'outcomp',{'w','p2','uor'}, ...
'tlist',[0.000001:0.01667:299.99999], ...
'tout','tlist');


%Press
fp=fopen(['Press_E' num2str(l) '_k' num2str(m) '.txt'],'wt');
for it = 1:15:17971
pd_press = posteval(fem,'p2','Solnum',it);
pd_press_data = transpose(pd_press.d);
Press = transpose(pd_press.d);
Max_Press = max(Press(:,1));
Min_Press = min(Press(:,1));
fprintf(fp,'%f %f \n',Min_Press',Max_Press');
end
fclose(fp);

clear pd_press
clear pd_press_data
clear Press

%er Strain
fp=fopen(['erStrain_E' num2str(l) '_k' num2str(m) '.txt'],'wt');
for it = 1:15:17971
pd_erStrain = posteval(fem,'er_smaxi','Solnum',it);
```

```
pd_erStrain_data = transpose(pd_erStrain.d);
erStrain = transpose(pd_erStrain.d);
Max_erStrain = max(erStrain(:,1));
Min_erStrain = min(erStrain(:,1));
fprintf(fp,'%f %f \n',Min_erStrain',Max_erStrain');
end
fclose(fp);

clear pd_erStrain
clear pd_erStrain_data
clear erStrain

%Shear
fp=fopen(['Shear_E' num2str(l) '_k' num2str(m) '.txt'],'wt');
for it = 1:15:17971
pd_Shear = posteval(fem,'srz_smaxi','Solnum',it);
pd_Shear_data = transpose(pd_Shear.d);
Shear = transpose(pd_Shear.d);
Max_Shear = max(Shear(:,1));
Min_Shear = min(Shear(:,1));
fprintf(fp,'%f %f \n',Min_Shear',Max_Shear');
end
fclose(fp);

clear pd_Shear
clear pd_Shear_data
```

```
        clear Shear

        %rVel
        fp=fopen(['rVel_E' num2str(l) '_k' num2str(m) '.txt'],'wt');
        for it = 1:15:17971
        pd_rVel = posteval(fem,'u_chdl','Solnum',it);
        pd_rVel_data = transpose(pd_rVel.d);
        rVel = transpose(pd_rVel.d);
        Max_rVel = max(rVel(:,1));
        Min_rVel = min(rVel(:,1));
        fprintf(fp,'%f %f \n',Min_rVel',Max_rVel');
        end
        fclose(fp);

        clear pd_rVel
        clear pd_rVel_data
        clear rVel

    m=m+1;
    l
    m
    end
    l=l+1;
end
 % Save current fem structure for restart purposes
fem0=fem;
```

Conclusion

As expected and validated, the developed model exhibited classic poroelastic behavior, having pressurized cores with low fluid flow and edges with high radial fluid velocities. This code was modified for the parametric analysis of scaffolds with 360 combinations of modulus and permeability. And as shown in chapter 3, this model can be successfully used for the analysis of dynamically compressing scaffolds and tissues.

APPENDIX D

Supplementary Data for Chapters 4

Introduction

The fourth aim of this dissertation detailed the response of chondrocytes to scaffold composition and dynamic compression. This appendix contains supplementary supporting data not included in the body of the chapters.

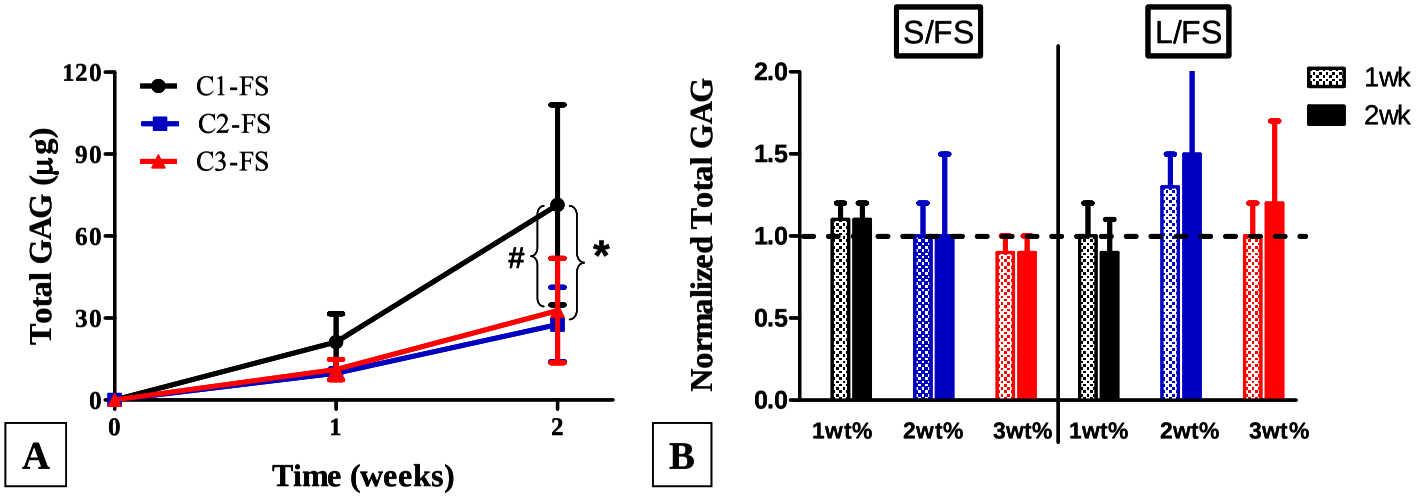

Average total GAG produced per gel as a function of scaffold composition and loading condition (n = 8 ± stdev.) displayed as raw data (Fig. A) or loaded conditions (Fig. B) normalized to free swell. Trends shown in free swell gels (Fig. A) is similar to those observed for static and loaded gels. # and * represent significant differences between 1wt% gels and 2 and 3wt% gels, respectively (all with $p<0.05$)

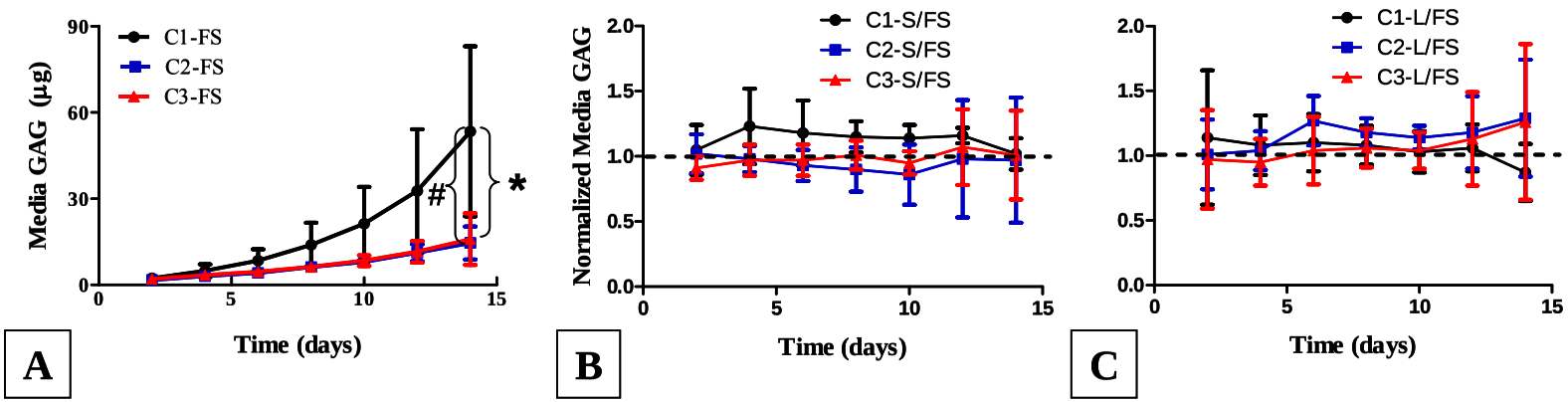

Average amount of GAG cumulatively released to the surrounding medium, as a function of scaffold composition and loading condition (n = 8 ± stdev.) displayed as raw data (Fig. A) or static (Fig. B) and dynamically loaded (Fig. C) conditions normalized to free swell values. # and * represent significant differences between 1wt% gels and 2 and 3wt% gels, respectively (all with $p<0.05$)

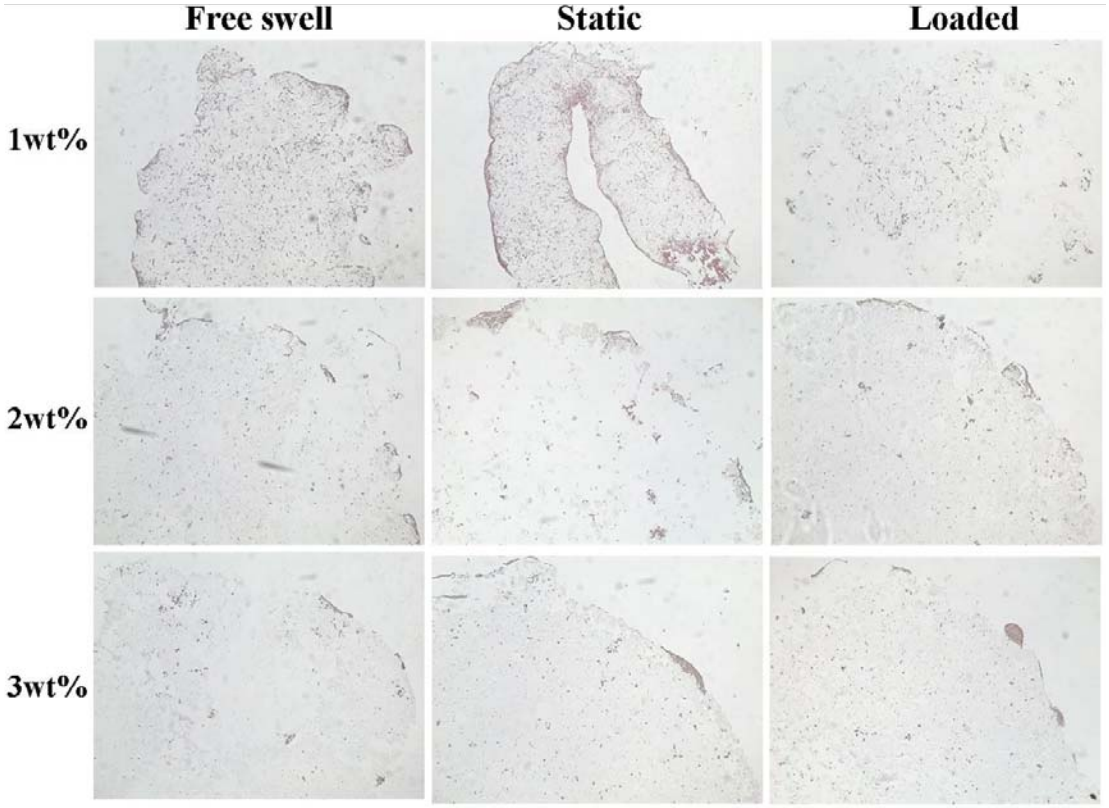

Sample images of gels stained for glycosaminoglycan via Safranin O by histological analysis on 2 week gels (images at 20X magnification)

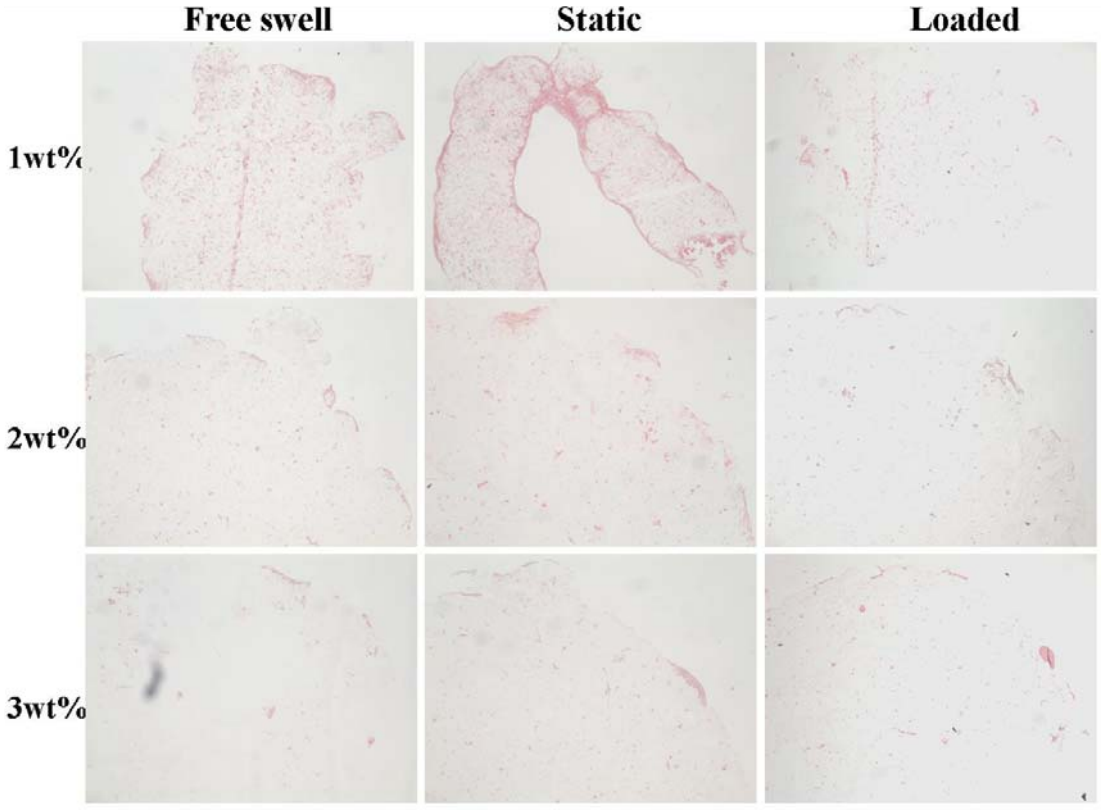

Sample images of gels stained for collagen via picrosirius red by histological analysis on 2 week gels (images at 20X magnification)

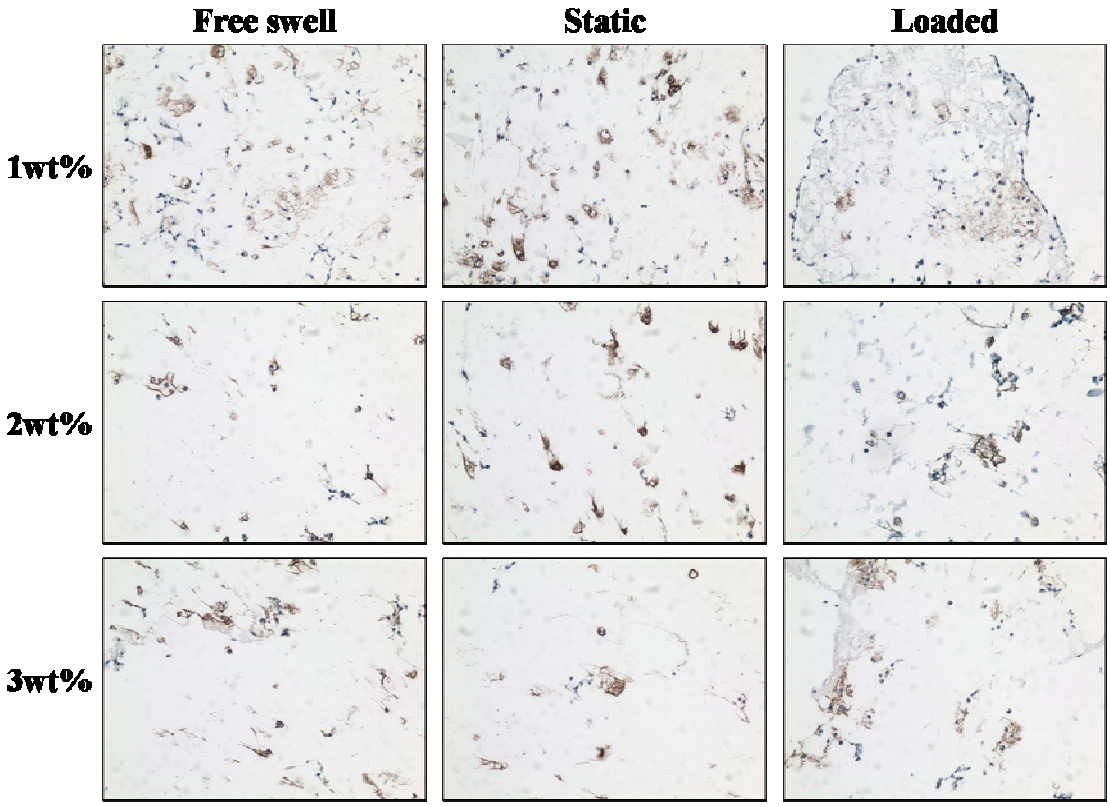

Sample images of gels analyzed for link protein using immunochemical analysis on gels at 2week (images at 20X magnification)

APPENDIX D

Finite Element Analysis of Dynamically Compressing Poly(ethylene) Glycol Scaffolds

Introduction

This appendix details the development of a finite element model of poly(ethylene glycol) scaffolds undergoing unconfined cyclic dynamic compression. These simulations were done as a collaborative effort with Dr. Stephanie Bryant at the University of Colorado. Relevant parameter of two PEG scaffolds with different material properties and loading regimens were incorporated into the developed finite element model of dynamically compressing scaffolds. The models of the two scaffolds were used to analyze the physical gradient present within their scaffolds.

Parameters Modeled

Weight Percent poly(ethylene glycol) dimethacrylate	Equilibrium Modulus (kPa)		Hydraulic Permeability, k (m^4/Ns)	Solid Density (g/cm^3)	Porosity
	Avg.	St. dev.			
10% (w/w)	46.09	3.23	9.19E-07	1.07	91.71%
15% (w/w)	201.33	24.77	9.40E-09	1.07	86.96%

Loading Waveform	Sinusoidal (displacement controlled)
Strain Amplitude	15% = 750μm
Offset	5% = 250μm
Frequency	0.3 Hz Period = 3.3s
Geometry	Cylinder
Dimensions	5mm height x 5mm diameter
loading function	= - offset (m) + amplitude (m) *Sin(2p*frequency (Hz)*t)
	= - 0.00025+0.00075*Sin(2p*0.3*t)

COMSOL code using properties of 10wt% PEG gel

```
% COMSOL Multiphysics Model M-file
% Generated by COMSOL 3.3a (COMSOL 3.3.0.511, $Date: 2007/02/02 19:05:58 $)

flclear fem

% COMSOL version
clear vrsn
vrsn.name = 'COMSOL 3.3';
vrsn.ext = 'a';
vrsn.major = 0;
vrsn.build = 511;
vrsn.rcs = '$Name:  $';
vrsn.date = '$Date: 2007/02/02 19:05:58 $';
fem.version = vrsn;

% Geometry
g1=rect2(1,0.4,'base','corner','pos',[0,0]);
g2=rect2('0.005','0.0015','base','corner','pos',{'0','0'},'rot','0');

% Analyzed geometry
clear s
s.objs={g2};
s.name={'R1'};
s.tags={'g2'};
```

```
fem.draw=struct('s',s);
fem.geom=geomcsg(fem);
% COMSOL Multiphysics Model M-file
% Generated by COMSOL 3.3a (COMSOL 3.3.0.511, $Date: 2007/02/02 19:05:58 $)

% Geometry
g1=rect2('0.00125','0.001','base','corner','pos',{'0','0'},'rot','0');

% Analyzed geometry
clear s
s.objs={g1};
s.name={'R1'};
s.tags={'g1'};

fem.draw=struct('s',s);
fem.geom=geomcsg(fem);
% COMSOL Multiphysics Model M-file
% Generated by COMSOL 3.3a (COMSOL 3.3.0.511, $Date: 2007/02/02 19:05:58 $)

% Geometry
g2=rect2('0.004','0.0020','base','corner','pos',{'0','0'},'rot','0');

% Analyzed geometry
clear s
s.objs={g2};
```

```
s.name={'R1'};
s.tags={'g2'};

fem.draw=struct('s',s);
fem.geom=geomcsg(fem);
% COMSOL Multiphysics Model M-file
% Generated by COMSOL 3.3a (COMSOL 3.3.0.511, $Date: 2007/02/02 19:05:58 $)

% Geometry
g1=rect2(0.0040,0.0010,'base','corner','pos',[0,0]);
g3=rect2('0.0040','0.0008','base','corner','pos',{'0','0'},'rot','0');
g4=rect2('0.0040','0.0007','base','corner','pos',{'0','0'},'rot','0');
g5=rect2('0.0040','0.0005','base','corner','pos',{'0','0'},'rot','0');
[g6]=geomcopy({g5});
g6=move(g6,[0,7.5E-4]);
g6=move(g6,[0,7.5E-4]);
g7=rect2(0.0010,0.0020,'base','corner','pos',[0.0030,0]);
g8=rect2('0.0005','0.0020','base','corner','pos',{'0.0030','0'},'rot','0');
g8=move(g8,[7.499999999999998E-4,0]);
g8=move(g8,[-0.0010,0]);
g9=rect2('5.0E-4','0.0020','base','corner','pos',{'0.004','0'},'rot','0');
g10=rect2('5.0E-4','0.0020','base','corner','pos',{'0.0005','0'},'rot','0');
g11=rect2('5.0E-4','0.0020','base','corner','pos',{'0.005','0'},'rot','0');
g12=rect2('5.0E-4','0.0020','base','corner','pos',{'0.05','0'},'rot','0');
g13=rect2('5.0E-4','0.0020','base','corner','pos',{'0.005','0'},'rot','0');
g14=rect2('5.0E-4','0.0020','base','corner','pos',{'0.004','0'},'rot','0');
```

```
g15=rect2('5.0E-4','0.0020','base','corner','pos',{'0.0045','0'},'rot','0');
g16=rect2('5.0E-4','0.0020','base','corner','pos',{'0.0035','0'},'rot','0');

% Analyzed geometry
clear s
s.objs={g2,g5,g6,g16};
s.name={'R1','R2','R3','R4'};
s.tags={'g2','g5','g6','g16'};

fem.draw=struct('s',s);
fem.geom=geomcsg(fem);
% COMSOL Multiphysics Model M-file
% Generated by COMSOL 3.3a (COMSOL 3.3.0.511, $Date: 2007/02/02 19:05:58 $)

% Geometry

% Geometry objects
clear s
s.objs={g2};
s.name={'R1'};
s.tags={'g2'};

fem.draw=struct('s',s);
% COMSOL Multiphysics Model M-file
% Generated by COMSOL 3.3a (COMSOL 3.3.0.511, $Date: 2007/02/02 19:05:58 $)
```

```
% Geometry

% Analyzed geometry
clear s
s.objs={g2};
s.name={'R1'};
s.tags={'g2'};

fem.draw=struct('s',s);
fem.geom=geomcsg(fem);
% COMSOL Multiphysics Model M-file
% Generated by COMSOL 3.3a (COMSOL 3.3.0.511, $Date: 2007/02/02 19:05:58 $)

% Geometry
g1=rect2('0.0030','0.0010','base','corner','pos',{'0','0'},'rot','0');

% Analyzed geometry
clear s
s.objs={g1};
s.name={'R1'};
s.tags={'g1'};

fem.draw=struct('s',s);
fem.geom=geomcsg(fem);
% COMSOL Multiphysics Model M-file
% Generated by COMSOL 3.3a (COMSOL 3.3.0.511, $Date: 2007/02/02 19:05:58 $)
```

```
% Geometry
g2=rect2('0.0025','0.005','base','corner','pos',{'0','0'},'rot','0');

% Analyzed geometry
clear s
s.objs={g2};
s.name={'R1'};
s.tags={'g2'};

fem.draw=struct('s',s);
fem.geom=geomcsg(fem);
% COMSOL Multiphysics Model M-file
% Generated by COMSOL 3.4 (COMSOL 3.4.0.248, $Date: 2007/10/10 16:07:51 $)

% COMSOL version
clear vrsn
vrsn.name = 'COMSOL 3.4';
vrsn.ext = '';
vrsn.major = 0;
vrsn.build = 248;
vrsn.rcs = '$Name:  $';
vrsn.date = '$Date: 2007/10/10 16:07:51 $';
fem.version = vrsn;

% Create mapped quad mesh
```

```
fem.mesh=meshmap(fem, ...
                'edgegroups',{{[2],[4],[3],[1]}}, ...
                'edgelem',{1,[0:0.5:2.5 3:1:7 7.5:0.5:10],2,[0 0.1801764433778299
0.32855770621241176 0.4507545858245572 0.5513877594590998
0.6342625077170205 0.7025126050830863 0.7587188185364379
0.8050064950773133 0.8431259282843007 0.874518542833419
0.9003713996395082 0.921662082643639 0.9391956645677698
0.9536351494368349 0.9655265430029726 0.9753194990694128
0.983384322421347 0.9900259713020967 0.9954955889155542 1],3,[0
0.1801764433778299 0.32855770621241176 0.4507545858245572
0.5513877594590998 0.6342625077170205 0.7025126050830863
0.7587188185364379 0.8050064950773133 0.8431259282843007
0.874518542833419 0.9003713996395082 0.921662082643639 0.9391956645677698
0.9536351494368349 0.9655265430029726 0.9753194990694128
0.983384322421347 0.9900259713020967 0.9954955889155542 1],4,[0:0.5:2.5 3:1:7
7.5:0.5:10]}, ...
                'hauto',5);

% (Default values are not included)

% Application mode 1
clear appl
appl.mode.class = 'SmeAxialSolid';
appl.mode.type = 'axi';
appl.module = 'SME';
appl.gporder = 4;
```

```
appl.cporder = 2;
appl.assignsuffix = '_smaxi';
clear prop
prop.analysis='quasi';
appl.prop = prop;
clear bnd
bnd.Tni = 1e6;
bnd.Rz = {0,0,0,'-0.00025-0.0003125*sin(2*pi*0.3*t)'};
bnd.Ttri = 1e6;
bnd.Ttzi = 1e6;
bnd.Hz = {0,0,0,1};
bnd.constrcond = {'free','sym','roller','displacement'};
bnd.pt = 'E_smaxi/h*min(1e-4*5^auglagiter,0.1)';
bnd.pn = 'E_smaxi/h*min(1e-4*5^auglagiter,0.1)';
bnd.ind = [2,3,4,1];
appl.bnd = bnd;
clear equ
equ.nu = 0.125;
equ.rho = 1070;
equ.betadK = 0.01;
equ.E = 1024E3;
equ.Fz = '-p2z';
equ.Fr = '-p2r';
equ.ind = [1];
appl.equ = equ;
fem.appl{1} = appl;
```

```
% Application mode 2
clear appl
appl.mode.class = 'DarcysLaw';
appl.mode.type = 'axi';
appl.dim = {'p2'};
appl.module = 'CHEM';
appl.shape = {'shlag(1,"p2")'};
appl.gporder = 2;
appl.cporder = 1;
appl.assignsuffix = '_chdl';
clear prop
clear weakconstr
weakconstr.value = 'off';
weakconstr.dim = {'lm3'};
prop.weakconstr = weakconstr;
appl.prop = prop;
clear bnd
bnd.p0 = {0,'p2',0};
bnd.type = {'ax','N0','P'};
bnd.ind = [1,2,3,3];
appl.bnd = bnd;
clear equ
equ.eta = 1e-3;
equ.F = '(-(diff(uaxir_smaxi,t)+diff(wz,t)))*1e3';
equ.epsilon = 0.9171;
```

```
equ.init = 0;
equ.k = 1.02E-13;
equ.rho = 1e3;
equ.ind = [1];
appl.equ = equ;
fem.appl{2} = appl;
fem.sdim = {'r','z'};
fem.frame = {'ref'};
fem.border = 1;
fem.outform = 'general';
clear units;
units.basesystem = 'SI';
fem.units = units;

% Multiphysics
fem=multiphysics(fem);
% COMSOL Multiphysics Model M-file
% Generated by COMSOL 3.4 (COMSOL 3.4.0.248, $Date: 2007/10/10 16:07:51 $)

% COMSOL version
clear vrsn
vrsn.name = 'COMSOL 3.4';
vrsn.ext = '';
vrsn.major = 0;
vrsn.build = 248;
vrsn.rcs = '$Name:  $';
```

```
vrsn.date = '$Date: 2007/10/10 16:07:51 $';
fem.version = vrsn;

% (Default values are not included)

% Application mode 1
clear appl
appl.mode.class = 'SmeAxialSolid';
appl.mode.type = 'axi';
appl.module = 'SME';
appl.gporder = 4;
appl.cporder = 2;
appl.assignsuffix = '_smaxi';
clear prop
prop.analysis='quasi';
appl.prop = prop;
clear bnd
bnd.Tni = 1e6;
bnd.Rz = {0,0,0,'-0.0003125-0.0003125*sin(2*pi*0.3*t)'};
bnd.Ttri = 1e6;
bnd.Ttzi = 1e6;
bnd.Hz = {0,0,0,1};
bnd.constrcond = {'free','sym','roller','displacement'};
bnd.pt = 'E_smaxi/h*min(1e-4*5^auglagiter,0.1)';
bnd.pn = 'E_smaxi/h*min(1e-4*5^auglagiter,0.1)';
bnd.ind = [2,3,4,1];
```

```
appl.bnd = bnd;
clear equ
equ.nu = 0.125;
equ.rho = 1070;
equ.betadK = 0.01;
equ.E = 46090;
equ.Fz = '-p2z';
equ.Fr = '-p2r';
equ.ind = [1];
appl.equ = equ;
fem.appl{1} = appl;

% Application mode 2
clear appl
appl.mode.class = 'DarcysLaw';
appl.mode.type = 'axi';
appl.dim = {'p2'};
appl.module = 'CHEM';
appl.shape = {'shlag(1,"p2")'};
appl.gporder = 2;
appl.cporder = 1;
appl.assignsuffix = '_chdl';
clear prop
clear weakconstr
weakconstr.value = 'off';
weakconstr.dim = {'lm3'};
```

```
prop.weakconstr = weakconstr;
appl.prop = prop;
clear bnd
bnd.p0 = {0,'p2',0};
bnd.type = {'ax','N0','P'};
bnd.ind = [1,2,3,3];
appl.bnd = bnd;
clear equ
equ.eta = 1e-3;
equ.F = '(-(diff(uaxir_smaxi,t)+diff(wz,t)))*1e3';
equ.epsilon = 0.9171;
equ.init = 0;
equ.k = 9.19E-10;
equ.rho = 1e3;
equ.ind = [1];
appl.equ = equ;
fem.appl{2} = appl;
fem.sdim = {'r','z'};
fem.frame = {'ref'};
fem.border = 1;
fem.outform = 'general';
clear units;
units.basesystem = 'SI';
fem.units = units;
 % Multiphysics
fem=multiphysics(fem);
```

REFERENCES

1. Mow VC, R. A., Woo SL-Y. Biomechanics of diarthrodial joints. New York: Springer; 1990.

2. Cowin, S. C., Doty, S. B. Tissue Mechanics. New York: Springer; 2007.

3. Hardingham, T. E., Fosang, A. J. 1992, "Proteoglycans: many forms and many functions," Faseb J, **6**(3), pp.861-70.

4. Kjellen, L., Lindahl, U. 1991, "Proteoglycans: structures and interactions," Annu Rev Biochem, **60** pp.443-75.

5. Maroudas, A., Muir, H., Wingham, J. 1969, "The correlation of fixed negative charge with glycosaminoglycan content of human articular cartilage," Biochim Biophys Acta, **177**(3), pp.492-500.

6. Aigner, T., Kurz, B., Fukui, N., Sandell, L. 2002, "Roles of chondrocytes in the pathogenesis of osteoarthritis," Curr Opin Rheumatol, **14**(5), pp.578-84.

7. Bailey, A. J. 2001, "Molecular mechanisms of ageing in connective tissues," Mech Ageing Dev, **122**(7), pp.735-55.

8. Martin, J. A., Buckwalter, J. A. 2002, "Aging, articular cartilage chondrocyte senescence and osteoarthritis," Biogerontology, **3**(5), pp.257-64.

9. Martin, J. A., Buckwalter, J. A. 2001, "Roles of articular cartilage aging and chondrocyte senescence in the pathogenesis of osteoarthritis," Iowa Orthop J, **21** pp.1-7.

10. Sandell, L. J., Aigner, T. 2001, "Articular cartilage and changes in arthritis. An introduction: cell biology of osteoarthritis," Arthritis Res, **3**(2), pp.107-13.

11. Barnett, C. H., Cochrane, W., Palfrey, A. J. 1963, "Age Changes in Articular Cartilage of Rabbits," Ann Rheum Dis, **22** pp.389-400.

12. Holmes, M. W., Bayliss, M. T., Muir, H. 1988, "Hyaluronic acid in human articular cartilage. Age-related changes in content and size," Biochem J, **250**(2), pp.435-41.

13. Kaplan, D., Meyer, K. 1959, "Ageing of human cartilage," Nature, **183**(4670), pp.1267-8.

14. Baker, C. L., Jr., Ferguson, C. M. 2005, "Future treatment of osteoarthritis," Orthopedics, **28**(2 Suppl), pp.s227-34.

15. Howell, D. S. 1986, "Pathogenesis of osteoarthritis," Am J Med, **80**(4B), pp.24-8.

16. Andersson, G., Bouchard, J., Bozic, K., Campbell, R., Cisternas, M., Correa, A., Cosman, F., Cragan, J., D'Andrea, K., Doernberg, N., Dormans, J., Elderkin, A., Fershteyn, Z., Foreman, A., Gitelis, S., Gnatz, S., Haralson, R., Helmick, C., Hu, S., Katz, J., King, T., Kirk, R., Kurtz, S., Lane, N., Miller, A., Novich, R., Olney, R., Panopalis, P., Pasta, D., Pollak, A., Puzas, J., Richards, B., Sestito, J., Siffel, C., Sponseller, P., St. Clair, E., Stuart, A., Templeton, K., Thompson, G., Tosi, L., Ward, W., Watkins-Castillo, S., Weinstein, S., Wright, J., Yelin, E. Burden of Musculoskeletal Diseases in the United States: Prevalence, Societal and Economic Cost. Rosemont, IL: American Academy of Orthopaedic Surgeons; 2008.

17. CDC. Arthrits related statistics. In: Program TA, editor.: Center for Disease Control and Prevention; 2009.

18. Helmick, C. G., Felson, D. T., Lawrence, R. C., Gabriel, S., Hirsch, R., Kwoh, C. K., Liang, M. H., Kremers, H. M., Mayes, M. D., Merkel, P. A., Pillemer, S. R., Reveille, J. D., Stone, J. H. 2008, "Estimates of the prevalence of arthritis and other rheumatic conditions in the United States. Part I," Arthritis Rheum, **58**(1), pp.15-25.

19. Martel-Pelletier, J. 1999, "Pathophysiology of osteoarthritis," Osteoarthritis Cartilage, **7**(4), pp.371-3.

20. Alfredson, H., Lorentzon, R. 1999, "Superior results with continuous passive motion compared to active motion after periosteal transplantation. A retrospective study of human patella cartilage defect treatment," Knee Surg Sports Traumatol Arthrosc, **7**(4), pp.232-8.

21. Akeson, W. H., Amiel, D., Abel, M. F., Garfin, S. R., Woo, S. L. 1987, "Effects of immobilization on joints," Clin Orthop Relat Res, (219), pp.28-37.

22. Bendele, A. M. 2001, "Animal models of osteoarthritis," J Musculoskelet Neuronal Interact, **1**(4), pp.363-76.

23. Vrahas, M. S., Mithoefer, K., Joseph, D. 2004, "The long-term effects of articular impaction," Clin Orthop Relat Res, (423), pp.40-3.

24. Chiang, H., Kuo, T. F., Tsai, C. C., Lin, M. C., She, B. R., Huang, Y. Y., Lee, H. S., Shieh, C. S., Chen, M. H., Ramshaw, J. A., Werkmeister, J. A., Tuan, R. S., Jiang, C. C. 2005, "Repair of porcine articular cartilage defect with autologous chondrocyte transplantation," J Orthop Res, **23**(3), pp.584-93.

25. Richardson, J. B., Caterson, B., Evans, E. H., Ashton, B. A., Roberts, S. 1999, "Repair of human articular cartilage after implantation of autologous chondrocytes," J Bone Joint Surg Br, **81**(6), pp.1064-8.

26. Ronga, M., Grassi, F. A., Bulgheroni, P. 2004, "Arthroscopic autologous chondrocyte implantation for the treatment of a chondral defect in the tibial plateau of the knee," Arthroscopy, **20**(1), pp.79-84.

27. Browne, J. E., Anderson, A. F., Arciero, R., Mandelbaum, B., Moseley, J. B., Jr., Micheli, L. J., Fu, F., Erggelet, C. 2005, "Clinical outcome of autologous chondrocyte implantation at 5 years in US subjects," Clin Orthop Relat Res, (436), pp.237-45.

28. Henderson, I., Francisco, R., Oakes, B., Cameron, J. 2005, "Autologous chondrocyte implantation for treatment of focal chondral defects of the knee--a clinical, arthroscopic, MRI and histologic evaluation at 2 years," Knee, **12**(3), pp.209-16.

29. Micheli, L. J., Browne, J. E., Erggelet, C., Fu, F., Mandelbaum, B., Moseley, J. B., Zurakowski, D. 2001, "Autologous chondrocyte implantation of the knee: multicenter experience and minimum 3-year follow-up," Clin J Sport Med, **11**(4), pp.223-8.

30. Palsson, B. O., Bhatia, S. N. Tissue Engineering: Prentice Hall; 2003.

31. Angele, P., Schumann, D., Angele, M., Kinner, B., Englert, C., Hente, R., Fuchtmeier, B., Nerlich, M., Neumann, C., Kujat, R. 2004, "Cyclic, mechanical compression enhances chondrogenesis of mesenchymal progenitor cells in tissue engineering scaffolds," Biorheology, **41**(3-4), pp.335-46.

32. Bonassar, L. J., Grodzinsky, A. J., Frank, E. H., Davila, S. G., Bhaktav, N. R., Trippel, S. B. 2001, "The effect of dynamic compression on the response of articular cartilage to insulin-like growth factor-I," J Orthop Res, **19**(1), pp.11-7.

33. Buschmann, M. D., Gluzband, Y. A., Grodzinsky, A. J., Hunziker, E. B. 1995, "Mechanical compression modulates matrix biosynthesis in chondrocyte/agarose culture," J Cell Sci, **108 (Pt 4)** pp.1497-508.

34. Campbell, J. J., Lee, D. A., Bader, D. L. 2006, "Dynamic compressive strain influences chondrogenic gene expression in human mesenchymal stem cells," Biorheology, **43**(3-4), pp.455-70.

35. Darling, E. M., Athanasiou, K. A. 2005, "Growth factor impact on articular cartilage subpopulations," Cell Tissue Res, **322**(3), pp.463-73.

36. Demarteau, O., Wendt, D., Braccini, A., Jakob, M., Schafer, D., Heberer, M., Martin, I. 2003, "Dynamic compression of cartilage constructs engineered from expanded human articular chondrocytes," Biochem Biophys Res Commun, **310**(2), pp.580-8.

37. Kisiday, J. D., Jin, M., DiMicco, M. A., Kurz, B., Grodzinsky, A. J. 2004, "Effects of dynamic compressive loading on chondrocyte biosynthesis in self-assembling peptide scaffolds," J Biomech, **37**(5), pp.595-604.

38. Kojima, K., Bonassar, L. J., Roy, A. K., Mizuno, H., Cortiella, J., Vacanti, C. A. 2003, "A composite tissue-engineered trachea using sheep nasal chondrocyte and epithelial cells," Faseb J, **17**(8), pp.823-8.

39. Lee, C. S., Gleghorn, J. P., Won Choi, N., Cabodi, M., Stroock, A. D., Bonassar, L. J. 2007, "Integration of layered chondrocyte-seeded alginate hydrogel scaffolds," Biomaterials, **28**(19), pp.2987-93.

40. Lima, E. G., Bian, L., Ng, K. W., Mauck, R. L., Byers, B. A., Tuan, R. S., Ateshian, G. A., Hung, C. T. 2007, "The beneficial effect of delayed compressive loading on tissue-engineered cartilage constructs cultured with TGF-beta3," Osteoarthritis Cartilage, **15**(9), pp.1025-33.

41. Mahmoudifar, N., Doran, P. M. 2005, "Tissue engineering of human cartilage and osteochondral composites using recirculation bioreactors," Biomaterials, **26**(34), pp.7012-24.

42. Mauck, R. L., Seyhan, S. L., Ateshian, G. A., Hung, C. T. 2002, "Influence of seeding density and dynamic deformational loading on the developing structure/function relationships of chondrocyte-seeded agarose hydrogels," Ann Biomed Eng, **30**(8), pp.1046-56.

43. Mauck, R. L., Soltz, M. A., Wang, C. C., Wong, D. D., Chao, P. H., Valhmu, W. B., Hung, C. T., Ateshian, G. A. 2000, "Functional tissue engineering of articular cartilage through dynamic loading of chondrocyte-seeded agarose gels," J Biomech Eng, **122**(3), pp.252-60.

44. Mercier, N. R., Costantino, H. R., Tracy, M. A., Bonassar, L. J. 2005, "Poly(lactide-co-glycolide) microspheres as a moldable scaffold for cartilage tissue engineering," Biomaterials, **26**(14), pp.1945-52.

45. Mouw, J. K., Connelly, J. T., Wilson, C. G., Michael, K. E., Levenston, M. E. 2007, "Dynamic compression regulates the expression and synthesis of chondrocyte-

specific matrix molecules in bone marrow stromal cells," Stem Cells, **25**(3), pp.655-663.

46. Chowdhury, T. T., Bader, D. L., Lee, D. A. 2006, "Dynamic compression counteracts IL-1beta induced iNOS and COX-2 activity by human chondrocytes cultured in agarose constructs," Biorheology, **43**(3-4), pp.413-29.

47. Elder, S. H., Sanders, S. W., McCulley, W. R., Marr, M. L., Shim, J. W., Hasty, K. A. 2006, "Chondrocyte response to cyclic hydrostatic pressure in alginate versus pellet culture," J Orthop Res, **24**(4), pp.740-7.

48. Hunter, C. J., Mouw, J. K., Levenston, M. E. 2004, "Dynamic compression of chondrocyte-seeded fibrin gels: effects on matrix accumulation and mechanical stiffness," Osteoarthritis and Cartilage, **12**(2), pp.117-130.

49. Mahmoudifar, N., Doran, P. M. 2005, "Tissue engineering of human cartilage in bioreactors using single and composite cell-seeded scaffolds," Biotechnol Bioeng, **91**(3), pp.338-55.

50. Ng, K. W., Mauck, R. L., Statman, L. Y., Lin, E. Y., Ateshian, G. A., Hung, C. T. 2006, "Dynamic deformational loading results in selective application of mechanical stimulation in a layered, tissue-engineered cartilage construct," Biorheology, **43**(3-4), pp.497-507.

51. Beaupre, G. S., Stevens, S. S., Carter, D. R. 2000, "Mechanobiology in the development, maintenance, and degeneration of articular cartilage," J Rehabil Res Dev, **37**(2), pp.145-51.

52. Carter, D. R., Beaupre, G. S., Wong, M., Smith, R. L., Andriacchi, T. P., Schurman, D. J. 2004, "The mechanobiology of articular cartilage development and degeneration," Clin Orthop Relat Res, (427 Suppl), pp.S69-77.

53. Heegaard, J. H., Beaupre, G. S., Carter, D. R. 1999, "Mechanically modulated cartilage growth may regulate joint surface morphogenesis," J Orthop Res, **17**(4), pp.509-17.

54. Henderson, J. H., Carter, D. R. 2002, "Mechanical induction in limb morphogenesis: the role of growth-generated strains and pressures," Bone, **31**(6), pp.645-53.

55. Lelkes, G. 1958, "Experiments in vitro on the role of movement in the development of joints," J Embryol Exp Morphol, **6**(2), pp.183-6.

56. Nowlan, N. C., Murphy, P., Prendergast, P. J. 2007, "Mechanobiology of embryonic limb development," Ann N Y Acad Sci, **1101** pp.389-411.

57. Rot-Nikcevic, I., Reddy, T., Downing, K. J., Belliveau, A. C., Hallgrimsson, B., Hall, B. K., Kablar, B. 2006, "Myf5-/- :MyoD-/- amyogenic fetuses reveal the importance of early contraction and static loading by striated muscle in mouse skeletogenesis," Dev Genes Evol, **216**(1), pp.1-9.

58. Mikic, B., Johnson, T. L., Chhabra, A. B., Schalet, B. J., Wong, M., Hunziker, E. B. 2000, "Differential effects of embryonic immobilization on the development of fibrocartilaginous skeletal elements," J Rehabil Res Dev, **37**(2), pp.127-33.

59. Osborne, A. C., Lamb, K. J., Lewthwaite, J. C., Dowthwaite, G. P., Pitsillides, A. A. 2002, "Short-term rigid and flaccid paralyses diminish growth of embryonic

chick limbs and abrogate joint cavity formation but differentially preserve pre-cavitated joints," J Musculoskelet Neuronal Interact, **2**(5), pp.448-56.

60. Carter, D. R., Beaupre, G. S., Giori, N. J., Helms, J. A. 1998, "Mechanobiology of skeletal regeneration," Clin Orthop Relat Res, (355 Suppl), pp.S41-55.

61. Carter, D. R., Orr, T. E., Fyhrie, D. P., Schurman, D. J. 1987, "Influences of mechanical stress on prenatal and postnatal skeletal development," Clin Orthop Relat Res, (219), pp.237-50.

62. Carter, D. R., Wong, M., Orr, T. E. 1991, "Musculoskeletal ontogeny, phylogeny, and functional adaptation," J Biomech, **24 Suppl 1** pp.3-16.

63. Pauwels, F. 1960, "[A new theory on the influence of mechanical stimuli on the differentiation of supporting tissue. The tenth contribution to the functional anatomy and causal morphology of the supporting structure.]," Z Anat Entwicklungsgesch, **121** pp.478-515.

64. Herzog, W., Federico, S. 2006, "Considerations on joint and articular cartilage mechanics," Biomech Model Mechanobiol, **5**(2-3), pp.64-81.

65. LeVeau, B. F., Bernhardt, D. B. 1984, "Developmental biomechanics. Effect of forces on the growth, development, and maintenance of the human body," Phys Ther, **64**(12), pp.1874-82.

66. Andriacchi, T. P., Koo, S., Scanlan, S. F. 2009, "Gait mechanics influence healthy cartilage morphology and osteoarthritis of the knee," J Bone Joint Surg Am, **91 Suppl 1** pp.95-101.

67. Vanwanseele, B., Eckstein, F., Knecht, H., Stussi, E., Spaepen, A. 2002, "Knee cartilage of spinal cord-injured patients displays progressive thinning in the absence of normal joint loading and movement," Arthritis Rheum, **46**(8), pp.2073-8.

68. Alenghat, F. J., Ingber, D. E. 2002, "Mechanotransduction: all signals point to cytoskeleton, matrix, and integrins," Sci STKE, **2002**(119), pp.pe6.

69. Chen, C. S., Tan, J., Tien, J. 2004, "Mechanotransduction at cell-matrix and cell-cell contacts," Annu Rev Biomed Eng, **6** pp.275-302.

70. Jalali, S., del Pozo, M. A., Chen, K., Miao, H., Li, Y., Schwartz, M. A., Shyy, J. Y., Chien, S. 2001, "Integrin-mediated mechanotransduction requires its dynamic interaction with specific extracellular matrix (ECM) ligands," Proc Natl Acad Sci U S A, **98**(3), pp.1042-6.

71. Gumbiner, B. M. 1996, "Cell adhesion: the molecular basis of tissue architecture and morphogenesis," Cell, **84**(3), pp.345-57.

72. Schwartz, M. A., Schaller, M. D., Ginsberg, M. H. 1995, "Integrins: emerging paradigms of signal transduction," Annu Rev Cell Dev Biol, **11** pp.549-99.

73. Shyy, J. Y., Chien, S. 1997, "Role of integrins in cellular responses to mechanical stress and adhesion," Curr Opin Cell Biol, **9**(5), pp.707-13.

74. Pazzano, D., Mercier, K. A., Moran, J. M., Fong, S. S., DiBiasio, D. D., Rulfs, J. X., Kohles, S. S., Bonassar, L. J. 2000, "Comparison of chondrogensis in static and perfused bioreactor culture," Biotechnol Prog, **16**(5), pp.893-6.

75. Knight, M. M., Toyoda, T., Lee, D. A., Bader, D. L. 2006, "Mechanical compression and hydrostatic pressure induce reversible changes in actin cytoskeletal

organisation in chondrocytes in agarose," Journal of Biomechanics, **39**(8), pp.1547-1551.

76. Freed, L. E., Langer, R., Martin, I., Pellis, N. R., Vunjak-Novakovic, G. 1997, "Tissue engineering of cartilage in space," Proc Natl Acad Sci U S A, **94**(25), pp.13885-90.

77. Li, W. J., Chiang, H., Kuo, T. F., Lee, H. S., Jiang, C. C., Tuan, R. S. 2009, "Evaluation of articular cartilage repair using biodegradable nanofibrous scaffolds in a swine model: a pilot study," J Tissue Eng Regen Med, **3**(1), pp.1-10.

78. Yang, Z., Shi, Y., Wei, X., He, J., Yang, S., Dickson, G., Tang, J., Xiang, J., Song, C., Li, G. 2009, "Fabrication and Characterization of a Novel Acellular Cartilage Matrix Scaffold for Tissue Engineering," Tissue Eng Part C Methods.

79. Chang, S. C., Rowley, J. A., Tobias, G., Genes, N. G., Roy, A. K., Mooney, D. J., Vacanti, C. A., Bonassar, L. J. 2001, "Injection molding of chondrocyte/alginate constructs in the shape of facial implants," J Biomed Mater Res, **55**(4), pp.503-11.

80. Darling, E. M., Athanasiou, K. A. 2005, "Rapid phenotypic changes in passaged articular chondrocyte subpopulations," J Orthop Res, **23**(2), pp.425-32.

81. Giannoni, P., Crovace, A., Malpeli, M., Maggi, E., Arbico, R., Cancedda, R., Dozin, B. 2005, "Species variability in the differentiation potential of in vitro-expanded articular chondrocytes restricts predictive studies on cartilage repair using animal models," Tissue Eng, **11**(1-2), pp.237-48.

82. Veilleux, N. H., Yannas, I. V., Spector, M. 2004, "Effect of passage number and collagen type on the proliferative, biosynthetic, and contractile activity of adult

canine articular chondrocytes in type I and II collagen-glycosaminoglycan matrices in vitro," Tissue Eng, **10**(1-2), pp.119-27.

83. Baksh, D., Song, L., Tuan, R. S. 2004, "Adult mesenchymal stem cells: characterization, differentiation, and application in cell and gene therapy," J Cell Mol Med, **8**(3), pp.301-16.

84. Caplan, A. I. 1991, "Mesenchymal stem cells," J Orthop Res, **9**(5), pp.641-50.

85. Kolf, C. M., Cho, E., Tuan, R. S. 2007, "Mesenchymal stromal cells. Biology of adult mesenchymal stem cells: regulation of niche, self-renewal and differentiation," Arthritis Res Ther, **9**(1), pp.204.

86. Pittenger, M. F., Mackay, A. M., Beck, S. C., Jaiswal, R. K., Douglas, R., Mosca, J. D., Moorman, M. A., Simonetti, D. W., Craig, S., Marshak, D. R. 1999, "Multilineage potential of adult human mesenchymal stem cells," Science, **284**(5411), pp.143-7.

87. Tuan, R. S. 2003, "Cellular signaling in developmental chondrogenesis: N-cadherin, Wnts, and BMP-2," J Bone Joint Surg Am, **85-A Suppl 2** pp.137-41.

88. Worster, A. A., Nixon, A. J., Brower-Toland, B. D., Williams, J. 2000, "Effect of transforming growth factor beta1 on chondrogenic differentiation of cultured equine mesenchymal stem cells," Am J Vet Res, **61**(9), pp.1003-10.

89. O'Driscoll, S. W., Saris, D. B., Ito, Y., Fitzimmons, J. S. 2001, "The chondrogenic potential of periosteum decreases with age," J Orthop Res, **19**(1), pp.95-103.

90. Young, H. E., Steele, T. A., Bray, R. A., Hudson, J., Floyd, J. A., Hawkins, K., Thomas, K., Austin, T., Edwards, C., Cuzzourt, J., Duenzl, M., Lucas, P. A., Black, A. C., Jr. 2001, "Human reserve pluripotent mesenchymal stem cells are present in the connective tissues of skeletal muscle and dermis derived from fetal, adult, and geriatric donors," Anat Rec, **264**(1), pp.51-62.

91. Gronthos, S., Franklin, D. M., Leddy, H. A., Robey, P. G., Storms, R. W., Gimble, J. M. 2001, "Surface protein characterization of human adipose tissue-derived stromal cells," J Cell Physiol, **189**(1), pp.54-63.

92. De Bari, C., Dell'Accio, F., Tylzanowski, P., Luyten, F. P. 2001, "Multipotent mesenchymal stem cells from adult human synovial membrane," Arthritis Rheum, **44**(8), pp.1928-42.

93. Pereira, R. F., Halford, K. W., O'Hara, M. D., Leeper, D. B., Sokolov, B. P., Pollard, M. D., Bagasra, O., Prockop, D. J. 1995, "Cultured adherent cells from marrow can serve as long-lasting precursor cells for bone, cartilage, and lung in irradiated mice," Proc Natl Acad Sci U S A, **92**(11), pp.4857-61.

94. Friedenstein, A. J., Piatetzky, S., II, Petrakova, K. V. 1966, "Osteogenesis in transplants of bone marrow cells," J Embryol Exp Morphol, **16**(3), pp.381-90.

95. Wang, Y., Kim, U. J., Blasioli, D. J., Kim, H. J., Kaplan, D. L. 2005, "In vitro cartilage tissue engineering with 3D porous aqueous-derived silk scaffolds and mesenchymal stem cells," Biomaterials, **26**(34), pp.7082-94.

96. Gleghorn, J. P., Jones, A. R., Flannery, C. R., Bonassar, L. J. 2007, "Boundary mode frictional properties of engineered cartilaginous tissues," Eur Cell Mater, **14** pp.20-8; discussion 28-9.

97. Aigner, J., Tegeler, J., Hutzler, P., Campoccia, D., Pavesio, A., Hammer, C., Kastenbauer, E., Naumann, A. 1998, "Cartilage tissue engineering with novel nonwoven structured biomaterial based on hyaluronic acid benzyl ester," J Biomed Mater Res, **42**(2), pp.172-81.

98. Grigolo, B., Roseti, L., Fiorini, M., Fini, M., Giavaresi, G., Aldini, N. N., Giardino, R., Facchini, A. 2001, "Transplantation of chondrocytes seeded on a hyaluronan derivative (hyaff-11) into cartilage defects in rabbits," Biomaterials, **22**(17), pp.2417-24.

99. Leddy, H. A., Awad, H. A., Guilak, F. 2004, "Molecular diffusion in tissue-engineered cartilage constructs: effects of scaffold material, time, and culture conditions," J Biomed Mater Res B Appl Biomater, **70**(2), pp.397-406.

100. Sams, A. E., Nixon, A. J. 1995, "Chondrocyte-laden collagen scaffolds for resurfacing extensive articular cartilage defects," Osteoarthritis Cartilage, **3**(1), pp.47-59.

101. Iwasa, J., Ochi, M., Uchio, Y., Katsube, K., Adachi, N., Kawasaki, K. 2003, "Effects of cell density on proliferation and matrix synthesis of chondrocytes embedded in atelocollagen gel," Artif Organs, **27**(3), pp.249-55.

102. Li, W. J., Cooper, J. A., Jr., Mauck, R. L., Tuan, R. S. 2006, "Fabrication and characterization of six electrospun poly(alpha-hydroxy ester)-based fibrous scaffolds for tissue engineering applications," Acta Biomater, **2**(4), pp.377-85.

103. Moran, J. M., Pazzano, D., Bonassar, L. J. 2003, "Characterization of polylactic acid-polyglycolic acid composites for cartilage tissue engineering," Tissue Eng, **9**(1), pp.63-70.

104. Nicodemus, G. D., Villanueva, I., Bryant, S. J. 2007, "Mechanical stimulation of TMJ condylar chondrocytes encapsulated in PEG hydrogels," J Biomed Mater Res A, **83**(2), pp.323-31.

105. Rotter, N., Ung, F., Roy, A. K., Vacanti, M., Eavey, R. D., Vacanti, C. A., Bonassar, L. J. 2005, "Role for interleukin 1alpha in the inhibition of chondrogenesis in autologous implants using polyglycolic acid-polylactic acid scaffolds," Tissue Eng, **11**(1-2), pp.192-200.

106. Lee, C. R., Grad, S., Gorna, K., Gogolewski, S., Goessl, A., Alini, M. 2005, "Fibrin-polyurethane composites for articular cartilage tissue engineering: a preliminary analysis," Tissue Eng, **11**(9-10), pp.1562-73.

107. Bryant, S. J., Arthur, J. A., Anseth, K. S. 2005, "Incorporation of tissue-specific molecules alters chondrocyte metabolism and gene expression in photocrosslinked hydrogels," Acta Biomater, **1**(2), pp.243-52.

108. Mauck, R. L., Wang, C. C., Oswald, E. S., Ateshian, G. A., Hung, C. T. 2003, "The role of cell seeding density and nutrient supply for articular cartilage tissue engineering with deformational loading," Osteoarthritis Cartilage, **11**(12), pp.879-90.

109. Platt, D., Wells, T., Bayliss, M. T. 1997, "Proteoglycan metabolism of equine articular chondrocytes cultured in alginate beads," Res Vet Sci, **62**(1), pp.39-47.

110. Yoo, H. S., Lee, E. A., Yoon, J. J., Park, T. G. 2005, "Hyaluronic acid modified biodegradable scaffolds for cartilage tissue engineering," Biomaterials, **26**(14), pp.1925-33.

111. Nerurkar, N. L., Baker, B. M., Chen, C. Y., Elliott, D. M., Mauck, R. L. 2006, "Engineering of fiber-reinforced tissues with anisotropic biodegradable nanofibrous scaffolds," Conf Proc IEEE Eng Med Biol Soc, **1** pp.787-90.

112. Miot, S., Woodfield, T., Daniels, A. U., Suetterlin, R., Peterschmitt, I., Heberer, M., van Blitterswijk, C. A., Riesle, J., Martin, I. 2005, "Effects of scaffold composition and architecture on human nasal chondrocyte redifferentiation and cartilaginous matrix deposition," Biomaterials, **26**(15), pp.2479-89.

113. Barry, J. J., Gidda, H. S., Scotchford, C. A., Howdle, S. M. 2004, "Porous methacrylate scaffolds: supercritical fluid fabrication and in vitro chondrocyte responses," Biomaterials, **25**(17), pp.3559-68.

114. Chaipinyo, K., Oakes, B. W., van Damme, M. P. 2002, "Effects of growth factors on cell proliferation and matrix synthesis of low-density, primary bovine chondrocytes cultured in collagen I gels," J Orthop Res, **20**(5), pp.1070-8.

115. Grande, D. A., Mason, J., Light, E., Dines, D. 2003, "Stem cells as platforms for delivery of genes to enhance cartilage repair," J Bone Joint Surg Am, **85-A Suppl 2** pp.111-6.

116. Mauck, R. L., Nicoll, S. B., Seyhan, S. L., Ateshian, G. A., Hung, C. T. 2003, "Synergistic action of growth factors and dynamic loading for articular cartilage tissue engineering," Tissue Eng, **9**(4), pp.597-611.

117. Worster, A. A., Brower-Toland, B. D., Fortier, L. A., Bent, S. J., Williams, J., Nixon, A. J. 2001, "Chondrocytic differentiation of mesenchymal stem cells sequentially exposed to transforming growth factor-beta1 in monolayer and insulin-like growth factor-I in a three-dimensional matrix," J Orthop Res, **19**(4), pp.738-49.

118. Li, W. J., Tuli, R., Okafor, C., Derfoul, A., Danielson, K. G., Hall, D. J., Tuan, R. S. 2005, "A three-dimensional nanofibrous scaffold for cartilage tissue engineering using human mesenchymal stem cells," Biomaterials, **26**(6), pp.599-609.

119. Yamaoka, H., Asato, H., Ogasawara, T., Nishizawa, S., Takahashi, T., Nakatsuka, T., Koshima, I., Nakamura, K., Kawaguchi, H., Chung, U. I., Takato, T., Hoshi, K. 2006, "Cartilage tissue engineering using human auricular chondrocytes embedded in different hydrogel materials," J Biomed Mater Res A, **78**(1), pp.1-11.

120. Almarza, A. J., Athanasiou, K. A. 2005, "Effects of initial cell seeding density for the tissue engineering of the temporomandibular joint disc," Ann Biomed Eng, **33**(7), pp.943-50.

121. Connelly, J. T., Vanderploeg, E. J., Levenston, M. E. 2004, "The influence of cyclic tension amplitude on chondrocyte matrix synthesis: experimental and finite element analyses," Biorheology, **41**(3-4), pp.377-87.

122. Lima, E. G., Mauck, R. L., Han, S. H., Park, S., Ng, K. W., Ateshian, G. A., Hung, C. T. 2004, "Functional tissue engineering of chondral and osteochondral constructs," Biorheology, **41**(3-4), pp.577-90.

123. Silva, P., Crozier, S., Veidt, M., Pearcy, M. J. 2005, "An experimental and finite element poroelastic creep response analysis of an intervertebral hydrogel disc model in axial compression," J Mater Sci Mater Med, **16**(7), pp.663-9.

124. Langer, R., Vacanti, J. P. 1993, "Tissue engineering," Science, **260**(5110), pp.920-6.

125. Sharma, B., Williams, C. G., Kim, T. K., Sun, D., Malik, A., Khan, M., Leong, K., Elisseeff, J. H. 2007, "Designing zonal organization into tissue-engineered cartilage," Tissue Eng, **13**(2), pp.405-14.

126. Sittinger, M., Perka, C., Schultz, O., Haupl, T., Burmester, G. R. 1999, "Joint cartilage regeneration by tissue engineering," Z Rheumatol, **58**(3), pp.130-5.

127. Xu, J. W., Zaporojan, V., Peretti, G. M., Roses, R. E., Morse, K. B., Roy, A. K., Mesa, J. M., Randolph, M. A., Bonassar, L. J., Yaremchuk, M. J. 2004, "Injectable tissue-engineered cartilage with different chondrocyte sources," Plast Reconstr Surg, **113**(5), pp.1361-71.

128. Fuchs, J. R., Terada, S., Hannouche, D., Ochoa, E. R., Vacanti, J. P., Fauza, D. O. 2002, "Engineered fetal cartilage: structural and functional analysis in vitro," J Pediatr Surg, **37**(12), pp.1720-5.

129. Mandl, E. W., van der Veen, S. W., Verhaar, J. A., van Osch, G. J. 2004, "Multiplication of human chondrocytes with low seeding densities accelerates cell yield without losing redifferentiation capacity," Tissue Eng, **10**(1-2), pp.109-18.

130. Mayne, R., Vail, M. S., Mayne, P. M., Miller, E. J. 1976, "Changes in type of collagen synthesized as clones of chick chondrocytes grow and eventually lose division capacity," Proc Natl Acad Sci U S A, **73**(5), pp.1674-8.

131. von der Mark, K., Gauss, V., von der Mark, H., Muller, P. 1977, "Relationship between cell shape and type of collagen synthesised as chondrocytes lose their cartilage phenotype in culture," Nature, **267**(5611), pp.531-2.

132. Mackay, A. M., Beck, S. C., Murphy, J. M., Barry, F. P., Chichester, C. O., Pittenger, M. F. 1998, "Chondrogenic differentiation of cultured human mesenchymal stem cells from marrow," Tissue Eng, **4**(4), pp.415-28.

133. Mauck, R. L., Yuan, X., Tuan, R. S. 2006, "Chondrogenic differentiation and functional maturation of bovine mesenchymal stem cells in long-term agarose culture," Osteoarthritis Cartilage, **14**(2), pp.179-89.

134. Tuan, R. S., Boland, G., Tuli, R. 2003, "Adult mesenchymal stem cells and cell-based tissue engineering," Arthritis Res Ther, **5**(1), pp.32-45.

135. Genes, N. G., Rowley, J. A., Mooney, D. J., Bonassar, L. J. 2004, "Effect of substrate mechanics on chondrocyte adhesion to modified alginate surfaces," Arch Biochem Biophys, **422**(2), pp.161-7.

136. Mauck, R. L., Byers, B. A., Yuan, X., Tuan, R. S. 2007, "Regulation of cartilaginous ECM gene transcription by chondrocytes and MSCs in 3D culture in response to dynamic loading," Biomechanics and Modeling in Mechanobiology, **6**(1-2), pp.113-125.

137. Enobakhare, B. O., Bader, D. L., Lee, D. A. 1996, "Quantification of sulfated glycosaminoglycans in chondrocyte/alginate cultures, by use of 1,9-dimethylmethylene blue," Anal Biochem, **243**(1), pp.189-91.

138. Kim, Y. J., Sah, R. L., Doong, J. Y., Grodzinsky, A. J. 1988, "Fluorometric assay of DNA in cartilage explants using Hoechst 33258," Anal Biochem, **174**(1), pp.168-76.

139. Mow, V. C., Kuei, S. C., Lai, W. M., Armstrong, C. G. 1980, "Biphasic creep and stress relaxation of articular cartilage in compression? Theory and experiments," J Biomech Eng, **102**(1), pp.73-84.

140. Quinn, T. M., Grodzinsky, A. J. 1993, "Longitudinal Modulus and Hydraulic Permeability of Poly(Methacrylic Acid) Gels - Effects of Charge-Density and Solvent Content," Macromolecules, **26**(16), pp.4332-4338.

141. Wong, M., Siegrist, M., Wang, X., Hunziker, E. 2001, "Development of mechanically stable alginate/chondrocyte constructs: effects of guluronic acid content and matrix synthesis," J Orthop Res, **19**(3), pp.493-9.

142. Kobayashi, S., Meir, A., Urban, J. 2008, "Effect of cell density on the rate of glycosaminoglycan accumulation by disc and cartilage cells in vitro," J Orthop Res, **26**(4), pp.493-503.

143. Mahmoudifar, N., Doran, P. M. 2006, "Effect of seeding and bioreactor culture conditions on the development of human tissue-engineered cartilage," Tissue Eng, **12**(6), pp.1675-85.

144. Panossian, A., Ashiku, S., Kirchhoff, C. H., Randolph, M. A., Yaremchuk, M. J. 2001, "Effects of cell concentration and growth period on articular and ear chondrocyte transplants for tissue engineering," Plast Reconstr Surg, **108**(2), pp.392-402.

145. Saini, S., Wick, T. M. 2003, "Concentric cylinder bioreactor for production of tissue engineered cartilage: effect of seeding density and hydrodynamic loading on construct development," Biotechnol Prog, **19**(2), pp.510-21.

146. Tran-Khanh, N., Hoemann, C. D., McKee, M. D., Henderson, J. E., Buschmann, M. D. 2005, "Aged bovine chondrocytes display a diminished capacity to produce a collagen-rich, mechanically functional cartilage extracellular matrix," J Orthop Res, **23**(6), pp.1354-62.

147. Nicodemus, G. D., Giunta, S. M., Bryant, S. J. Rational design of 3D hydrogels to capture and retain ECM molecules within mechanically stimulated PRG gels. In: Transactions of the Orthopaedic Research Society; 2009; Las Vegas, NV; 2009. p. 0572.

148. Uhthoff, H. K., Jaworski, Z. F. 1978, "Bone loss in response to long-term immobilisation," J Bone Joint Surg Br, **60-B**(3), pp.420-9.

149. Smith, R. L., Thomas, K. D., Schurman, D. J., Carter, D. R., Wong, M., van der Meulen, M. C. 1992, "Rabbit knee immobilization: bone remodeling precedes cartilage degradation," J Orthop Res, **10**(1), pp.88-95.

150. Behrens, F., Kraft, E. L., Oegema, T. R., Jr. 1989, "Biochemical changes in articular cartilage after joint immobilization by casting or external fixation," J Orthop Res, **7**(3), pp.335-43.

151. Langenskiold, A., Michelsson, J. E., Videman, T. 1979, "Osteoarthritis of the knee in the rabbit produced by immobilization. Attempts to achieve a reproducible model for studies on pathogenesis and therapy," Acta Orthop Scand, **50**(1), pp.1-14.

152. Kim, Y. J., Bonassar, L. J., Grodzinsky, A. J. 1995, "The role of cartilage streaming potential, fluid flow and pressure in the stimulation of chondrocyte biosynthesis during dynamic compression," J Biomech, **28**(9), pp.1055-66.

153. Cioffi, M., Boschetti, F., Raimondi, M. T., Dubini, G. 2006, "Modeling evaluation of the fluid-dynamic microenvironment in tissue-engineered constructs: a micro-CT based model," Biotechnol Bioeng, **93**(3), pp.500-10.

154. Lacroix, D., Chateau, A., Ginebra, M. P., Planell, J. A. 2006, "Micro-finite element models of bone tissue-engineering scaffolds," Biomaterials, **27**(30), pp.5326-34.

155. Chatchawalsaisin, J., Podczeck, F., Newton, J. M. 2004, "The influence of chitosan and sodium alginate and formulation variables on the formation and drug release from pellets prepared by extrusion/spheronisation," International Journal of Pharmaceutics, **275**(1-2), pp.41-60.

156. Fourest, E., Volesky, B. 1997, "Alginate properties and heavy metal biosorption by marine algae," Applied Biochemistry and Biotechnology, **67**(3), pp.215-226.

157. Matsukawa, M., Sasaki, K., Akimoto, T., Otani, T. 2002, "Application of a suspension theory to particle-dispersed agarose gels," Jpn. J. Appl. Phys., **41**(5B), pp.3163-3167.

158. Serwer, P. 1983, "Agarose Gels - Properties and Use for Electrophoresis," Electrophoresis, **4**(6), pp.375-382.

159. Spilker, R. L., Suh, J. K., Mow, V. C. 1990, "Effects of friction on the unconfined compressive response of articular cartilage: a finite element analysis," J Biomech Eng, **112**(2), pp.138-46.

160. Chowdhury, T. T., Bader, D. L., Lee, D. A. 2003, "Dynamic compression counteracts IL-1 beta-induced release of nitric oxide and PGE2 by superficial zone chondrocytes cultured in agarose constructs," Osteoarthritis Cartilage, **11**(9), pp.688-96.

161. Lima, E. G., Bian, L., Mauck, R. L., Byers, B. A., Tuan, R. S., Ateshian, G. A., Hung, C. T. 2006, "The effect of applied compressive loading on tissue-engineered cartilage constructs cultured with TGF-beta3," Conf Proc IEEE Eng Med Biol Soc, **1** pp.779-82.

162. Pingguan-Murphy, B., Lee, D. A., Bader, D. L., Knight, M. M. 2005, "Activation of chondrocytes calcium signalling by dynamic compression is independent of number of cycles," Archives of Biochemistry and Biophysics, **444**(1), pp.45-51.

163. Shelton, J. C., Bader, D. L., Lee, D. A. 2003, "Mechanical conditioning influences the metabolic response of cell-seeded constructs," Cells Tissues Organs, **175**(3), pp.140-50.

164. Ma, P. X., Schloo, B., Mooney, D., Langer, R. 1995, "Development of biomechanical properties and morphogenesis of in vitro tissue engineered cartilage," J Biomed Mater Res, **29**(12), pp.1587-95.

165. Waldman, S. D., Spiteri, C. G., Grynpas, M. D., Pilliar, R. M., Hong, J., Kandel, R. A. 2003, "Effect of biomechanical conditioning on cartilaginous tissue formation in vitro," J Bone Joint Surg Am, **85-A**(2), pp.101-5.

166. O'Brien, F. J., Harley, B. A., Waller, M. A., Yannas, I. V., Gibson, L. J., Prendergast, P. J. 2007, "The effect of pore size on permeability and cell attachment in collagen scaffolds for tissue engineering," Technol Health Care, **15**(1), pp.3-17.

167. Hoemann, C. D., Sun, J., McKee, M. D., Chevrier, A., Rossomacha, E., Rivard, G. E., Hurtig, M., Buschmann, M. D. 2007, "Chitosan-glycerol phosphate/blood implants elicit hyaline cartilage repair integrated with porous subchondral bone in microdrilled rabbit defects," Osteoarthritis Cartilage, **15**(1), pp.78-89.

168. Hung, C. T., Mauck, R. L., Wang, C. C., Lima, E. G., Ateshian, G. A. 2004, "A paradigm for functional tissue engineering of articular cartilage via applied physiologic deformational loading," Ann Biomed Eng, **32**(1), pp.35-49.

169. Huang, C. Y., Hagar, K. L., Frost, L. E., Sun, Y., Cheung, H. S. 2004, "Effects of cyclic compressive loading on chondrogenesis of rabbit bone-marrow derived mesenchymal stem cells," Stem Cells, **22**(3), pp.313-23.

170. Waldman, S. D., Spiteri, C. G., Grynpas, M. D., Pilliar, R. M., Kandel, R. A. 2004, "Long-term intermittent compressive stimulation improves the composition and mechanical properties of tissue-engineered cartilage," Tissue Eng, **10**(9-10), pp.1323-31.

171. Babalola, O. M., Bonassar, L. J. 2009, "Parametric finite element analysis of physical stimuli resulting from mechanical stimulation of tissue engineered cartilage," J Biomech Eng, **131**(6), pp.061014.

172. Gleghorn, J. P., Bonassar, L. J. 2008, "Lubrication mode analysis of articular cartilage using Stribeck surfaces," J Biomech, **41**(9), pp.1910-8.

173. Bryant, S. J., Anseth, K. S. 2003, "Controlling the spatial distribution of ECM components in degradable PEG hydrogels for tissue engineering cartilage," J Biomed Mater Res A, **64**(1), pp.70-9.

174. Bryant, S. J., Chowdhury, T. T., Lee, D. A., Bader, D. L., Anseth, K. S. 2004, "Crosslinking density influences chondrocyte metabolism in dynamically loaded photocrosslinked poly(ethylene glycol) hydrogels," Ann Biomed Eng, **32**(3), pp.407-17.

175. Chou, A. I., Akintoye, S. O., Nicoll, S. B. 2009, "Photo-crosslinked alginate hydrogels support enhanced matrix accumulation by nucleus pulposus cells in vivo," Osteoarthritis Cartilage, **17**(10), pp.1377-84.

176. Nehrer, S., Breinan, H. A., Ramappa, A., Young, G., Shortkroff, S., Louie, L. K., Sledge, C. B., Yannas, I. V., Spector, M. 1997, "Matrix collagen type and pore size influence behaviour of seeded canine chondrocytes," Biomaterials, **18**(11), pp.769-76.

177. Stops, A. J., McMahon, L. A., O'Mahoney, D., Prendergast, P. J., McHugh, P. E. 2008, "A finite element prediction of strain on cells in a highly porous collagen-glycosaminoglycan scaffold," J Biomech Eng, **130**(6), pp.061001.

178. Kunisaki, S. M., Fuchs, J. R., Steigman, S. A., Fauza, D. O. 2007, "A comparative analysis of cartilage engineered from different perinatal mesenchymal progenitor cells," Tissue Eng, **13**(11), pp.2633-44.

179. Wu, J. Z., Herzog, W. 2006, "Analysis of the mechanical behavior of chondrocytes in unconfined compression tests for cyclic loading," Journal of Biomechanics, **39**(4), pp.603-616.

180. Wernike, E., Li, Z., Alini, M., Grad, S. 2008, "Effect of reduced oxygen tension and long-term mechanical stimulation on chondrocyte-polymer constructs," Cell and Tissue Research, **331** pp.473-483.

181. Lee, C. R., Grodzinsky, A. J., Spector, M. 2001, "The effects of cross-linking of collagen-glycosaminoglycan scaffolds on compressive stiffness, chondrocyte-mediated contraction, proliferation and biosynthesis," Biomaterials, **22**(23), pp.3145-54.

182. Caterson, E. J., Nesti, L. J., Li, W. J., Danielson, K. G., Albert, T. J., Vaccaro, A. R., Tuan, R. S. 2001, "Three-dimensional cartilage formation by bone marrow-derived cells seeded in polylactide/alginate amalgam," J Biomed Mater Res, **57**(3), pp.394-403.

183. Murata, M., Bonassar, L. J., Wright, M., Mankin, H. J., Towle, C. A. 2003, "A role for the interleukin-1 receptor in the pathway linking static mechanical compression to decreased proteoglycan synthesis in surface articular cartilage," Arch Biochem Biophys, **413**(2), pp.229-35.

184. Haudenschild, A. K., Hsieh, A. H., Kapila, S., Lotz, J. C. 2009, "Pressure and distortion regulate human mesenchymal stem cell gene expression," Ann Biomed Eng, **37**(3), pp.492-502.

185. Kisiday, J. D., Lee, J. H., Siparsky, P. N., Frisbie, D. D., Flannery, C. R., Sandy, J. D., Grodzinsky, A. J. 2009, "Catabolic responses of chondrocyte-seeded peptide hydrogel to dynamic compression," Ann Biomed Eng, **37**(7), pp.1368-75.

186. Thorpe, S. D., Buckley, C. T., Vinardell, T., O'Brien, F. J., Campbell, V. A., Kelly, D. J. 2008, "Dynamic compression can inhibit chondrogenesis of mesenchymal stem cells," Biochem Biophys Res Commun, **377**(2), pp.458-62.

187. Yanagisawa, M., Suzuki, N., Mitsui, N., Koyama, Y., Otsuka, K., Shimizu, N. 2007, "Effects of compressive force on the differentiation of pluripotent mesenchymal cells," Life Sci, **81**(5), pp.405-12.

188. Chowdhury, T. T., Bader, D. L., Shelton, J. C., Lee, D. A. 2003, "Temporal regulation of chondrocyte metabolism in agarose constructs subjected to dynamic compression," Arch Biochem Biophys, **417**(1), pp.105-11.

189. Akens, M. K., Hurtig, M. B. 2005, "Influence of species and anatomical location on chondrocyte expansion," BMC Musculoskelet Disord, **6** pp.23.

190. Park, S., Hung, C. T., Ateshian, G. A. 2004, "Mechanical response of bovine articular cartilage under dynamic unconfined compression loading at physiological stress levels," Osteoarthritis Cartilage, **12**(1), pp.65-73.

191. Stoltz, J. F., Dumas, D., Wang, X., Payan, E., Mainard, D., Paulus, F., Maurice, G., Netter, P., Muller, S. 2000, "Influence of mechanical forces on cells and tissues," Biorheology, **37**(1-2), pp.3-14.

192. Almeida, E. S., Spilker, R. L. 1998, "Mixed and Penalty Finite Element Models for the Nonlinear Behavior of Biphasic Soft Tissues in Finite Deformation: Part II - Nonlinear Examples," Comput Methods Biomech Biomed Engin, **1**(2), pp.151-170.

193. Prendergast, P. J., van Driel, W. D., Kuiper, J. H. 1996, "A comparison of finite element codes for the solution of biphasic poroelastic problems," Proc Inst Mech Eng [H], **210**(2), pp.131-6.

194. Spilker, R. L., de Almeida, E. S., Donzelli, P. S. 1992, "Finite element methods for the biomechanics of soft hydrated tissues: nonlinear analysis and adaptive control of meshes," Crit Rev Biomed Eng, **20**(3-4), pp.279-313.

195. Lee, J. H., Fitzgerald, J. B., DiMicco, M. A., Cheng, D. M., Flannery, C. R., Sandy, J. D., Plaas, A. H., Grodzinsky, A. J. 2009, "Co-culture of mechanically injured cartilage with joint capsule tissue alters chondrocyte expression patterns and increases ADAMTS5 production," Arch Biochem Biophys, **489**(1-2), pp.118-26.

196. Rodriguez-Manzaneque, J. C., Westling, J., Thai, S. N., Luque, A., Knauper, V., Murphy, G., Sandy, J. D., Iruela-Arispe, M. L. 2002, "ADAMTS1 cleaves aggrecan at multiple sites and is differentially inhibited by metalloproteinase inhibitors," Biochem Biophys Res Commun, **293**(1), pp.501-8.

197. Bryant, S. J., Nicodemus, G. D., Villanueva, I. 2008, "Designing 3D photopolymer hydrogels to regulate biomechanical cues and tissue growth for cartilage tissue engineering," Pharm Res, **25**(10), pp.2379-86.

198. Connelly, J. T., Garcia, A. J., Levenston, M. E. 2007, "Inhibition of in vitro chondrogenesis in RGD-modified three-dimensional alginate gels," Biomaterials, **28**(6), pp.1071-83.

199. Hsu, S. H., Chang, S. H., Yen, H. J., Whu, S. W., Tsai, C. L., Chen, D. C. 2006, "Evaluation of biodegradable polyesters modified by type II collagen and Arg-

Gly-Asp as tissue engineering scaffolding materials for cartilage regeneration," Artif Organs, **30**(1), pp.42-55.

200. Abell, J. E., Hootman, J. M., Zack, M. M., Moriarty, D., Helmick, C. G. 2005, "Physical activity and health related quality of life among people with arthritis," J Epidemiol Community Health, **59**(5), pp.380-5.